

# MANIPULATION OF FLOODING AND NUTRIENTS INFLUENCES PLANT-MICROBE INTERACTIONS AND WETLAND FUNCTION

by

Regina Ann Bellon Bledsoe

May 2020

Director of Dissertation: Ariane L. Peralta, Ph.D., Department of Biology

Major Department: Interdisciplinary Doctoral Program in Biological Sciences

## **Abstract**

The largest global stocks of organic carbon are in soils, where plants fix atmospheric carbon dioxide into biomass at higher rates than soil organic carbon is lost through decomposition and microbial respiration. Specifically, wetlands store about 30% of global carbon stocks, but changes in soil hydrology and nutrient concentrations can stimulate microbial activities and result in soil organic matter decomposition. This leads to carbon loss as carbon dioxide and decreases wetland carbon storage potential. The aim of this work was to determine the degree that soil hydrology and nutrient status interact to affect plant-microbe relationships, microbial community structure, and functions related to carbon and nitrogen cycling within wetlands. A combination of field and laboratory mesocosm manipulations in constructed, restored, and natural wetland ecosystems were used to examine wetland plant-soil-microbial interactions. In a constructed (Chapter 1) and restored (Chapter 2) wetland, hydrology explained variation in microbial community composition and function, while plant presence also mediated soil carbon loss (methane and carbon dioxide). Further, in a nutrient-poor coastal plain

wetland experiment (Chapters 3 and 4), long-term nutrient additions stimulated plant-microbial feedbacks in a way that increased microbial activity and carbon losses in these wetland soils. Together, these results highlight how plant-microbial interactions regulate carbon loss and nitrogen cycling in wetland soils and the need to include these interactions to improve predictions of wetland carbon storage potential. In addition, considering hydrologic and nutrient controls on plant-microbial regulation of microbial functions could enhance wetland construction and restoration efforts. Results from this dissertation provide insights in how plant-microbial interactions can be leveraged to enhance soil carbon storage and increase climate change mitigation potential from wetlands ecosystems.



MANIPULATION OF FLOODING AND NUTRIENTS INFLUENCES PLANT-MICROBE  
INTERACTIONS AND WETLAND FUNCTION

A Dissertation

Presented To

The Faculty of the Interdisciplinary Doctoral Program in Biological Sciences

In Association with the Department of Biology,

Thomas Harriot College of Arts and Sciences

East Carolina University

In Partial Fulfillment of the Requirements for the Degree

Doctor of Philosophy

Interdisciplinary Doctoral Program of Biological Sciences

by

Regina Ann Bellon Bledsoe

May 2020

© Regina Ann Bellon Bledsoe, 2020

MANIPULATION OF FLOODING AND NUTRIENTS INFLUENCES PLANT-MICROBE  
INTERACTIONS AND WETLAND FUNCTION

by

Regina Ann Bellon Bledsoe

APPROVED BY:

DIRECTOR OF  
DISSERTATION:

\_\_\_\_\_  
Ariane L. Peralta, Ph.D.

COMMITTEE MEMBER:

\_\_\_\_\_  
Erin K. Field, Ph.D.

COMMITTEE MEMBER:

\_\_\_\_\_  
Lauren Kinsman-Costello, Ph.D.

COMMITTEE MEMBER:

\_\_\_\_\_  
Michael W. McCoy, Ph.D.

CHAIR OF THE DEPARTMENT  
OF BIOLOGY:

\_\_\_\_\_  
David R. Chalcraft, PhD.

DEAN OF THE  
GRADUATE SCHOOL:

\_\_\_\_\_  
Paul J. Gemperline, Ph.D.

## **ACKNOWLEDGMENTS**

Over the past several years, I have had the opportunity to study the most interesting organisms on the planet – soil bacteria and fungi. I am thankful for my advisor, Dr. Ariane Peralta for her advice and guidance through my studies. I am grateful for research funding provided by National Science Foundation Graduate Research Fellowship Program, North Carolina Sea Grant and Water Resources Research Institute, Mycological Society of America, and the Department of Biology at East Carolina University. I am appreciative of my committee (Dr. Erin Field, Dr. Lauren Kinsman-Costello, and Dr. Michael McCoy) for helpful feedback and advice. Last but not least, I would like to thank the many friends, colleagues, and acquaintances I have met along the way that have provided support during this journey.

## TABLE OF CONTENTS

<b>LIST OF TABLES</b> .....	<b>vii</b>
<b>LIST OF FIGURES</b> .....	<b>viii</b>
<b>LIST OF ABBREVIATIONS</b> .....	<b>ix</b>
<b>INTRODUCTION</b> .....	<b>1</b>
References .....	5
<b>CHAPTER 1: A MICROBIAL PERSPECTIVE ON BALANCING TRADE-OFFS IN ECOSYSTEM FUNCTIONS IN A CONSTRUCTED STORMWATER WETLAND</b> .	<b>8</b>
Abstract .....	8
Introduction .....	10
Methods .....	14
Results .....	20
Discussion .....	25
Figures and Tables.....	32
Supplemental Figures and Tables .....	40
References .....	45
<b>CHAPTER 2: PLANT-MEDIATED REDUCTION OF GREENHOUSE GASES UNDER DYNAMIC HYDROLOGY</b> .....	<b>51</b>
Abstract .....	51
Introduction .....	53
Methods .....	58
Results .....	68
Discussion .....	72
Figures and Tables.....	76
Supplemental Figures and Tables .....	84
References .....	90
<b>CHAPTER 3: LONG-TERM NUTRIENT ENRICHMENT OF AN OLIGOTROPH-DOMINATED WETLAND INCREASES BACTERIAL DIVERSITY IN BULK SOILS AND PLANT RHIZOSPHERES</b> .....	<b>95</b>

Abstract .....	95
Introduction .....	97
Methods .....	101
Results .....	107
Discussion .....	110
Figures and Tables.....	116
Supplemental Figures and Tables .....	122
References .....	128
<b>CHAPTER 4: LONG-TERM NUTRIENT ENRICHMENT OF AN OLIGOTROPH-DOMINATED WETLAND SHIFTS MICROBIAL DIVERSITY AND INCREASES CARBON AND NITROGEN CYCLING .....</b>	<b>136</b>
Abstract .....	136
Introduction .....	138
Methods .....	143
Results .....	152
Discussion .....	158
Figures and Tables.....	161
Supplemental Figures and Tables .....	167
References .....	175
<b>CONCLUSION .....</b>	<b>181</b>
References .....	186

## LIST OF TABLES

Table 1.1 Soil and water properties .....	33
Table S1.1 Mixed-effects models for greenhouse gas fluxes .....	40
Table S1.2 Estimated marginal means for greenhouse gas fluxes .....	41
Table S1.3 Mixed-effects models for potential denitrification N <sub>2</sub> O fluxes .....	42
Table S1.4 Estimated marginal means for potential denitrification N <sub>2</sub> O fluxes....	42
Table S1.5 Summary of bacterial indicator species analysis.....	44
Table 2.1 Soil properties .....	79
Table S2.1 Mixed-effects models for greenhouse gas fluxes .....	84
Table S2.2 Summary of PERMANOVA comparing microbial communities.....	85
Table S2.3 Summary of bacterial indicator species analysis.....	85
Table 3.1 Soil properties .....	116
Table S3.1 Soil properties ANOVA summary.....	122
Table S3.2 Bacterial diversity ANOVA summary.....	122
Table S3.3 Copiotroph to oligotroph ratio ANOVA summary.....	123
Table S3.4 Bacterial composition PERMANOVA summary .....	123
Table S3.5 Summary of bacterial indicator species analysis.....	126
Table 4.1 Soil properties .....	161
Table S4.1 Soil properties ANOVA summary.....	167
Table S4.2 Fungal and bacterial diversity ANOVA summary .....	167
Table S4.3 Fungal and bacterial community PERMANOVA summary.....	168
Table S4.4 Fungal indicator species analysis summary.....	169
Table S4.5 Bacterial indicator species analysis summary.....	171
Table S4.6 C, N, and P AWCD ANOVA summary .....	173
Table S4.7 C, N, and P diversity ANOVA summary .....	174

## LIST OF FIGURES

Figure 1.1 Constructed wetland experimental setup .....	32
Figure 1.2 Boxplots of greenhouse gas fluxes .....	35
Figure 1.3 Stacked bar plot of global warming potentials.....	36
Figure 1.4 Boxplots of potential denitrification rates.....	37
Figure 1.5 PCoA plot of microbial community .....	38
Figure 1.6 Heat map of relative abundance of top 1% taxa.....	39
Figure S1.1 Images of greenhouse gas chambers.....	40
Figure 2.1 Image of study site .....	76
Figure 2.2 Images of mesocosm experimental setup.....	77
Figure 2.3 Boxplots of percent pain removed form IRIS tubes.....	78
Figure 2.4 Boxplots of CH <sub>4</sub> concentrations .....	80
Figure 2.5 Boxplots of CO <sub>2</sub> concentrations.....	81
Figure 2.6 Boxplots of N <sub>2</sub> O concentrations.....	82
Figure 2.7 PCoA plot of microbial community .....	83
Figure S2.1 Images of Indicator of Reduction in Soils tubes.....	84
Figure 3.1 Boxplots of bacterial diversity.....	117
Figure 3.2 Boxplots of copiotroph oligotroph ratios .....	118
Figure 3.3 PCoA of bacterial community composition.....	119
Figure 3.4 Heat map of grass rhizosphere core taxa.....	120
Figure 3.5 Heat map of forb rhizosphere core taxa .....	121
Figure S3.1 Regression of bacterial diversity and copiotroph oligotroph ratio...	124
Figure S3.2 Boxplots of bulk soil top OTU relative abundances.....	125
Figure 4.1 Boxplots of fungal and bacterial diversity .....	163
Figure 4.2 PCoA of fungal community composition.....	164
Figure 4.3 PCoA of bacterial community composition.....	165
Figure 4.4 Boxplots C, N, and P AWCD and diversity .....	166

## LIST OF SYMBOLS OR ABBREVIATIONS

$\Delta$	Delta, refers to a change in quantity
%	Percent
$\mu\text{g}$	Microgram
$\mu\text{L}$	Microliter
$\mu\text{m}$	Micrometer
$\mu\text{M}$	Micromolar
abs	Absorbance value
AICc	Corrected Akaike information criterion
ANOVA	Analysis of variance
AWCD	Average well color development
$^{\circ}\text{C}$	Degrees Celsius
C	Carbon
C3	C3 photosynthetic pathway in plants, Calvin cycle
C4	C4 photosynthetic pathway in plants, Hatch-Slack pathway
$\text{CH}_4$	Methane
$\text{CO}_2$	Carbon dioxide
cm	Centimeter
CW	Constructed wetland
DM	Dry mass
DNA	Deoxyribonucleic acid
$\text{Fe}^{2+}$	Iron (II)
Fig	Figure
FWS	Free water surface
g	Gram
GHG	Greenhouse gas
GWP	Global warming potential

ha	Hectare
HCl	Hydrochloric acid
hr	Hour
HSD	Honestly significant difference
IndVal	Indicator value
IRIS	Indicator of Reduction in Soil
ITS2	Internal transcribed spacer region 2
KCl	Potassium chloride
KNO <sub>3</sub>	Potassium nitrate
kg	Kilogram
L	Liter
L.	Carl Linnaeus
M	Molar
m <sup>2</sup>	Meter squared
MDL	Below detection limit
Mton	Metric ton
N	North
mg	Milligram
Mg(NO <sub>3</sub> )	Magnesium nitrate
mL	Milliliter
mm	Millimeter
mM	Millimolar
mV	Millivolt
ng	Nanogram
N	Nitrogen
NADH	Nicotinamide adenine dinucleotide
N <sub>2</sub>	Dinitrogen

N <sub>2</sub> O	Nitrous oxide
NH <sub>4</sub> <sup>+</sup>	Ammonium
NO <sub>2</sub> <sup>-</sup>	Nitrite
NO <sub>3</sub> <sup>-</sup>	Nitrate
OM	Organic matter
OTU	Operational taxonomic unit
Pg	Pentagram
P	Phosphorus
PCR	Polymerase chain reaction
PCoA	Principal coordinates of analysis
PERMANOVA	Permutational analysis of variance
PO <sub>4</sub> <sup>3-</sup>	Phosphate
ppm	Parts per million
PVC	Polyvinyl Chloride
rRNA	Ribosomal ribonucleic acid
RDP	Ribosomal database program
RPM	Rotations per minute
SCM	Stormwater control measure
SD	Standard deviation
SOM	Soil organic matter
Tg	Teragram
W	West
wt	Weight
x g	Relative centrifugal force
v	Version
yr	Year

## INTRODUCTION

Soils represent the largest global carbon (C) stocks with concentrations exceeding those found in both plant biomass and the atmosphere (Scharlemann et al., 2014). While representing only 5-8% of terrestrial land surface (Mitsch et al., 2013), wetland ecosystems are estimated to store 450 Pg C, or ~30%, of the estimated 1,500 Pg C found in global soil organic C pools (Lal, 2008). In addition to C storage, wetlands provide another important ecosystem function through the removal of pollutants and excess nutrients from surface waters and agricultural runoff (Koch et al., 2014; Reisinger et al., 2016). However, land use conversion of wetlands to urban and agricultural development results in the loss of these important functions that improve water quality and mitigate climate change. Soil microorganisms and plants control wetland C storage and nutrient removal functions, but abiotic factors particularly soil hydrology and nutrient concentrations also contribute to regulating ecosystem functions (Leff et al., 2015; Mitsch and Gosslink, 2007). Therefore, better understandings of how abiotic and biotic factors interact to control microbial functions and promote ecosystem benefits are needed when wetlands are restored or constructed.

In Chapter 1, I explore trade-offs in microbially driven ecosystem functions responsible for nitrogen removal (service) and greenhouse gas production (disservice) in a constructed stormwater wetland. Complete inorganic nitrogen removal via denitrification ( $\text{NO}_3^- \rightarrow \text{N}_2$ ) is an anaerobic microbial process that decreases nitrogen loads in stormwater runoff resulting in improved downstream water quality (Lee et al., 2009). These same anoxic soil conditions can also support production of the greenhouse gas methane (via methanogenesis), which could decrease long-term C

storage and climate change mitigation benefits of wetlands (Demuzere et al., 2014).

The goal of this study was to better understand which design features of a constructed wetland best supports denitrification but also decreases methanogenesis.

Next, in Chapter 2, I examine how the duration of soil saturation and plant presence influence microbial community structure and greenhouse gas production using a mesocosm experiment. Soil hydrology strongly relates to soil oxygen concentrations or redox status (Burgin et al., 2011; Truu et al., 2009). As such, soil redox status is a good predictor of microbial processes since oxygen availability limits microbial physiology and cellular respiration. Since hydrology is a strong environmental filter that affects microbial community structure and function, the duration and magnitude of a strong environmental can affect microbial response to hydrology in unexpected ways (Peralta et al., 2014). Additionally, the presence of plants has been shown to increase and decrease greenhouse gas production due to gas transport via plant tissues which can alter soil redox status (Chanton, 2005; Sundberg et al., 2007). Therefore, the presence of plants can also impact microbial community structure and function. However, the inclusion of plants in studies measuring GHG production is often overlooked (Günther et al., 2014; Luan and Wu, 2014). A deeper understanding of abiotic (hydrology) and biotic (plants) controls on microbial processes in wetlands can help improve estimations of wetland C storage potential.

In Chapter 3 and 4, I investigate how long-term nutrient additions to soils influence C and N cycling in bulk soils and plant rhizospheres in a coastal plain wetland. Industrial agricultural use of inorganic fertilizer is responsible for increased atmospheric deposition of both nitrogen and phosphorus (Peñuelas et al., 2012; Wang et al., 2015).

This indirect nutrient enrichment can stimulate both plant and microbial growth resulting in a positive feedback that promotes soil organic matter (SOM) decomposition (Bengtson et al., 2012; Meier et al., 2017; Riggs et al., 2015; Song et al., 2011). In Chapter 3, results suggested that fertilization increase bacterial diversity in bulk soils and plant rhizospheres. Based on another study, microbial diversity may contribute to enhanced N-mining when nutrients are limiting, which leads to increased SOM decomposition (Weidner et al., 2015). Additionally, if fertilization increases labile C substrates within plant rhizosphere soils, this could fuel microbial activity that promotes decomposition of more recalcitrant SOM which could decrease soil C stocks (i.e., soil priming) (Nowinski et al., 2008). If nutrient additions increase rates of SOM decomposition within plant rhizospheres and lead to net C losses, then estimates of wetland C storage potential could be overestimated.

Conservation, protection, and enhancement of wetland C stocks require a holistic understanding of the interactions between soil microorganisms and plants along with abiotic constraints (i.e., hydrology and nutrients) that regulate microbial C and N processes. This dissertation examines facets of plant-microbial interactions within wetlands to reveal mechanisms controlling wetland C cycling. Soil hydrologic status is a primary determinant in microbial community structure and function due to the relationship of decreasing oxygen levels with increasing soil saturation, which selects for particular subsets of microbial taxa adapted to those oxygen levels (Burgin et al., 2011; Truu et al., 2009). This dissertation demonstrates that the duration of hydrologic events can have lasting impacts on both microbial community structure and function. These studies also demonstrate that plant presence can increase oxygen availability

and decrease GHG emissions in saturated soils. In terms of climate change and shifting weather patterns, increasing intensity and magnitude of drought and flooded conditions could have dramatic effects on microbial functions by directly altering soil hydrology or plant community abundance and composition. Another important determinant of microbial community structure and function is the availability of nutrients. Soil C and N limitations and availability can affect plant-microbe interactions in ways that enhance plant-microbe feedbacks and SOM decomposition in soils, which can decrease wetland C storage potential (Bengtson et al., 2012; Nowinski et al., 2008). These studies demonstrate that low-nutrient ecosystems may be particularly sensitive to nutrient additions altering C cycling rates. Therefore, if industrial agriculture continues to fuel commercial fertilization demand, then resultant atmospheric nutrient deposition is expected to destabilize soil C storage capacity of low-nutrient ecosystems. An extension of the studies presented here could examine the extent that nutrient additions force wetlands to a tipping point between C storage and C loss. This future work could improve nutrient management with the goal of decreasing atmospheric nutrient concentrations to conserve and enhance global C stocks.

## References

- Bengtson, P., Barker, J., Grayston, S.J., 2012. Evidence of a strong coupling between root exudation, C and N availability, and stimulated SOM decomposition caused by rhizosphere priming effects. *Ecol. Evol.* 2, 1843–1852. <https://doi.org/10.1002/ece3.311>
- Burgin, A.J., Yang, W.H., Hamilton, S.K., Silver, W.L., 2011. Beyond carbon and nitrogen: how the microbial energy economy couples elemental cycles in diverse ecosystems. *Front. Ecol. Environ.* 9, 44–52. <https://doi.org/10.1890/090227>
- Chanton, J.P., 2005. The effect of gas transport on the isotope signature of methane in wetlands. *Org. Geochem.* 36, 753–768. <https://doi.org/10.1016/j.orggeochem.2004.10.007>
- Demuzere, M., Orru, K., Heidrich, O., Olazabal, E., Geneletti, D., Orru, H., Bhave, A.G., Mittal, N., Feliu, E., Faehle, M., 2014. Mitigating and adapting to climate change: Multi-functional and multi-scale assessment of green urban infrastructure. *J. Environ. Manage.* 146, 107–115. <https://doi.org/10.1016/j.jenvman.2014.07.025>
- Günther, A., Jurasinski, G., Huth, V., Glatzel, S., 2014. Opaque closed chambers underestimate methane fluxes of *Phragmites australis* (Cav.) Trin. ex Steud. *Environ. Monit. Assess.* 186, 2151–2158. <https://doi.org/10.1007/s10661-013-3524-5>
- Koch, B.J., Febria, C.M., Gevrey, M., Wainger, L.A., Palmer, M.A., 2014. Nitrogen Removal by Stormwater Management Structures: A Data Synthesis. *J. Am. Water Resour. Assoc.* 50, 1594–1607. <https://doi.org/10.1111/jawr.12223>
- Lal, R., 2008. Carbon sequestration. *Philos. Trans. R. Soc. B Biol. Sci.* <https://doi.org/10.1098/rstb.2007.2185>
- Lee, C.G., Fletcher, T.D., Sun, G., 2009. Nitrogen removal in constructed wetland systems. *Eng. Life Sci.* 9, 11–22. <https://doi.org/10.1002/elsc.200800049>
- Leff, J.W., Jones, S.E., Prober, S.M., Barberán, A., Borer, E.T., Firn, J.L., Harpole, W.S., Hobbie, S.E., Hofmockel, K.S., Knops, J.M.H., McCulley, R.L., La Pierre, K., Risch, A.C., Seabloom, E.W., Schütz, M., Steenbock, C., Stevens, C.J., Fierer, N., 2015. Consistent responses of soil microbial communities to elevated nutrient inputs in grasslands across the globe. *Proc. Natl. Acad. Sci.* 201508382. <https://doi.org/10.1073/pnas.1508382112>
- Luan, J., Wu, J., 2014. Gross photosynthesis explains the “artificial bias” of methane fluxes by static chamber (opaque versus transparent) at the hummocks in a boreal peatland. *Environ. Res. Lett.* 9. <https://doi.org/10.1088/1748-9326/9/10/105005>
- Meier, I.C., Finzi, A.C., Phillips, R.P., 2017. Soil Biology & Biochemistry Root exudates increase N availability by stimulating microbial turnover of fast-cycling N pools. *Soil Biol. Biochem.* 106, 119–128. <https://doi.org/10.1016/j.soilbio.2016.12.004>

- Mitsch, W.J., Bernal, B., Nahlik, A.M., Mander, Ü., Zhang, L., Anderson, C.J., Jørgensen, S.E., Brix, H., 2013. Wetlands, carbon, and climate change. *Landsc. Ecol.* 28, 583–597. <https://doi.org/10.1007/s10980-012-9758-8>
- Mitsch, W.J., Gosslink, J.G., 2007. *Wetlands*, 4th ed. John Wiley & Sons, Hoboken.
- Nowinski, N.S., Trumbore, S.E., Schuur, E.A.G., Mack, M.C., Shaver, G.R., 2008. Nutrient addition prompts rapid destabilization of organic matter in an arctic tundra ecosystem. *Ecosystems* 11, 16–25. <https://doi.org/10.1007/s10021-007-9104-1>
- Peñuelas, J., Sardans, J., Rivas-ubach, A., Janssens, I.A., 2012. The human-induced imbalance between C, N and P in Earth's life system. *Glob. Chang. Biol.* 18, 3–6. <https://doi.org/10.1111/j.1365-2486.2011.02568.x>
- Peralta, A.L., Matthews, J.W., Kent, A.D., 2014. Habitat Specialization Along a Wetland Moisture Gradient Differs Between Ammonia-oxidizing and Denitrifying Microorganisms. *Microb. Ecol.* 68, 339–350. <https://doi.org/10.1007/s00248-014-0407-4>
- Reisinger, A.J., Groffman, P.M., Rosi-Marshall, E.J., 2016. Nitrogen-cycling process rates across urban ecosystems. *FEMS Microbiol. Ecol.* 92, fiw198. <https://doi.org/10.1093/femsec/fiw198>
- Riggs, C.E., Hobbie, S.E., Bach, E.M., Hofmockel, K.S., Kazanski, C.E., 2015. Nitrogen addition changes grassland soil organic matter decomposition. *Biogeochemistry* 125, 203–219. <https://doi.org/10.1007/s10533-015-0123-2>
- Scharlemann, J.P.W., Tanner, E.V.J., Hiederer, R., Kapos, V., 2014. Global soil carbon: Understanding and managing the largest terrestrial carbon pool. *Carbon Manag.* 5, 81–91. <https://doi.org/10.4155/cmt.13.77>
- Song, L., Bao, X., Liu, X., Zhang, Y., Christie, P., Fangmeier, A., Zhang, F., 2011. Nitrogen enrichment enhances the dominance of grasses over forbs in a temperate steppe ecosystem. *Biogeosciences* 8, 2341–2350. <https://doi.org/10.5194/bg-8-2341-2011>
- Sundberg, C., Jenny, J.S., Tonderski, K., Lindgren, P.E., 2007. Overland flow systems for treatment of landfill leachates-Potential nitrification and structure of the ammonia-oxidising bacterial community during a growing season. *Soil Biol. Biochem.* 39, 127–138. <https://doi.org/10.1016/j.soilbio.2006.06.016>
- Truu, M., Juhanson, J., Truu, J., 2009. Microbial biomass, activity and community composition in constructed wetlands. *Sci. Total Environ.* 407, 3958–3971. <https://doi.org/10.1016/j.scitotenv.2008.11.036>
- Wang, R., Balkanski, Y., Boucher, O., Ciais, P., Peñuelas, J., Tao, S., 2015. Significant contribution of combustion-related emissions to the atmospheric phosphorus budget. *Nat. Geosci.* 8, 48–54. <https://doi.org/10.1038/ngeo2324>

Weidner, S., Koller, R., Latz, E., Kowalchuk, G., Bonkowski, M., Scheu, S., Jousset, A., 2015. Bacterial diversity amplifies nutrient-based plant-soil feedbacks. *Funct. Ecol.* 29, 1341–1349. <https://doi.org/10.1111/1365-2435.12445>

# CHAPTER 1: A MICROBIAL PERSPECTIVE ON BALANCING TRADE-OFFS IN ECOSYSTEM FUNCTIONS IN A CONSTRUCTED STORMWATER WETLAND

In Review at  
*Ecological Engineering*, 2020

## **Abstract**

Green stormwater infrastructure, such as constructed wetlands (CWs), is a type of stormwater control measure that can decrease nutrient and pollutant loads in urban stormwater runoff. Nutrient and pollutant removal processes (i.e., benefit) within wetlands are primarily driven by microbial functions that can result in disservices such as greenhouse gas (GHG) emissions, which can negate climate change mitigation. Specifically, microbial respiration by facultative anaerobes in anoxic conditions is the primary pathway for nitrogen removal. Similar anoxic conditions that support denitrifiers can also support obligate anaerobes that produce methane via methanogenesis. In this study, we examined nitrogen removal potential, GHG production, and microbial community structure within flooded and shallow land areas of a stormwater CW to identify spatial zones for optimization. Our results indicate that permanently flooded zones are sources of methane emissions and have the greatest contribution to climate change. However, denitrification potential rates were similar across both flooded and shallow land zones. This suggests that shallow land areas can provide nitrogen removal services with decreased GHG emissions compared to flooded zones. In the case of this particular CW, a reduction of permanently flooded zones within the wetland could decrease GHG emissions (i.e., disservice) without limiting denitrification potential (i.e., benefit) of the wetland. We conclude that holistic development and design of stormwater control measures that accounts for microbial functions provides the opportunity to

maximize benefits (i.e., nutrient and pollutant removal) and decrease disservices (i.e., GHG emissions) in these structures.

## Introduction

In urban areas, impervious surfaces increase nutrient and pollutant loads in stormwater runoff, thereby decreasing water quality within neighboring watersheds (Bell et al., 2019; Line and White, 2007; O'Driscoll et al., 2010). Nutrient loadings are of particular concern due to adverse effects in downstream water quality (Paerl et al., 2014; Rabalais et al., 2009). Green stormwater infrastructure, such as constructed wetlands (CWs), are stormwater control measures (SCMs) that are designed to mimic natural ecosystems and can decrease flooding from stormwater runoff and improve water quality in and around urban areas. The physical, chemical, and biological treatment processes that naturally occur in wetlands make CWs an effective approach to decreasing nutrient loads in stormwater runoff (Koch et al., 2014; Mitsch et al., 2013; Payne et al., 2014; Reisinger et al., 2016). Thus, entities such as the North Carolina Department of Environmental Quality encourage use of SCMs as a way to decrease nutrient loadings to nutrient sensitive waterways by offering nutrient reduction credits. CWs that have a ponding depth of less than 12 inches and a hydraulic residence time of two to five days are credited with 40% removal of nitrogen (N) from stormwater runoff (NCDEQ, 2018) However, this nutrient reduction policy and similar policies outside of North Carolina do not consider the potential trade-off of water quality and air quality via greenhouse gas (GHG) emissions associated with nitrogen removal processes. The unintended GHG production from stormwater CWs could negatively affect climate change mitigation and adaptation by simultaneously releasing multiple GHGs (Demuzere et al., 2014). Therefore, in order to meet management goals in a more holistic way (i.e., enhancing total nitrogen removal and decreasing GHG emissions), a

deeper understanding of microbial and plant mediated processes occurring within CWs are needed to optimize wetland design.

Plants and microorganisms carry out nutrient and pollutant removal processes that occur within wetlands. While plants and microorganisms can assimilate ammonium ( $\text{NH}_4^+$ ) and nitrate ( $\text{NO}_3^-$ ) ions into biomass, the primary pathway of complete nitrogen (N) removal from the system is microbial respiration via denitrification and to a lesser degree anaerobic ammonium oxidation or anammox (Lee et al., 2009). Denitrification is typically coupled with nitrification in which  $\text{NH}_4^+$  is first transformed to nitrite ( $\text{NO}_2^-$ ) and then  $\text{NO}_3^-$  by aerobic nitrifying microorganisms (Lee et al., 2009). In the process of anammox,  $\text{NO}_2^-$  is directly converted to dinitrogen gas ( $\text{N}_2$ ) and in the process of denitrification  $\text{NO}_3^-$  is reduced to nitric oxide (NO), then to nitrous oxide ( $\text{N}_2\text{O}$ ), a potent GHG, and finally to  $\text{N}_2$ , an inert and abundant atmospheric gas (Knowles, 1982; Lee et al., 2009; Smith and Tiedje, 1979). Denitrification is an anaerobic microbial process that requires anoxic conditions such as those found in saturated and flooded soils within wetlands (Marton et al., 2015; Smith and Tiedje, 1979). Many denitrifying microorganisms are facultatively anaerobic. These microorganisms can perform aerobic respiration when oxygen is available but can use other alternate electron acceptors (i.e., nitrate) when anoxic soil conditions arise (Tiedje, 1988). Due to this facultative anaerobic metabolism, these microorganisms respond to hydrologic change with varying degrees depending on past environmental conditions (Peralta et al., 2014; Peralta et al., 2013).

Similar anoxic conditions that support the beneficial process of complete denitrification (transformation of  $\text{N}_2\text{O}$  to  $\text{N}_2$ ) can also support production of methane

(CH<sub>4</sub>), a GHG, which is considered an ecosystem disservice (Demuzere et al., 2014). Methanogens are obligate anaerobes that produce CH<sub>4</sub> via methanogenesis but only under anoxic conditions when the environment is depleted of other electron acceptors (e.g., nitrate, sulfate, and ferric iron) (Fetzer and Conrad, 1993; Liu et al., 2008). When organic matter is decomposed by fermentation, methanogens can use the byproducts of acetate, hydrogen, and CO<sub>2</sub> for energy and produce CH<sub>4</sub> (Conrad, 2007). The other side of CH<sub>4</sub> cycling is the consumption of CH<sub>4</sub> by aerobic methanotrophs, which have been reported to consume 45-90% of CH<sub>4</sub> produced (Brindha and Vasudevan, 2018; Conrad, 2007; Le Mer and Roger, 2001). Systems in which the ratio of methanogens is greater than methanotrophs are typically sources of methane (Altshuler et al., 2019; Rey-Sanchez et al., 2019; Wen et al., 2018). Since methanogens are obligate anaerobes, even low amounts of oxygen can suppress methanogenesis (Fetzer and Conrad, 1993; Le Mer and Roger, 2001). However, the majority of methanotrophs are aerobes, and there is typically greater CH<sub>4</sub> oxidation in pulsing systems that are not permanently inundated (Chowdhury and Dick, 2013). Therefore, anoxic conditions that can support complete denitrification also often result in GHG emissions, especially when nitrate is limiting.

The three major biogenic GHGs of concern, CO<sub>2</sub>, CH<sub>4</sub>, and N<sub>2</sub>O, are known to contribute to increased atmospheric warming and thereby influence global climate change. While CO<sub>2</sub> is the most abundant GHG and is therefore most concerning, CH<sub>4</sub> and N<sub>2</sub>O gases have a greater global warming potential (GWP) than CO<sub>2</sub> (IPCC, 2014). Specifically, per molecule, CH<sub>4</sub> and N<sub>2</sub>O have GWP of 28 and 265, respectively, over a 100 year time-scale when compared to CO<sub>2</sub> which is equal to 1 (IPCC, 2014).

Generally, atmospheric quantities of CH<sub>4</sub> are lower than CO<sub>2</sub> and N<sub>2</sub>O is typically measured in the lowest atmospheric quantities, but the increased GWP of these gases contribute disproportionately to atmospheric warming.

To improve CW water quality management in the urban landscape, both ecosystem services (e.g., complete denitrification) and disservices (e.g., GHGs) should be taken into account during the planning and design phase (Demuzere et al., 2014). This study focuses on a free surface water CW which are common due to low construction cost. To accommodate stormwater runoff and water quality functions, CWs generally have four main zones: upland (rarely submerged except during large runoff events), shallow land (soil is saturated but only temporarily inundated following runoff events), shallow pools (designed to be permanently inundated except during droughts) and deep pools (permanently inundated) (NCDEQ, 2019). In CWs, ammonification and nitrification are optimized to occur in the shallow land zones as stormwater percolates into aerated soils as runoff enters. If soils in shallow lands are saturated for sufficient durations, denitrification is expected to eventually occur as well. It is in the shallow water zones where denitrification is conventionally thought to occur due to saturated, anoxic conditions. In this study we focus on complete denitrification as the ecosystem service since this process typically accounts for the most nitrogen removal in constructed wetlands (Rahman et al., 2019).

The goal of this study is to identify areas within a stormwater CW that supports denitrification and decreases GHG emissions, especially due to methanogenesis. We hypothesize that the redox status of different locations within the wetland identified as shallow land and flooded zones will both support the anaerobic process of

denitrification, while only the flooded zones will be a source of CH<sub>4</sub> gas. If CH<sub>4</sub> emissions are greater than CO<sub>2</sub> production, the overall GWP of the wetland will increase since methane has a higher GWP than CO<sub>2</sub>. However, due to the facultative nature of microbes residing in the shallow land zones, denitrification will still occur in shallow land zones after a short period of flooding if nitrate is not limiting. To test these hypotheses, we monitored GHG fluxes monthly for one year and sampled sediments and surface water for chemical analyses seasonally. To determine bacterial and archaeal community structure in sediments, we carried out 16s rRNA V4 amplicon sequencing. We also determined potential denitrification rates across the wetland using a short-term incubation experiment. We examined the potential benefits and disservices occurring within this CW by combining GHG rates with potential denitrification rates, sediment and water chemistry parameters along with microbial community composition.

## **Methods**

### *Study site*

The study location is a recently constructed (2015) stormwater wetland located on East Carolina University's main campus in Greenville, NC (N 35°35'22.4", W 77°22'13.4"). The 0.13 acre CW receives runoff from a 5.7 acre parking lot in a highly urbanized area of the city. The temporary ponding depth (30.5 cm) of the wetland is equal to 0.51 cm of runoff within the impervious drainage area (Fig. 1.1). The total surface area is divided among main zones (% surface area): shallow land (35%), shallow water (35%), deep pools (10%), forebay (10%), and outlet pool (10%) (NCDEQ,

2019). The dominant plants within saturated areas of the wetland are *Typha latifolia* L., *Pontederia cordata*, and L., and *Iris versicolor* L. The shallow land area along the water's edge is dominated by *Carex lupulina* Muhl. ex Willd.

### *GHG monitoring and flux calculations*

We used a static chamber method to measure GHG fluxes. At the CW, we established 13 GHG sampling plots along two main transects that follow the central channel within the wetland and flows from inlet to outlet (Fig. 1.1). Of those 13 plots, five chambers were placed in shallow water and deep pools (flooded zones), and 10 chambers were placed in shallow land zones along the outside edge of the main channel. Each sampling plot in shallow land zones (n=8) was fitted with a GHG chamber bottom installed 6 cm belowground. During sampling events, chamber tops (height = 30 cm and diameter = 15 cm) were attached to an aboveground groove, and the groove was filled with water to create a gas tight seal. GHG chamber tops in flooded zones were fitted with a Styrofoam float allowing 2-3 cm of the chamber top below the surface water.

We collected GHG samples monthly for one year (2017). Sampling events occurred at least 48 hours after a rain event of > 0.51 cm. Gas samples were collected at 0, 12, 24, and 36 minutes using 20 mL syringes. Each gas sample was divided between two 3.7 mL Exetainers® (Labco, Lampeter, Wales, UK) with dual septa and stored upside at room temperature until analyzed. We measure GHG concentrations using a Shimadzu 2014 gas chromatograph (Shimadzu Scientific Instruments,

Columbia, Maryland) fitted with an electron capture detector to measure N<sub>2</sub>O and flame ionization detector to measure CH<sub>4</sub> and CO<sub>2</sub>. Monthly GHG fluxes were calculated using the linear change in concentration and the ideal gas law (Millar et al. 2018). Seasonal estimates were calculated by averaging monthly flux measurements: spring = March-May, summer = June-August, fall = September-November and winter = December-February. In addition, the equivalent CO<sub>2</sub> flux (CO<sub>2</sub>e) for methane was calculated by multiplying CH<sub>4</sub> flux by 28, which is equal to the increase in warming potential in methane versus carbon dioxide.

#### *Soil collection and chemical properties*

We characterize soil physicochemical properties seasonally (May, July, October, and December). Each CW composite soil sample represented three cores (3.1 cm diameter, 12 cm depth) that were adjacent to each GHG sampling chamber. We homogenized each composite sample by passing the sample through a 4 mm sieve, and then processed subsamples for soil gravimetric moisture, pH, extractable ammonium and nitrate, total carbon, and total nitrogen. Briefly, we combined 5 g of field moist soil and 45 mL of 2M potassium chloride (KCl) and shook samples for 1 hour before gravity filtration to collect soil extracts. Ammonium and nitrate concentrations were colorimetrically measured using a SmartChem 200 auto analyzer (Unity Scientific Milford, Massachusetts, USA) at the East Carolina University Environmental Research Laboratory. Using a 20-30 g subsample, we measured field-moist and oven-dry (dried 24 hours at 105°C) soil weights to determine moisture content by measuring the mass

of water divided by the mass of oven-dried soil. Using a mortar and pestle, we coarsely ground a oven-dried subsample of soil and combined 10 g of soil with 10 mL of Nanopure® water to measure soil pH. On another oven-dried subsample, we finely ground the soil for elemental carbon and nitrogen analysis using an elemental analyzer (2400 CHNS Analyzer; Perkin Elmer; Waltham, Massachusetts, USA) at the Environmental and Agricultural Testing Service laboratory (Department of Crop and Soil Sciences at NC State). Finally, we measured organic matter content based on the loss on ignition method by ashing 20 g oven-dried soil at 550 °C (Hoogsteen et al., 2015) for 2 hours, this duration may underestimate organic carbon content (Heiri et al., 2001). In addition, a subsample of field-moist soil was stored at 4 °C until we performed denitrification potential assays. Another subsample of field-moist soil was stored at -80 °C until DNA extraction for bacterial amplicon sequencing.

### *Seasonal denitrification potential*

Within 72 hours of soil collection, we measured potential denitrification rates using the acetylene block denitrification enzyme assay (Schaller et al., 2004; Tiedje et al., 1989; Wall et al., 2005). We weighed triplicate 25 g subsamples of field-moist soil and transferred samples into 125 mL Wheaton bottles fitted with a phenolic cap and butyl septa. In each bottle, we added 75 mL of 1 mM potassium chloride ( $\text{KNO}_3$ ) to provide an abundant nitrogen supply and 1.3 mL of chloramphenicol ( $100 \text{ mg mL}^{-1}$ ) to inhibit new denitrification enzyme production. Bottles were sealed with septa-centered caps, shook, and purged with helium for 5 minutes. We removed 15 mL of helium from

the headspace and replaced with 15 mL of pure acetylene gas. At each hour for 3 hours, we collected a 10 mL gas sample (time point T0, T1, T2, T3) from each bottle and stored gas sample in a 3.7 mL Exetainer®. We shook each bottle to equilibrate N<sub>2</sub>O in aqueous and sediment phases before each sample collection. We added 10 mL of 10% acetylene mixture to the headspace after each sample collection. N<sub>2</sub>O fluxes were calculated as described for GHG fluxes.

### *Microbial Community Analysis*

We extracted DNA from soils using the Qiagen DNeasy Powerlyzer PowerSoil Kit. Genomic DNA was amplified using barcoded primers 515FB/806R primer set, originally developed by the Earth Microbiome Project to target the V4-V5 region of the bacterial 16S subunit of the ribosomal RNA gene (Apprill et al., 2015; Caporaso et al., 2010; Parada et al., 2016). For each sample, three 50 µL polymerase chain reaction (PCR) libraries were combined and then cleaned using the AMPure XP magnetic bead protocol (Axygen, Union City, California, USA). Cleaned PCR products were quantified using QuantIT dsDNA broad range assay (Thermo Scientific, Waltham, Massachusetts, USA) and diluted to a concentration of 10 ng µL<sup>-1</sup>. We combined barcoded PCR samples (5 ng µL<sup>-1</sup>) in equimolar concentration and sequenced the pooled library using the Illumina MiSeq platform paired end read approach (Illumina Reagent Kit v2, 500 reaction kit) at the Indiana University Center for Genomics and Bioinformatics Sequencing Facility.

Sequences were processed using a standard mothur pipeline (v1.40.1)(Kozich et al., 2013; Schloss et al., 2009). We assembled contigs from the paired end reads, quality trimmed using a moving average quality score (minimum quality score 35), aligned sequences to the Silva Database (Quast et al. 2013; SSURef v123), and removed chimeric sequences using the VSEARCH algorithm (Rognes et al., 2016). We created operational taxonomic units (OTUs) by first splitting sequences based on taxonomic class and then binning into OTUs based on 97% sequence similarity. The Silva database was used to assign taxonomy to each OTU.

### *Statistical Analysis*

All statistical analyses were completed in the R statistical environment (RStudio v1.1.383, Rv3.4.0) (R Core Team, 2019). We constructed linear mixed effects models with sampling plot as a random effect, using the *lme4* R package (Bates et al., 2015), to determine the importance of hydrology, season, and distance from the inlet on GHG fluxes and denitrification potential fluxes within the constructed wetland. We then conducted model comparisons using sample size corrected Akaike information criteria (AICc) model comparisons, which adjust for small sample size, to determine which combinations of fixed effects (hydrology and season) had the most explanatory power (Gorsky et al., 2019; Hurvich and Tsai, 1993). Estimated marginal means with Tukey post-hoc adjustment in the R package *emmeans* (Lenth, 2017) was used to determine significance ( $p < 0.05$ ) in gas flux rates between treatment groups and the *multcomp* R package (Hothorn et al., 2020) was used to assign Tukey post-hoc groups. Lastly, we

used the *MuMIn* R package to determine the proportion of variance explained by fixed effects (marginal) and the complete model (conditional) (Barton, 2019; Gorsky et al., 2019). The CH<sub>4</sub>, CO<sub>2</sub>, and N<sub>2</sub>O fluxes were transformed to the log of the cube root and denitrification potential rates were log transformed to meet normality assumptions of the statistical models.

Principal Coordinates of Analysis (PCoA) based on Bray-Curtis dissimilarity was used to visualize patterns of bacterial diversity among treatments and sampling dates. Permutated analysis of variance (PERMANOVA) was run, using the *adonis* function in the *vegan* package (Oksanen, 2015), to test clustering significance. We performed a Dufrene-Legendre indicator species analysis using the *labdsv* R package (Roberts, 2016) to identify specific microbial community members that represented each hydrologic treatment. Next, we examined the relationship between individual GHG fluxes and microbial community Bray-Curtis dissimilarity matrix using distance based partial least square regression in the *dbstats* R package (Boj et al., 2017). Finally, we used Mantel R statistic function in the *vegan* R package (Oksanen, 2015) to examine the relationship between all soil properties (moisture %, pH, organic matter %, ammonium and nitrate concentrations, total C%, total N%, and C:N) and microbial composition.

## **Results**

### *Sediments and water properties*

Over the one year study period in 2017, water depth in flooded plots ranged from 8-28 cm in shallow water areas and 25-53 cm in deep pools. Shallow land plots were not flooded during sampling events. Temperatures varied seasonally with July having the highest average ( $\pm$  SD) temperature ( $26.5 \pm 1.8^\circ\text{C}$ ) and December the lowest ( $4.9 \pm 1.3^\circ\text{C}$ ) (Table 1.1). Sediments in the wetland were acidic ( $4.6 \pm 0.3$  pH) with a range of pH 4.08-5.28. Ammonium and nitrate concentrations were generally lower in sediments ( $0.089 \pm 0.066$  mg  $\text{NH}_4^+\text{-N g}^{-1}$  dry mass and  $0.023 \pm 0.008$  mg  $\text{NO}_3^-\text{-N g}^{-1}$  dry mass) and in the water column ( $2.57 \pm 19.6$  mg  $\text{NH}_4^+ \text{ L}^{-1}$  and  $0.328 \pm 0.803$  mg  $\text{NO}_3^-\text{-N L}^{-1}$ ) throughout the wetland. Sediment C:N ratios along with other sediment parameters (C%, N%, and C:N) and water column phosphate ( $\text{PO}_4^{3-}$ ) concentrations were similar across space (hydrologic zone) and time (season) within the wetland (Table 1.1).

### *Methane flux*

Across the wetland,  $\text{CH}_4$  fluxes differed by hydrology and season (Fig. 1.2A). Average ( $\pm$  SD)  $\text{CH}_4$  fluxes across all seasons were lowest in shallow land plots ( $2.32 \pm 9.33$  mg  $\text{CH}_4\text{-C m}^{-2} \text{ hr}^{-1}$ ) and highest in flooded plots ( $80.80 \pm 118.31$  mg  $\text{CH}_4\text{-C m}^{-2} \text{ hr}^{-1}$ ). Within flooded plots, the highest mean  $\text{CH}_4$  fluxes ( $160.24 \pm 156.28$  mg  $\text{CH}_4\text{-C m}^{-2} \text{ hr}^{-1}$ ) were detected during summer months, and the lowest  $\text{CH}_4$  fluxes were detected in winter and spring months ( $45.02 \pm 88.74$  and  $46.98 \pm 59.40$  mg  $\text{CH}_4\text{-C m}^{-2} \text{ hr}^{-1}$ , respectively). Within shallow land plots, the highest mean  $\text{CH}_4$  fluxes ( $6.38 \pm 16.44$  mg  $\text{CH}_4\text{-C m}^{-2} \text{ hr}^{-1}$ ) were detected during spring months and the lowest  $\text{CH}_4$  fluxes were detected in winter ( $0.09 \pm 0.42$  mg  $\text{CH}_4\text{-C m}^{-2} \text{ hr}^{-1}$ ). The model that included hydrology

and seasonal interaction explained the most variation in CH<sub>4</sub> fluxes based on a  $\Delta\text{AICc}$  score of 0 and an AICc weight of 1 (Table S1.1). In this model the interaction of hydrology and season and random effects accounted for 73% variation in CH<sub>4</sub> fluxes, while the interaction alone explained 63% of that variation (Table S1.1).

### *Carbon dioxide flux*

Carbon dioxide fluxes varied seasonally but were generally highest in flooded plots compared to shallow land plots (Fig. 1.2B). Across all seasons CO<sub>2</sub> fluxes were lowest in shallow land plots ( $3.95 \pm 43.96$  mg CO<sub>2</sub>-C m<sup>-2</sup> hr<sup>-1</sup>) and highest in flooded plots ( $73.52 \pm 100.24$  mg CO<sub>2</sub>-C m<sup>-2</sup> hr<sup>-1</sup>). We measured similar CO<sub>2</sub> flux rates ( $20.82 \pm 46.36$ ,  $14.37 \pm 44.68$ , and  $18.88 \pm 24.23$  mg CO<sub>2</sub>-C m<sup>-2</sup> hr<sup>-1</sup>) during spring, fall, and winter seasons, while CO<sub>2</sub> flux rates ( $63.13 \pm 133.21$  mg CO<sub>2</sub>-C m<sup>-2</sup> hr<sup>-1</sup>) were highest during the summer. The model with season only explained the most variation in CO<sub>2</sub> fluxes based on a  $\Delta\text{AICc}$  score of 0 and AICc weight of 0.93 (Table S1.1). The fixed effect of season explained 26% of the variation and the full model explained 50% of the variation in CO<sub>2</sub> fluxes (Table S1.1).

### *Nitrous oxide flux*

Nitrous oxide fluxes were near zero in all plots across all seasons (Fig. 1.2C). Specifically, N<sub>2</sub>O fluxes were highest in shallow land plots ( $-0.006 \pm 0.117$  mg N<sub>2</sub>O-N m<sup>-2</sup> hr<sup>-1</sup>) and lowest in flooded plots ( $-0.083 \pm 0.243$  mg N<sub>2</sub>O-N m<sup>-2</sup> hr<sup>-1</sup>). Average N<sub>2</sub>O flux

rates across seasons ranged from  $-0.05 \pm 0.20$  to  $-0.02 \pm 0.15$  mg N<sub>2</sub>O-N m<sup>-2</sup> hr<sup>-1</sup>. Unlike CH<sub>4</sub> and CO<sub>2</sub> fluxes, hydrology and season did not influence N<sub>2</sub>O fluxes. In this case, the null model had a  $\Delta$ AICc score of 0 and the greatest AICc weight (0.69) (Table S1.1). However, the models with hydrology or season had similar  $\Delta$ AICc scores (2.98, 3.98) but lower AICc weights (0.15, 0.11) when compared to the null model. Comparison of parameters hydrology and season using estimated marginal means at 95% confidence level suggest season has the greatest impact on N<sub>2</sub>O fluxes (Table S1.2).

#### *Global warming potential*

In terms of GWP, flooded plots have a two-fold increase in magnitude of total warming potential than shallow land plots especially during warmer months (2418.63, 58.46 CO<sub>2</sub> equivalents (mg m<sup>-2</sup> hr<sup>-1</sup>), respectively) (Fig. 1.3). This is primarily due to increases in CH<sub>4</sub> concentrations, which make up 99% of the CO<sub>2</sub> equivalents in both flooded and shallow land plots (Fig. 1.3). Over one year, flooded areas within the wetland have the potential to produce about 7161.27 kg CO<sub>2</sub> equivalents, while shallow land areas produced about 93.20 kg CO<sub>2</sub> equivalents. The N<sub>2</sub>O emissions were not included in this evaluation because rates were near zero for all sampling events.

#### *Denitrification potential*

When nitrate limitation is relieved and anoxic conditions are present, sediments from flooded and shallow land zones have similar denitrification potential (Fig. 1.4). In

flooded and shallow land plots across all seasons, potential denitrification rates were  $24.45 \pm 20.18$  and  $20.29 \pm 15.14$  ng N<sub>2</sub>O-N hr<sup>-1</sup> g<sup>-1</sup> dry mass, respectively. However, denitrification potential varied by season; we measured higher rates in spring and summer ( $34.12 \pm 21.09$  and  $25.16 \pm 13.51$  ng N<sub>2</sub>O N hr<sup>-1</sup> g<sup>-1</sup> dry mass) than in fall and winter ( $10.55 \pm 6.17$  and  $16.45 \pm 13.72$  N<sub>2</sub>O ng N hr<sup>-1</sup> g<sup>-1</sup> dry mass) months. The model with season only explained the most variation in potential denitrification rates based on a  $\Delta$ AICc score of 0 and AICc weight of 0.78 (Table S1.3). The fixed effect of season explained 18% of the variation; however, the null model explained the majority of variation (42%) (Table S1.3). We selected the season only model even though the model with hydrology and season had a similar  $\Delta$ AICc (1.27) and AICc weight of 0.21, but there was little improvement in marginal and conditional R<sup>2</sup> values (Table S1.3).

### *Microbial community analysis*

Hydrology, and to a lesser extent season, influenced microbial community composition. Illumina amplicon sequencing of the 16S rRNA V4 region resulted in 454,709 reads, where each sample (n=22) contained between 13,235 and 33,678 reads before removing singletons and doubletons. Microbial community composition in flooded plots were distinct from shallow land plots (PERMANOVA, R<sup>2</sup>= 0.0886, p=0.007; Fig. 1.5). Indicator species analysis identified 1 Operational Taxonomic Unit (OTU; microbial taxon defined at 97% sequence similarity), in the family Syntrophaceae, that was unique to flooded plots and identified eight OTUs that represented the shallow land plots. The shallow land indicator taxa included OTUs from two unclassified

bacteria, two Betaproteobacteria, one Acidobacteria Gp6, and one *Geobacter* (Table S1.5). Further examination of taxa with >0.6% relative abundance of the total community suggests that flooded zones are dominated by taxa putatively involved in methanogenic degradation of hydrocarbons (e.g., Methanomicrobia, Methylocystis, and Syntrophaceae), while shallow land zones have fewer methanogens in comparison to flooded zones (Fig. 1.6). In addition, shallow land zones are enriched with taxa putatively involved in nitrogen cycle transformations (e.g., Bradyrhizobium, Nitrososphaera, Rhizobiales) (Fig. 1.6).

#### *Analyses of relationship between GHGs, sediment chemistry, and bacterial and archaeal community composition*

Distance-based partial least square regression suggests that bacterial and archaeal community composition explained 82.4%, 78.6%, and 79.1%, of variation in CH<sub>4</sub>, CO<sub>2</sub>, and N<sub>2</sub>O, respectively, by components 1 and 2. Sediment chemistry components 1 and 2 best explained variation in N<sub>2</sub>O production (51.4%) but less so for CH<sub>4</sub> or CO<sub>2</sub> production (21.0%, 16.6%). Mantel correlation analyses revealed a positive relationship between patterns in microbial community composition and soil properties ( $r = 0.52$ ,  $p = 0.003$ ).

## **Discussion**

After examining microbial processes occurring at permanently and periodically inundated locations within a stormwater CW, results revealed that modifications to

wetland design could enhance water quality (via denitrification) and decrease GHG production. Other studies comparing different types of CWs indicate that free water surface (FWS) wetlands, like this study site, are known to produce copious amounts of GHGs compared to vertical or horizontal subsurface flow CWs (Mander et al., 2014; McPhillips and Walter, 2015). While vertical or subsurface CWs may decrease GHG production, this type of installation is more costly than FWS wetlands and may not always be practical. We recognize that this study focuses on a single CW; however, our results demonstrate the need for more comprehensive studies exploring CW design features that can be modified to enhance beneficial microbial ecosystem services (i.e., denitrification) while decreasing ecosystem disservices (i.e., GHG emissions).

At our focal CW, CH<sub>4</sub> was the dominant GHG produced in flooded plots across all seasons. Hydrologic conditions accounted for the most variation in CH<sub>4</sub> fluxes and microbial community composition. Since high NO<sub>3</sub><sup>-</sup> concentrations suppress methanogenesis (Kim et al., 2015), it is likely the combination of anoxic conditions (McPhillips and Walter, 2015), low NO<sub>3</sub><sup>-</sup> concentrations in sediments and water, and availability of organic carbon in flooded plots provided optimal conditions for CH<sub>4</sub> production (Rahman et al., 2019). However, season and microbial community composition were stronger predictors of CO<sub>2</sub> and N<sub>2</sub>O rates within the wetland. In other studies, temperature and substrate availability strongly determined rates of organic decomposition and denitrification (Davidson and Janssens, 2006; Knowles, 1982; Moinet et al., 2018). Seasonal differences in temperature and vegetation status (i.e., organic carbon inputs) within this study influenced CO<sub>2</sub> and N<sub>2</sub>O rates to a greater degree than hydrology.

In order to simultaneously compare the biogenic GHGs within the CW, we quantified GWP associated with flooded and shallow land zones. In terms of GWP, CH<sub>4</sub> from flooded plots was the primary carbon source within the wetland. While both CO<sub>2</sub> and CH<sub>4</sub> production was greatest in flooded zones compared to shallow land zones, CH<sub>4</sub> production greatly exceeded CO<sub>2</sub> production leading to high GWP within the wetland. Compared to surface flow wastewater treatment wetlands receiving municipal or agricultural runoff, CO<sub>2</sub> emissions at our study wetland in flooded plots were similar but approximately 95% lower in shallow land plots (Jahangir et al., 2016; Mander et al., 2014). In contrast, CH<sub>4</sub> emissions at our study wetland had similar CH<sub>4</sub> rates in shallow land plots when compared to wastewater treatment wetlands, but approximately 94% greater emissions in flooded plots compared to wastewater treatment wetlands (Jahangir et al., 2016; Mander et al., 2014). In terms of GWP, flooded plots in our study wetland have a GWP that is 98% greater than in wastewater treatment wetlands. High nitrate concentrations tend to inhibit methanogenesis; therefore, high methane emissions in our study wetland are likely due to low nitrate concentrations in sediments and surface water. Overall, compared to wastewater treatment wetlands, flooded plots within our study wetland represent a considerable source of GWP primarily due to CH<sub>4</sub> emissions.

Further, GHG emissions could be partially explained by microbial community structure. This is due to hydrologic conditions in flooded zones providing optimal habitat for obligate anaerobes that participate in methanogenesis. Methanogenesis is suppressed by even low oxygen concentrations (Fetzer et al., 1993; Liu et al., 2008); and methane emissions were near zero or greatly decreased in shallow land areas,

which can fluctuate between oxic and anoxic conditions compared to flooded areas. Additionally, analysis of microbial community structure suggests that hydrocarbon degradation, a potential microbial ecosystem benefit, may be occurring in flooded plots. Hydrocarbons are becoming recognized as a common contaminant in urban wetlands with the potential to reduce and even harm wildlife taking refuge in these habitats (Clevenot et al., 2018; Mahler et al., 2014). This finding demonstrates the value of examining the microbial community composition when evaluating beneficial wetland ecosystem functions.

In retrospect of this study we identified three CW features for consideration to decrease ecosystem function disservices: (i) surface area of hydrologic zones, (ii) incoming nutrient and pollutant loads, and (iii) the anticipated number of rain days. In this study flooded soils produced the most GHGs, which was due, in part, to low nitrogen levels in sediments and surface waters, therefore altering the amount of surface area dedicated to flooded zones could reduce GHG emissions. Further, high nitrate levels should inhibit methanogenesis making nutrient loads a potential control mechanism. The number of rain days directly influences both hydrology and nutrient loads within this wetland which is why we consider this an important feature. Results from this study and others indicate that areas that fluctuate between oxic and anoxic conditions, which occur in CW shallow land areas in this study, are sites of decreased CH<sub>4</sub> production. This is due to the inhibition of methanogenesis and a greater abundance of methanotrophs which consume methane (Chowdhury and Dick, 2013; Lew and Glińska-Lewczuk, 2018). Additionally, even in CWs with low nitrate availability, shallow land areas could potentially support enhanced denitrification due to coupling of

nitrification, which occurs during oxic periods, and steady organic carbon inputs from vegetation (Mander et al., 2014; Rahman et al., 2019). Flooded zones increase water storage capacity and provide habitat for predator species that control nuisance species; therefore, elimination of flooded zones may not be desirable. However, an increase in shallow land area and a reduction in surface area of flooded zones could decrease GHG emissions without sacrificing benefits of flooded zones.

Secondly, substrate availability can directly impact microbial process rates. Compared to the neighboring Tar River ( $0.52 \text{ mg NO}_3\text{-N L}^{-1}$ ), seasonal  $\text{NO}_3^-$  concentrations within the surface water of the CW were much lower ( $0.007\text{-}0.173 \text{ mg NO}_3\text{-N L}^{-1}$ ) except during winter ( $0.769 \text{ mg NO}_3\text{-N L}^{-1}$ ) (Humphrey et al., 2019). Considering that  $\text{NO}_3^-$  availability limits denitrification, ecosystems that receive runoff from agriculture, livestock, or are adjacent to a high density of septic systems are areas of high denitrification potential and low methane production (Naylor et al., 2018). Recent studies show that iron (II) ( $\text{Fe}^{2+}$ ) additions can increase N removal from vertical and horizontal subsurface CWs due to coupled iron  $\text{NO}_3^-$  reduction (Song et al., 2016; Zhang et al., 2019). Additionally iron (II) amendments could also support anaerobic ammonium oxidation in sediments (Liu and Ni, 2015). In the case of existing wetlands, further investigation into iron (II) amendments as a potential way to increase denitrification is warranted. Additionally, depending on the upstream runoff source, pollutants such as hydrocarbons may be better targets for remediation within intentionally designed CWs.

Lastly, we suggest that the frequency of rain days or inter-event duration is taken into account during SCM planning (Andersen et al., 2017). Our results represent

ambient conditions, at least 48 hours after a storm event, which represent more than half the year for this CW. There were 268 days without precipitation. Within this particular wetland, decreasing the permanently flooded surface area could decrease GHGs while still providing N removal benefits. In areas where rain events are less frequent (i.e., greater inter-event durations) and more intense, SCMs that are not permanently flooded, such as dry infiltration basins or dry detention basins, could provide relief for runoff events with decreased GHG production (McPhillips and Walter, 2015; Morse et al., 2017). Therefore, we suggest frequency of rain events as another factor to consider when planning SCM design.

Context matters when designing CWs in urban watersheds. This study demonstrates the importance of considering microbial controls on biogeochemical processes within SCMs in order to decrease tradeoffs between water quality and GHG production. In the case of this urban stormwater CW, which is located in a parking lot of a highly urbanized area, we suggest that decreasing flooded areas and increasing shallow land area would decrease GHG emissions while still providing nutrient removal benefit. However, our analysis of the microbial community also indicates that potential hydrocarbon decomposition could be supported in flooded zones and warrants a deeper investigation in this potential service. This study also highlights the need for a comprehensive study of CW design features to better understand which design features and when those features provide the most ecosystem benefits. By examining both microbial process rates and the microbial community composition, we can approach SCM design and implementation in a holistic way that accounts for ecosystem services and disservices.

## **Acknowledgements**

We thank B. Hinckley, A. Garcia, and L. Armstrong for assistance with field research and sample processing. We also thank Sound Rivers for installation of the constructed wetland and ECU Grounds personnel and manager J. Gill for site maintenance. This work was supported by East Carolina University and the North Carolina Sea Grant/Water Resources Research Institute Graduate Student Research Fellowship and the National Science Foundation Graduate Research Fellowship to RBB. All code and data used in this study can be found in a public GitHub repository (<https://github.com/PeraltaLab/ConstructedStormwaterWetland>) and the NCBI SRA (BioProject PRJNA613095).

## Figures and Tables



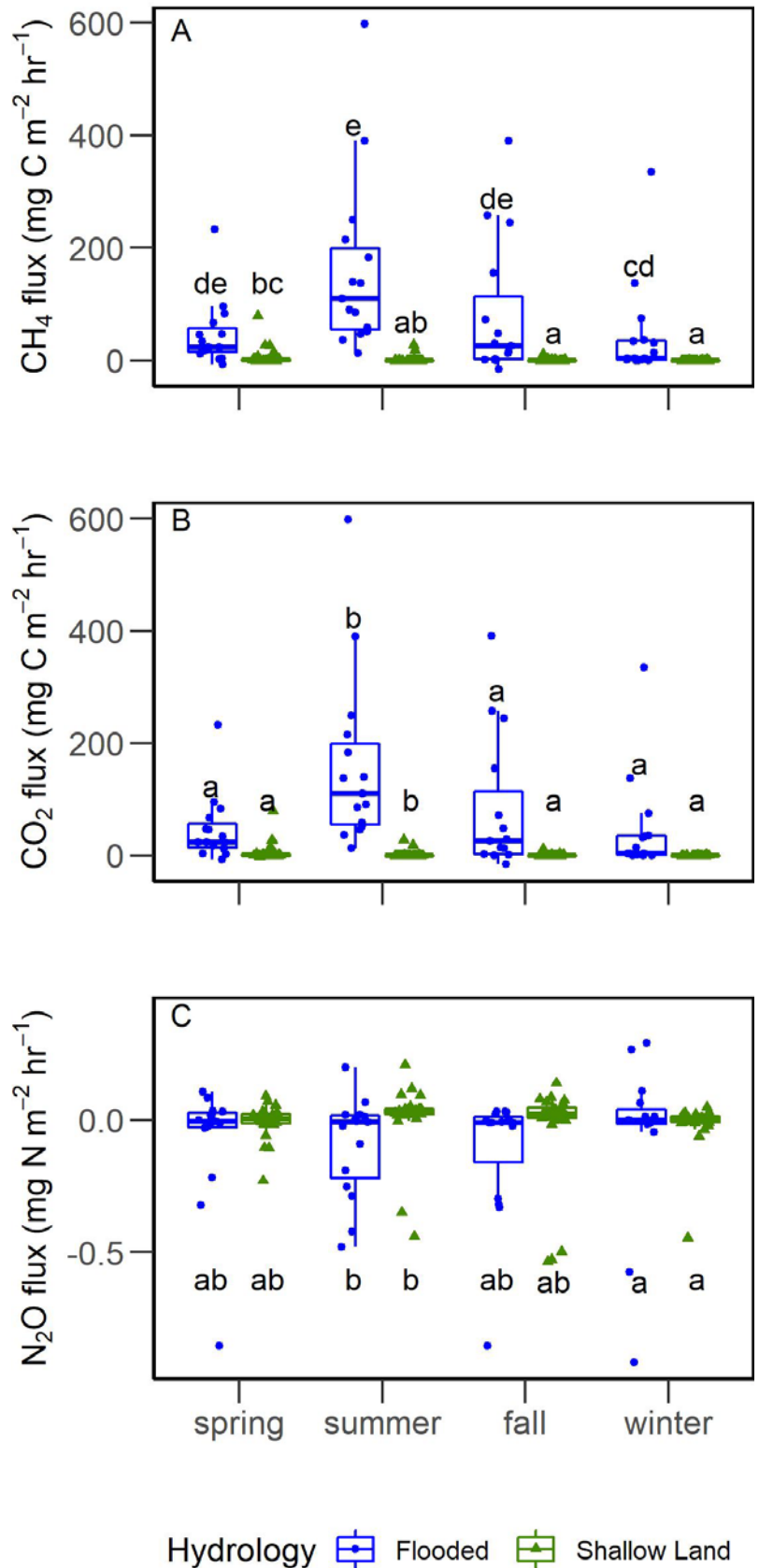
**Figure 1.1.** Left: Picture of wetland. Center: Google Earth image of wetland and parking lot (top left, outlined in red). Right: Google Earth image of wetland representing GHG and sediment sampling locations; white circles indicate shallow land and blue circles flooded sampling plots.

1 **Table 1.1.** Summary of mean (range) of soil and water properties measured at the constructed wetland. Annual wetland  
2 values are averages of all samples for the entire sampling period. Hydrology values are averages of samples collected in  
3 May (spring), July (summer), October (fall), and December (winter) for each hydrology type. Seasonal sediment values  
4 are averages from of all plots based on samples collected in May (spring), July (summer), October (fall), and December  
5 (winter). Seasonal water values are averages of monthly samples from flooded plots where spring = May-June, summer  
6 = July-September, fall = October-November, and winter = December-February. (Abbreviations: DM = dry mass. MDL =  
7 below detection limit).

8

	Whole Wetland	Hydrology Flooded	Shallow land	Season Spring	Summer	Fall	Winter
<b>Soil</b>							
temperature (°C)	18.6 (3.0-30.0)	-	-	19.6 (16.8-23.0)	26.5 (25.0-30.0)	21.3 (20.0-24.0)	4.9 (3.0-7.0)
moisture (%)	33.3 (18.3-51.9)	36.2 (23.2-51.9)	31.5 (18.3-46.2)	32.1 (26.6-42.9)	35.3 (27.0-48.1)	35.6 (26.6-51.9)	29.3 (18.3-44.1)
pH	4.6 (4.1-5.3)	4.7 (4.2-5.3)	4.6 (4.1-5.2)	4.7 (4.4-5.2)	4.6 (4.2-5.1)	4.5 (4.1-5.2)	4.7 (4.2-5.3)
organic matter (%)	6.20 (3.40-10.17)	6.54 (3.41-10.17)	6.01 (3.56-8.42)	6.32 (5.12-8.83)	6.26 (4.13-10.09)	6.68 (3.75-10.17)	5.39 (3.41-8.39)
mg NH <sub>4</sub> <sup>+</sup> -N g <sup>-1</sup> DM	0.089 (0.023-0.457)	0.129 (0.049-0.457)	0.066 (0.023-0.148)	0.085 (0.023-0.148)	0.089 (0.036-0.204)	0.098 (0.028-0.457)	0.082 (0.040-0.201)
mg NO <sub>3</sub> <sup>-</sup> -N g <sup>-1</sup> DM	0.023 (0.012-0.050)	0.027 (0.14-0.050)	0.021 (0.012-0.038)	0.020 (0.016-0.027)	0.025 (0.017-0.038)	0.023 (0.014-0.034)	0.026 (0.012-0.050)
Total C (%)	1.66 (0.27-3.61)	1.78 (0.27-3.61)	1.60 (0.57-2.81)	1.57 (0.62-2.74)	1.78 (0.27-3.61)	1.80 (0.48-2.81)	1.46 (0.33-3.49)
Total N (%)	0.10 (0.02-0.20)	0.11 (0.02-0.20)	0.10 (0.04-0.16)	0.10 (0.04-0.17)	0.11 (0.02-0.19)	0.11 (0.03-0.16)	0.09 (0.03-0.20)
C:N (wt: wt)	15.78 (11.00-19.00)	15.88 (11.00-19.00)	15.73 (13.88-18.44)	16.0 (15.0-18.4)	16.2 (13.5-19.0)	15.9 (13.9-17.6)	14.9 (11.0-17.5)
<b>Water</b>							
mg NH <sub>4</sub> <sup>+</sup> -N L <sup>-1</sup>	-	-	-	0.101 (MDL-0.474)	.206 (0.019-0.923)	0.263 (0.068-1.065)	9.972 (MDL-197.441)
mg NO <sub>3</sub> <sup>-</sup> -N L <sup>-1</sup>	-	-	-	0.173 (MDL-1.118)	0.007 (MDL-0.020)	0.169 (MDL-0.413)	0.769 (MDL-4.055)
Total Dissolved mg PO <sub>4</sub> <sup>3-</sup> L <sup>-1</sup>	-	-	-	0.035 (MDL-0.087)	0.088 (0.27-0.286)	0.072 (0.025-0.176)	0.075 (MDL-0.245)

**Figure 1.2.** Boxplots of seasonal methane (A), carbon dioxide (B), and nitrous oxide (C) fluxes for flooded (blue circles) and shallow land (green triangles) plots. Spring = Mar-May, Summer = Jun-Aug, Fall = Sep-Nov, Winter = Dec-Feb. Letters indicate significantly different groups based on estimated marginal means with Tukey post-hoc assessment at  $p < 0.05$  and based on 95% confidence levels (Table S1.2).



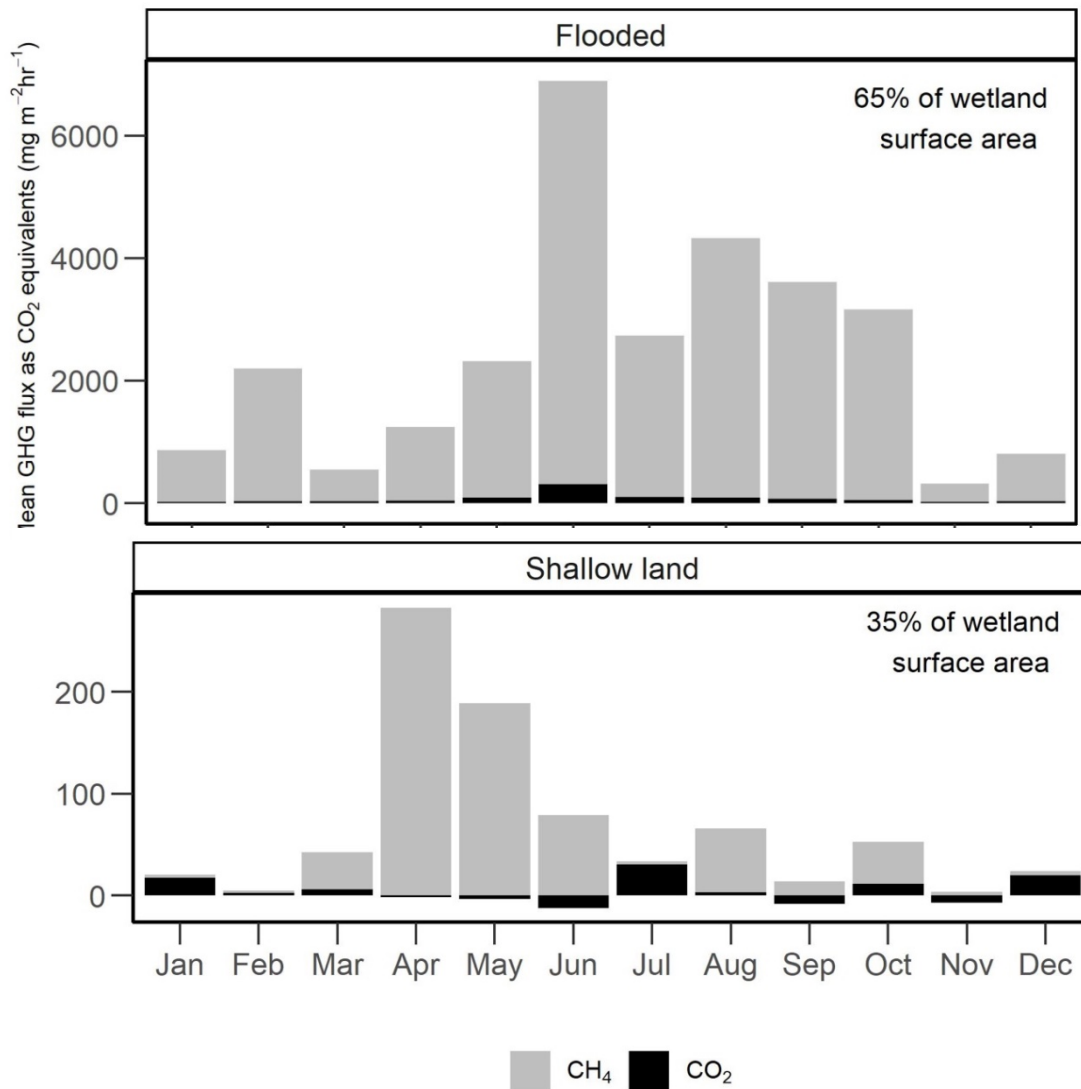


**Figure 1.3.** Global warming potentials of methane and carbon dioxide evaluated as carbon dioxide equivalents measure over a year at a constructed wetland. Proportion of grey for each bar represents mg CH<sub>4</sub>-C m<sup>-2</sup> hr<sup>-1</sup> converted to CO<sub>2</sub> equivalents and proportion of black for each bar represents mg CO<sub>2</sub>-C m<sup>-2</sup> hr<sup>-1</sup>. Average mg CH<sub>4</sub>-C m<sup>-2</sup> hr<sup>-1</sup> was multiplied by 28, which is the estimated increased radiative force of methane when compared to carbon dioxide.

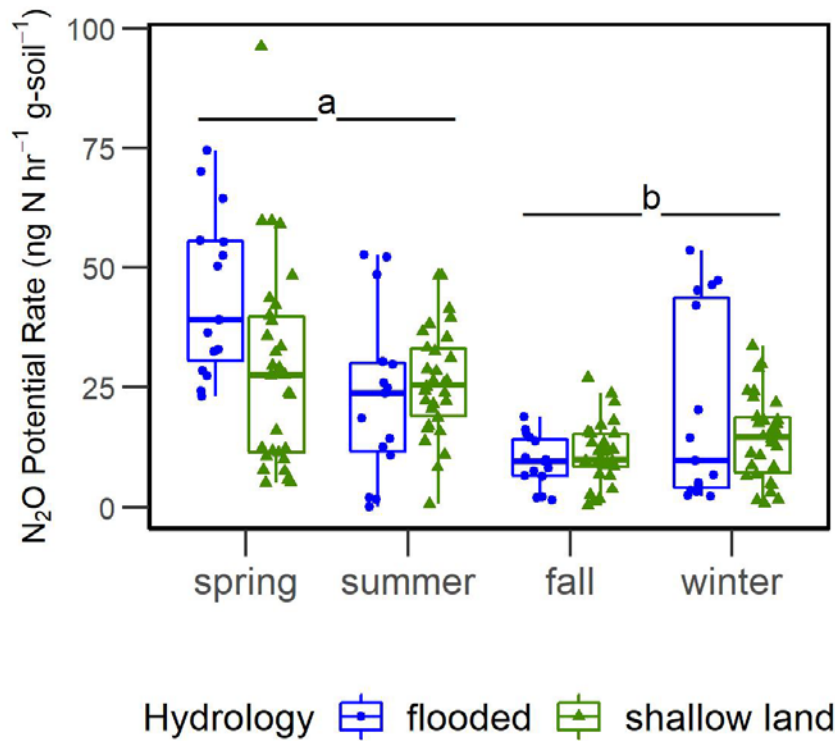


**Figure 1.4.** Boxplots of potential denitrification rates according to hydrology and season based on denitrification enzyme assay using the acetylene block method. Spring = Mar-May, Summer = Jun-Aug, Fall = Sep-Nov, Winter = Dec-Feb. Different letters indicate significantly different groups by Tukey adjusted estimated marginal means  $p < 0.05$  and based on 95% confidence levels. Blue circles indicate flooded plots and green triangles shallow land.

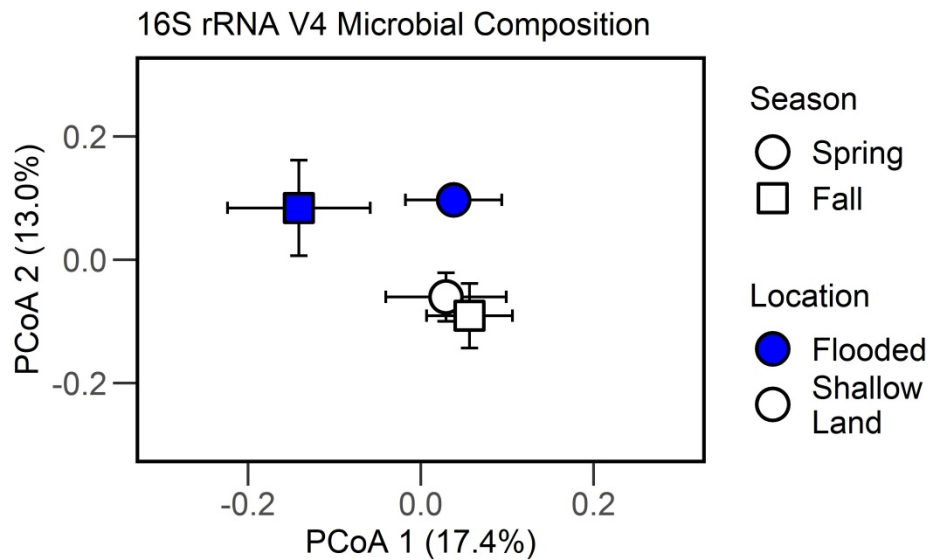


**Figure 1.5.** Ordination plot based on Principal Coordinates Analysis depicting sediment bacterial and archaeal community composition. Each point represents the centroid and range across season and sampling location. Symbols represent sampling period (circle = spring, square = fall). Spring samples were collected in May and fall samples were collected in October. Colors represent sampling plots (blue = flooded, green = shallow land).

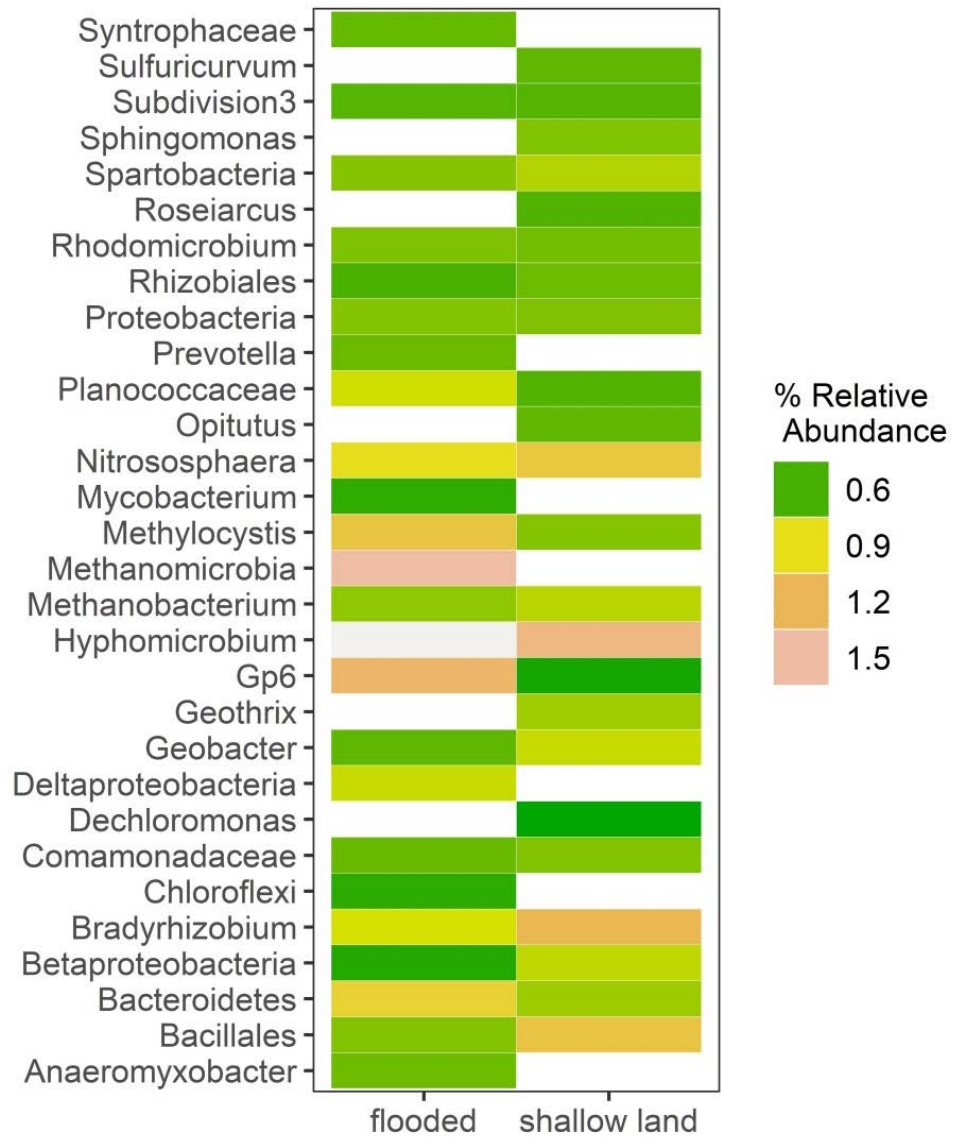


**Figure 1.6.** Heat map of bacterial and archaeal taxa found at >0.6% relative abundance. Color gradient (cool to warm, green to red) represents microbial relative abundance ~0.6 to 1.5%.

## Supplemental Figures and Tables



**Figure S1.** Images of GHG chambers. Left: Chamber top and bottom. Middle: Shallow land chamber installed on sampling plot. Right: Flooded plot chamber on Styrofoam float. Board-walks were set up prior to sampling to allow access into flooded plots.

**Table S1.1.** Mixed-effects models for GHG fluxes with sample plot as a random effect.

H = hydrology, S = season, D = distance from inlet.

Model	k	AICc	$\Delta$ AICc	AICc Wt	R <sup>2</sup> Marg	R <sup>2</sup> Cond
<b>CH<sub>4</sub></b>						
H*S	10	313.70	0	1	0.63	0.73
Hydrology	4	338.78	25.07	0	0.55	0.65
H*D	9	342.44	28.73	0	0.60	0.64
Season	6	343.41	29.70	0	0.05	0.69
H*D*S	30	344.69	30.69	0	0.70	0.75
Null	3	361.39	47.68	0	-	0.64
Distance	6	366.64	52.94	0	0.05	0.64
<b>CO<sub>2</sub></b>						
Season	6	45.54	0	0.93	0.26	0.50
H*S	10	50.71	5.16	0.07	0.46	0.50

Hydrology	4	68.40	22.86	0	0.22	0.23
Null	3	78.06	32.51	0	0	0.24
H*D	9	86.67	41.12	0	0.26	0.26
Distance	6	87.37	41.82	0	0.07	0.28
H*D*S	29	109.20	63.65	0	0.56	0.56
<b>N2O</b>						
Null	3	264.19	0	0.69	0	0.17
Hydrology	4	267.17	2.98	0.15	0.02	0.19
Season	6	267.88	3.69	0.11	0.05	0.23
Distance	6	270.11	5.93	0.04	0.07	0.20
H*D	9	271.91	7.72	0.01	0.08	0.26
H*S	10	278.96	14.77	0	0.17	0.21
H*D*S	30	316.91	52.72	0	0.27	0.32

**Table S1.2.** GHG flux estimated marginal means at 95% confidence levels (CL) with Tukey ( $\alpha=0.05$ ) adjusted post-hoc analysis of the selected model parameter based on AICc analysis. Log cuberoot transformed values. SL = shallow land, F = flooded, W = winter, FA = fall, SM = summer, SP = spring

Parameter	emmean	SE	df	lower.CL	upper.CL	group
<b>CH4:</b>						
interaction						
SL*W	-0.828	0.162	44.3	-1.154	0.501	a
SL*FA	-0.725	0.159	41.4	-1.046	-0.404	a
SL*SM	-0.634	0.159	41.2	-0.955	-0.314	ab
SL*SP	-0.191	0.160	42.8	-0.515	0.132	bc
F*W	0.574	0.221	39	0.127	1.021	cd
F*FA	0.949	0.221	39.0	0.503	1.396	de
F*SP	1.085	0.221	39.0	0.638	1.532	de
F*SM	1.554	0.221	39.0	1.107	2.001	e
<b>CO2:</b>						
Season						
Winter	0.602	0.0468	57.1	0.508	0.696	a
Spring	0.743	0.0473	58.4	0.648	0.837	a
Fall	0.744	0.0505	63.8	0.643	0.845	a
Summer	1.059	0.0481	58.3	0.963	1.156	b
<b>N2O:</b>						
Hydrology						

F	-1.29	0.089	13.4	-1.48	-1.094	a
SL	-1.13	0.123	12.2	-1.40	-0.862	a
Season						
Winter	-1.42	0.101	46.1	-1.62	-1.218	a
Spring	-1.28	0.100	46.1	-1.48	-1.078	ab
Fall	-1.18	0.098	42.6	-1.38	-0.986	ab
Summer	-1.06	0.099	43.7	-1.26	-0.861	b

**Table S1.3.** Mixed-effects models for DEA N<sub>2</sub>O flux potentials with sample plot as a random effect. H = hydrology, S = season, D = distance from inlet.

Model	k	AICc	ΔAICc	AICc Wt	R <sup>2</sup> Marg	R <sup>2</sup> Cond
H*S	10	478.74	0	0.65	0.21	.047
Season	6	480.01	1.27	0.35	0.18	0.42
H*D*S	18	513.69	34.95	0	0.38	0.55
Null	3	516.17	37.42	0	-	0.23
Distance	6	518.36	39.62	0	0.08	0.27
Hydrology	4	518.68	39.94	0	0.00	0.25
H*D	6	529.25	50.50	0	0.10	0.26

**Table S1.4.** DEA N<sub>2</sub>O flux potentials estimated marginal means at 95% confidence levels (CL) with Tukey (alpha=0.05) adjusted post-hoc analysis of the selected model parameter based on AICc analysis. Log cuberoot transformed values. SL = shallow land, F = flooded, W = winter, FA = fall, SM = summer, SP = spring

Parameter	emmean	SE	df	lower.CL	upper.CL	group
Interaction						
F*FA	2.03	0.322	26.7	1.37	2.69	ab
SL*FA	2.16	0.229	27.4	1.69	2.63	a
SL*W	2.37	0.227	26.7	1.91	2.84	a
F*W	2.43	0.322	26.7	1.77	3.09	ab
F*SM	2.52	0.322	26.7	1.86	3.18	ab
SL*SP	3.08	0.227	26.7	2.61	3.55	bc
SL*SM	3.10	0.227	26.7	2.63	3.57	bc

PI*SP	3.73	0.322	26.7	3.07	4.39	c
Season						
Fall	2.12	0.184	31.7	1.74	2.49	a
Winter	2.39	0.183	31.1	2.02	2.76	a
Summer	2.91	0.183	31.1	2.53	3.28	b
Spring	3.29	0.183	31.1	2.92	3.67	b

**Table S1.5.** Summary of bacterial taxa (OTUs) characteristic to flooded (F) and shallow land (SL) plots based on indicator species analysis. These are the top OTUs that are significantly associated with each hydrology.

OTU	Cluster	IndVal	Prob	Phylum	Order	Class	Family	Genus
Otu00037	F	0.730	0.002	Proteobacteria	Deltaproteobacteria	Syntrophobacterales	Syntrophaceae	unclassified
Otu00007	SL	0.632	0.002	Verrucomicrobia	Spartobacteria	unclassified	unclassified	unclassified
Otu00010	SL	0.604	0.006	Bacteria	unclassified	unclassified	unclassified	unclassified
Otu00013	SL	0.630	0.007	Acidobacteria	Acidobacteria_Gp6	Gp6	unclassified	unclassified
Otu00014	SL	0.576	0.02	Proteobacteria	Betaproteobacteria	unclassified	unclassified	unclassified
Otu00025	SL	0.680	0.006	Proteobacteria	Betaproteobacteria	unclassified	unclassified	unclassified
Otu00031	SL	0.597	0.033	Bacteria	unclassified	unclassified	unclassified	unclassified
Otu00032	SL	0.596	0.019	Proteobacteria	Deltaproteobacteria	Desulfuromonadales	Geobacteraceae	Geobacter

## References

- Altshuler, I., Hamel, J., Turney, S., Magnuson, E., Lévesque, R., Greer, C.W., Whyte, L.G., 2019. Species interactions and distinct microbial communities in high Arctic permafrost affected cryosols are associated with the CH<sub>4</sub> and CO<sub>2</sub> gas fluxes. *Environ. Microbiol.* 21, 3711–3727. <https://doi.org/10.1111/1462-2920.14715>
- Andersen, J.S., Lerer, S.M., Backhaus, A., Jensen, M.B., Danielsen Sørup, H.J., 2017. Characteristic rain events: A methodology for improving the amenity value of stormwater control measures. *Sustain.* 9. <https://doi.org/10.3390/su9101793>
- Apprill, A., McNally, S., Parsons, R., Weber, L., 2015. Minor revision to V4 region SSU rRNA 806R gene primer greatly increases detection of SAR11 bacterioplankton. *Aquat. Microb. Ecol.* 75, 129–137. <https://doi.org/10.3354/ame01753>
- Barton, K., 2019. Package “MuMIn.”
- Bates, D., Machler, M., Bolker, B., Walker, S., 2015. Fitting Linear Mixed-Effects Models Using lme4. *J. Stat. Softw.* 67, 1–48. <https://doi.org/10.18637/jss.v067.i01>
- Bell, C.D., Tague, C.L., McMillan, S.K., 2019. Modeling Runoff and Nitrogen Loads From a Watershed at Different Levels of Impervious Surface Coverage and Connectivity to Storm Water Control Measures. *Water Resour. Res.* 55, 2690–2707. <https://doi.org/10.1029/2018WR023006>
- Boj, E., Caballe, A., Delicado, P., Fortiana, J., 2017. Package ‘dbstats.’
- Brindha, R.K., Vasudevan, N., 2018. Methane oxidation capacity of methanotrophs isolated from different soil ecosystems. *Int. J. Environ. Sci. Technol.* 15, 1931–1940. <https://doi.org/10.1007/s13762-017-1546-1>
- Caporaso, J.G., Lauber, C.L., Walters, W.A., Berg-lyons, D., Lozupone, C.A., Turnbaugh, P.J., Fierer, N., Knight, R., 2010. <Global patterns of 16S rRNA diversity at a depth of millions of sequences per sample.pdf>. *Proc. Natl. Acad. Sci. U. S. A.* 108, 4516–4522. <https://doi.org/10.1073/pnas.1000080107/-/DCSupplemental.www.pnas.org/cgi/doi/10.1073/pnas.1000080107>
- Chowdhury, T.R., Dick, R.P., 2013. Ecology of aerobic methanotrophs in controlling methane fluxes from wetlands. *Appl. Soil Ecol.* 65, 8–22. <https://doi.org/10.1016/j.apsoil.2012.12.014>
- Clevenot, L., Carré, C., Pech, P., 2018. A Review of the factors that determine whether stormwater ponds are ecological traps and/or high-quality breeding sites for amphibians. *Front. Ecol. Evol.* 6, 1–12. <https://doi.org/10.3389/fevo.2018.00040>
- Conrad, R., 2007. Microbial Ecology of Methanogens and Methanotrophs. *Adv. Agron.* 96, 1–63. [https://doi.org/10.1016/S0065-2113\(07\)96005-8](https://doi.org/10.1016/S0065-2113(07)96005-8)

- Davidson, E.A., Janssens, I.A., 2006. Temperature sensitivity of soil carbon decomposition and feedbacks to climate change. *Nature* 440, 165–173. <https://doi.org/10.1038/nature04514>
- Demuzere, M., Orru, K., Heidrich, O., Olazabal, E., Geneletti, D., Orru, H., Bhawe, A.G., Mittal, N., Feliu, E., Faehnle, M., 2014. Mitigating and adapting to climate change: Multi-functional and multi-scale assessment of green urban infrastructure. *J. Environ. Manage.* 146, 107–115. <https://doi.org/10.1016/j.jenvman.2014.07.025>
- Fetzer, S., Bak, F., Conrad, R., 1993. Sensitivity of methanogenic bacteria from paddy soil to oxygen and desiccation. *FEMS Microbiol. Ecol.* 12, 107–115. <https://doi.org/10.1111/j.1574-6941.1993.tb00022.x>
- Fetzer, S., Conrad, R., 1993. Effect of redox potential on methanogenesis by *Methanosarcina barkeri*. *Arch. Microbiol.* 160, 108–113. <https://doi.org/10.1007/BF00288711>
- Gorsky, A.L., Racanelli, G.A., Belvin, A.C., Chambers, R.M., 2019. Greenhouse gas flux from stormwater ponds in southeastern Virginia (USA). *Anthropocene* 28. <https://doi.org/10.1016/j.ancene.2019.100218>
- Heiri, O., Lotter, A., Lemcke, G., 2001. Loss on ignition as a method for estimating organic and carbonate content in sediments. *J. Paleolimnol.* 25, 101–110. <https://doi.org/10.1017/CBO9781107415324.004>
- Hoogsteen, M.J.J., Lantinga, E.A., Bakker, E.J., Groot, J.C.J., Tittonell, P.A., 2015. Estimating soil organic carbon through loss on ignition: Effects of ignition conditions and structural water loss. *Eur. J. Soil Sci.* 66, 320–328. <https://doi.org/10.1111/ejss.12224>
- Hothorn, T., Bretz, F., Westfall, P., Heiberger, R.M., Schuetzenmeister, A., Scheibe, S., 2020. Package 'multcomp'.
- Humphrey, C., Iverson, G., Skibieli, C., Sanderford, C., Blackmon, J., 2019. Geochemistry of Flood Waters from the Tar River, North Carolina Associated with Hurricane Matthew. *Resources* 8, 48. <https://doi.org/10.3390/resources8010048>
- Hurvich, C., Tsai, C., 1993. A CORRECTED AKAIKE INFORMATION CRITERION FOR VECTOR AUTOREGRESSIVE MODEL SELECTION. *J. Time Ser. Anal.* 14, 271–279.
- IPCC, 2014. Climate Change 2014: Synthesis Report. Contribution of Working Groups I, II and III to the Fifth Assessment Report of the Intergovernmental Panel on Climate Change, Ipcc.
- IPCC - Intergovernmental Panel on Climate Change, 2014. Climate Change 2014 Synthesis Report (Unedited Version).
- Jahangir, M.M.R., Richards, K.G., Healy, M.G., Gill, L., Müller, C., Johnston, P., Fenton, O., 2016. Carbon and nitrogen dynamics and greenhouse gas emissions in

- constructed wetlands treating wastewater: A review. *Hydrol. Earth Syst. Sci.* 20, 109–123. <https://doi.org/10.5194/hess-20-109-2016>
- Kim, S.Y., Veraart, A.J., Meima-Franke, M., Bodelier, P.L.E., 2015. Combined effects of carbon, nitrogen and phosphorus on CH<sub>4</sub> production and denitrification in wetland sediments. *Geoderma* 259–260, 354–361. <https://doi.org/10.1016/j.geoderma.2015.03.015>
- Knowles, R., 1982. Denitrification. *Microbiol. Rev.* 46, 43–70.
- Koch, B.J., Febria, C.M., Gevrey, M., Wainger, L.A., Palmer, M.A., 2014. Nitrogen Removal by Stormwater Management Structures: A Data Synthesis. *J. Am. Water Resour. Assoc.* 50, 1594–1607. <https://doi.org/10.1111/jawr.12223>
- Kozich, J.J., Westcott, S.L., Baxter, N.T., Highlander, S.K., Schloss, P.D., 2013. Development of a dual-index sequencing strategy and curation pipeline for analyzing amplicon sequence data on the miseq illumina sequencing platform. *Appl. Environ. Microbiol.* 79, 5112–5120. <https://doi.org/10.1128/AEM.01043-13>
- Le Mer, J., Roger, P., 2001. Production, oxidation, emission and consumption of methane by soils: A review. *Eur. J. Soil Biol.* 37, 25–50. [https://doi.org/10.1016/S1164-5563\(01\)01067-6](https://doi.org/10.1016/S1164-5563(01)01067-6)
- Lee, C.G., Fletcher, T.D., Sun, G., 2009. Nitrogen removal in constructed wetland systems. *Eng. Life Sci.* 9, 11–22. <https://doi.org/10.1002/elsc.200800049>
- Lenth, R., 2017. Package 'lsmeans'. <https://doi.org/10.1080/00031305.1980.10483031>>.NOTE
- Lew, S., Glińska-Lewczuk, K., 2018. Environmental controls on the abundance of methanotrophs and methanogens in peat bog lakes. *Sci. Total Environ.* 645, 1201–1211. <https://doi.org/10.1016/j.scitotenv.2018.07.141>
- Line, D.E., White, N.M., 2007. Effects of Development on Runoff and Pollutant Export. *Water Environ. Res.* 79, 185–190. <https://doi.org/10.2175/106143006x111736>
- Liu, C. Te, Miyaki, T., Aono, T., Oyaizu, H., 2008. Evaluation of methanogenic strains and their ability to endure aeration and water stress. *Curr. Microbiol.* 56, 214–218. <https://doi.org/10.1007/s00284-007-9059-7>
- Liu, Y., Ni, B.J., 2015. Appropriate Fe (II) addition significantly enhances anaerobic ammonium oxidation (anammox) activity through improving the bacterial growth rate. *Sci. Rep.* 5, 1–7. <https://doi.org/10.1038/srep08204>
- Mahler, B.J., Van Metre, P.C., Foreman, W.T., 2014. Concentrations of polycyclic aromatic hydrocarbons (PAHs) and azaarenes in runoff from coal-tar- and asphalt-sealcoated pavement. *Environ. Pollut.* 188, 81–87. <https://doi.org/10.1016/j.envpol.2014.01.008>

- Mander, Ü., Dotro, G., Ebie, Y., Towprayoon, S., Chiemchaisri, C., Nogueira, S.F., Jamsranjav, B., Kasak, K., Truu, J., Tournebize, J., Mitsch, W.J., 2014. Greenhouse gas emission in constructed wetlands for wastewater treatment: A review. *Ecol. Eng.* 66, 19–35. <https://doi.org/10.1016/j.ecoleng.2013.12.006>
- Marton, J.M., Creed, I.F., Lewis, D.B., Lane, C.R., Basu, N.B., Cohen, M.J., Craft, C.B., 2015. Geographically isolated wetlands are important biogeochemical reactors on the landscape. *Bioscience* 65, 408–418. <https://doi.org/10.1093/biosci/biv009>
- McPhillips, L., Walter, M.T., 2015. Hydrologic conditions drive denitrification and greenhouse gas emissions in stormwater detention basins. *Ecol. Eng.* 85, 67–75. <https://doi.org/10.1016/j.ecoleng.2015.10.018>
- Mitsch, W.J., Bernal, B., Nahlik, A.M., Mander, Ü., Zhang, L., Anderson, C.J., Jørgensen, S.E., Brix, H., 2013. Wetlands, carbon, and climate change. *Landsc. Ecol.* 28, 583–597. <https://doi.org/10.1007/s10980-012-9758-8>
- Moinet, G.Y.K., Hunt, J.E., Kirschbaum, M.U.F., Morcom, C.P., Midwood, A.J., Millard, P., 2018. The temperature sensitivity of soil organic matter decomposition is constrained by microbial access to substrates. *Soil Biol. Biochem.* 116, 333–339. <https://doi.org/10.1016/j.soilbio.2017.10.031>
- Morse, N.R., McPhillips, L.E., Shapleigh, J.P., Walter, M.T., 2017. The Role of Denitrification in Stormwater Detention Basin Treatment of Nitrogen. *Environ. Sci. Technol.* 51, 7928–7935. <https://doi.org/10.1021/acs.est.7b01813>
- Naylor, E., Humphrey, C., Kelley, T., Easter, L., Iverson, G., 2018. Evaluation of nitrate concentrations and potential sources of nitrate in private water supply wells in North Carolina. *J. Environ. Health* 80, 16–23.
- NCDEQ, 2019. Stormwater Design Manual: C-4 Stormwater Wetland [WWW Document]. North Carolina Dep. Environ. Qual. URL <https://deq.nc.gov/sw-bmp-manual>
- NCDEQ, 2018. Stormwater Control Measure Credit Document [WWW Document]. North Carolina Dep. Environ. Qual. URL <https://deq.nc.gov/sw-bmp-manual>
- O’Driscoll, M., Clinton, S., Jefferson, A., Manda, A., McMillan, S., 2010. Urbanization effects on watershed hydrology and in-stream processes in the southern United States. *Water (Switzerland)* 2, 605–648. <https://doi.org/10.3390/w2030605>
- Oksanen, J., 2015. Vegan : ecological diversity 1, 1–12. <https://doi.org/10.1029/2006JF000545>
- Paerl, H.W., Hall, N.S., Peierls, B.L., Rossignol, K.L., 2014. Evolving Paradigms and Challenges in Estuarine and Coastal Eutrophication Dynamics in a Culturally and Climatically Stressed World. *Estuaries and Coasts* 37, 243–258. <https://doi.org/10.1007/s12237-014-9773-x>

- Parada, A.E., Needham, D.M., Fuhrman, J.A., 2016. Every base matters: Assessing small subunit rRNA primers for marine microbiomes with mock communities, time series and global field samples. *Environ. Microbiol.* 18, 1403–1414. <https://doi.org/10.1111/1462-2920.13023>
- Payne, E.G.I., Fletcher, T.D., Cook, P.L.M., Deletic, A., Hatt, B.E., 2014. Processes and drivers of nitrogen removal in stormwater biofiltration. *Crit. Rev. Environ. Sci. Technol.* 44, 796–846. <https://doi.org/10.1080/10643389.2012.741310>
- Peralta, A.L., Ludmer, S., Kent, A.D., 2013. Hydrologic history influences microbial community composition and nitrogen cycling under experimental drying/wetting treatments. *Soil Biol. Biochem.* 66, 29–37. <https://doi.org/10.1016/j.soilbio.2013.06.019>
- Peralta, A.L., Ludmer, S., Matthews, J.W., Kent, A.D., 2014. Bacterial community response to changes in soil redox potential along a moisture gradient in restored wetlands. *Ecol. Eng.* 73, 246–253. <https://doi.org/10.1016/j.ecoleng.2014.09.047>
- R Core Team, 2019. R: A language and environment for statistical computing. R Found. Stat. Comput. Vienna, Austria.
- Rabalais, N.N., Turner, R.E., Díaz, R.J., Justić, D., 2009. Global change and eutrophication of coastal waters. *ICES J. Mar. Sci.* 66, 1528–1537. <https://doi.org/10.1093/icesjms/fsp047>
- Rahman, M.M., Roberts, K.L., Warry, F., Grace, M.R., Cook, P.L.M., 2019. Factors controlling dissimilatory nitrate reduction processes in constructed stormwater urban wetlands. *Biogeochemistry* 142, 375–393. <https://doi.org/10.1007/s10533-019-00541-0>
- Reisinger, A.J., Groffman, P.M., Rosi-Marshall, E.J., 2016. Nitrogen-cycling process rates across urban ecosystems. *FEMS Microbiol. Ecol.* 92, fiw198. <https://doi.org/10.1093/femsec/fiw198>
- Rey-Sanchez, C., Bohrer, G., Slater, J., Li, Y.F., Grau-Andrés, R., Hao, Y., Rich, V.I., Davies, G.M., 2019. The ratio of methanogens to methanotrophs and water-level dynamics drive methane transfer velocity in a temperate kettle-hole peat bog. *Biogeosciences* 16, 3207–3231. <https://doi.org/10.5194/bg-16-3207-2019>
- Roberts, D., 2016. Package ‘labdsv.’
- Rognes, T., Flouri, T., Nichols, B., Quince, C., Mahé, F., 2016. VSEARCH: a versatile open source tool for metagenomics. *PeerJ* 4, e2584. <https://doi.org/10.7717/peerj.2584>
- Schaller, J.L., Royer, T. V., David, M.B., Tank, J.L., 2004. Denitrification associated with plants and sediments in an agricultural stream. *J. North Am. Benthol. Soc.* 23, 667–676. [https://doi.org/10.1899/0887-3593\(2004\)023<0667:DAWPAS>2.0.CO;2](https://doi.org/10.1899/0887-3593(2004)023<0667:DAWPAS>2.0.CO;2)

- Schloss, P.D., Westcott, S.L., Ryabin, T., Hall, J.R., Hartmann, M., Hollister, E.B., Lesniewski, R.A., Oakley, B.B., Parks, D.H., Robinson, C.J., Sahl, J.W., Stres, B., Thallinger, G.G., Van Horn, D.J., Weber, C.F., 2009. Introducing mothur: Open-source, platform-independent, community-supported software for describing and comparing microbial communities. *Appl. Environ. Microbiol.* 75, 7537–7541. <https://doi.org/10.1128/AEM.01541-09>
- Smith, M.S., Tiedje, J.M., 1979. Phases of denitrification following oxygen depletion in soil. *Soil Biol. Biochem.* 11, 261–267. [https://doi.org/10.1016/0038-0717\(79\)90071-3](https://doi.org/10.1016/0038-0717(79)90071-3)
- Song, X., Wang, S., Wang, Y., Zhao, Z., Yan, D., 2016. Addition of Fe<sup>2+</sup> increase nitrate removal in vertical subsurface flow constructed wetlands. *Ecol. Eng.* 91, 487–494. <https://doi.org/10.1016/j.ecoleng.2016.03.013>
- Tiedje, J.M., 1988. Ecology of denitrification and dissimilatory nitrate reduction to ammonium. *Environ. Microbiol. Anaerobes* 179–244.
- Tiedje, J.M., Simkins, S., Groffman, P.M., 1989. Perspectives on measurement of denitrification in the field including recommended protocols for acetylene based methods. *Plant Soil* 115, 261–284. <https://doi.org/10.1007/BF02202594>
- Wall, L.G., Tank, J.L., Royer, T. V., Bernot, M.J., 2005. Spatial and temporal variability in sediment denitrification within an agriculturally influenced reservoir. *Biogeochemistry* 76, 85–111. <https://doi.org/10.1007/s10533-005-2199-6>
- Wen, X., Unger, V., Jurasinski, G., Koebsch, F., Horn, F., Rehder, G., Sachs, T., Zak, D., Lischeid, G., Knorr, K.H., Böttcher, M.E., Winkel, M., Bodelier, P.L.E., Liebner, S., 2018. Predominance of methanogens over methanotrophs in rewetted fens characterized by high methane emissions. *Biogeosciences* 15, 6519–6536. <https://doi.org/10.5194/bg-15-6519-2018>
- Zhang, Y., Liu, X., Fu, C., Li, X., Yan, B., Shi, T., 2019. Effect of Fe<sup>2+</sup> addition on chemical oxygen demand and nitrogen removal in horizontal subsurface flow constructed wetlands. *Chemosphere* 220, 259–265. <https://doi.org/10.1016/j.chemosphere.2018.12.144>

## CHAPTER 2: PLANT-MEDIATED REDUCTION OF GREENHOUSE GASES UNDER DYNAMIC HYDROLOGY

### Abstract

While wetlands represent a small fraction (~7%) of the world's land surface, it is estimated that one third of wetlands have been lost due to human activities. Wetland habitat loss decreases ecosystem functions such as improving water quality and mitigating climate change. These microbially mediated functions are dependent on particular soil redox conditions, which are altered by soil moisture and the presence of plants. Differences in microbial physiology allow certain taxa (aerobes and facultative anaerobes) to adapt to fluctuating (dry/wet) hydrologic conditions, while other taxa (obligate anaerobes) are better adapted to continually saturated conditions. Therefore, the duration of hydrologic periods can affect soil microbial community structure and function. Further, plant-derived carbon, nutrients, and air are released by diffusion belowground which also impacts microbial activity in soils. In this study, we hypothesized that redox status due to continuous flooding would support greater abundance of microbial taxa involved in methanogenesis (obligate anaerobes), but plant-mediated oxygen transport would decrease methane emissions. Using a mesocosm design, we manipulated duration of hydrologic condition (i.e., stable dry, stable flooding, and alternating wet/dry) and presence of plants to induce soil redox changes in wetland soils. We measured soil redox status, used targeted amplicon sequencing to characterize the bacterial and archaeal communities, and measured greenhouse gas production to assess microbial function. Hydrology and to a lesser degree plant presence influenced soil redox conditions. Hydrologic history strongly

influenced microbial community composition, but plant presence and hydrologic treatment altered microbial function to a great degree. As predicted, plant presence decreased greenhouse gas production in the wetland mesocosms. While previous studies do not often include plants when assessing greenhouse gas emissions, this study highlights that plant-mediated decreases in greenhouse gas emissions are significant. If plant-mediated effects are not considered when estimating the carbon balance of ecosystems, then wetland carbon storage could be underestimated.

## Introduction

Wetlands represent only 5-8% of terrestrial land surface (Mitsch et al., 2013); however, it is estimated that we have lost at least 33% of wetlands as of 2009 (Davidson et al., 2018). Loss of important functions is a consequence of land use conversion of wetlands to urban and agricultural development. These wetland ecosystems provide valuable services such as improving water quality by decreasing nutrient and pollutant loads and mitigating climate change by sequestering carbon. Therefore, there is an interest in conserving, restoring, and constructing wetlands for these ecosystem benefits. Examples of valuable wetland ecosystem functions are anaerobic microbial processes associated with saturated soils that promote complete inorganic nitrogen ( $\text{NO}_3^- \rightarrow \text{N}_2$ ) removal via denitrification and suppress aerobic decomposition of organic matter. These same anoxic soil conditions can also support methane production (via methanogenesis), which could decrease long-term carbon storage and climate change mitigation benefits of wetlands. Microbial functions associated with delivery of ecosystem services have the potential to be managed to enhance beneficial wetland services (Peralta et al., 2014a). To achieve microbial management, a deeper understanding of the controls on wetland microbial ecosystem functions is needed.

In order to produce cellular energy, adenosine triphosphate, microorganisms catalyze a series of oxidative-reduction (redox) reactions. Aerobic respiration yields the greatest amount of energy and is expected under dry conditions but as water fills soil pore spaces, the soil matrix shifts to a reducing environment (Mitsch et al., 2013; Truu et al., 2009). Reducing environments favor anaerobic respiration in which other

molecules such as nitrate, manganese, ferric iron, sulfate, and carbon dioxide are used as terminal electron acceptors (Burgin et al., 2011). As soil moisture increases, oxygen availability and soil redox potentials decrease, which corresponds to a shift in available electron acceptors (Truu et al., 2009). Redox potentials measured between +600 and +250 mV are considered oxidative conditions while redox potentials measured from +250 to -400 mV are considered reducing conditions (Truu et al., 2009). Therefore, measuring soil redox potential is useful for predicting which biogeochemical processes are likely to be carried out by soil microbes.

In order to manage microbial functions in support of nitrogen removal and retention but with decreased methane production, a better understanding of the extent that the presence of vegetation and changes in hydrology (e.g., flooding, drying) affect microbial communities is needed. Complex interactions between abiotic factors, such as soil physicochemical properties, redox status and nutrient availability, and biotic factors, including abundance of vegetation and microbial community structure, influence microbial functions to varying degrees. A microbial community is composed of many taxa with varying physiologies which respond differently to changes in the local environment (Mentzer et al., 2006; Nygaard and Ejrnæs, 2009). Particular microbes may be more adapted to specific hydrologic conditions in their environment, where only a subset of microbial taxa can persist in response to frequent changes in soil moisture (Peralta et al., 2014b; Truu et al., 2009). However, unexpected microbial responses can also occur due to dormancy of soil bacterial taxa (Lennon and Jones, 2011; Rocca et al., 2015). As such, hydrologic changes in wetlands due to drought, draining, and re-wetting cause shifts in soil redox status and microbial community composition and

metabolism, which can influence the relative rates of anaerobic processes such as denitrification and methanogenesis (Kim et al., 2008; Peralta et al., 2014b; Truu et al., 2009).

If drying and re-wetting events are periodic, a cycle of activity and dormancy can maintain high microbial diversity compared to more stable environmental conditions (Peralta et al., 2014b). For example, denitrifiers are facultative anaerobes and are capable of using oxygen; but in anoxic conditions, denitrifiers can switch to reducing nitrate ( $\text{NO}_3^-$ ) to nitrous oxide ( $\text{N}_2\text{O}$ ) and dinitrogen ( $\text{N}_2$ ) gas during respiration (Mitsch and Gosslink, 2007). In addition, methanogens are dominant in the most anoxic conditions such as flooded wetlands, and are responsible for converting carbon dioxide to methane gas (Mitsch and Gosslink, 2007). Fluctuating hydrologic conditions can shift the microbial community to one that can only tolerate transitional zones. As hydrologic changes occur, anoxic-oxic interfaces provide environmental conditions that sometimes support methanotrophs that convert methane to carbon dioxide and denitrifiers (Conrad, 2009; McDonald and Murrell, 1997; Mitsch and Gosslink, 2007). Therefore, the availability of electron acceptor/s (e.g., oxygen, nitrate) in the soil environment influences the relative abundance of microbial functional groups (i.e., subset of microbes capable of using a suite of electron acceptors), rates and types of microbial processes.

While hydrology is a primary determinant of soil redox potential, plants also modify the soil environment. The soil microenvironments that are in contact with plant roots are hotspots of microbial activity involved in transporting nutrients, oxygen, and carbon belowground (Chanton, 2005; Kuzyakov, 2010; Philippot et al., 2013). Plants

can transport methane aboveground through aerenchyma in stems (Carmichael et al., 2014; Hu et al., 2015). Also, radial oxygen loss from plant roots can increase soil redox potentials around the root zone producing microenvironments that can support aerobic microbial processes (Chanton, 2005; Sundberg et al., 2007).

The aim of this study is to provide insight into how the duration of hydrologic change (i.e., dry, interim, wet), and the presence of vegetation in wetland soils change the structure of the microbial community, redox conditions, and greenhouse gas rates. We hypothesize that dry and dry/wet transition conditions will support similar microbial communities but that redox status and greenhouse gas rates will differ between manipulated hydrologic treatment conditions. We expect that dry conditions with and without vegetation will support higher redox potentials (i.e., oxidative conditions) and a higher rate of carbon dioxide production with some nitrous oxide production but little or no methane production. We expect this because dry and transition conditions should support similar communities of facultative anaerobes that can switch between respiration pathways depending on current soil saturation levels. Additionally, in dry conditions soils are already aerated so plant-mediated gas transport belowground should not alter redox status. However, in fluctuating wet conditions, we expect that redox conditions will shift between oxidative and reducing conditions due to soil saturation. Also, plant presence will increase redox potentials during saturated periods, due to plant-mediated gas transport belowground, compared to treatments where vegetation is absent. Due to lower oxygen levels when saturated conditions are present, we expect decreased carbon dioxide production but increased nitrous oxide production with plants and negative nitrous oxide rates without plants indicating incomplete or

complete denitrification processes, respectively. Also, we expect methane production will be lower due to methanogens being obligate anaerobes. Flooded conditions will support different microbial communities than dry or fluctuating environments due to consistently low redox potentials (i.e., reducing conditions) resulting in the highest rates of methane production and complete denitrification rates since these are both anaerobic processes. Although, other studies (Carmichael et al., 2014; Hu et al., 2015) have found increased methane rates in the presence of some plant species, in the present study, we expect that soils with plants will have lower methane production compared to flooded soils without plants. This is expected due to oxygen transport from roots supporting aerobic methanotrophic microbial taxa that consume methane.

To test these hypotheses, we conducted a mesocosm experiment in which we manipulated hydrology (i.e., dry, interim, and wet) and presence of plants in wetland soils from different hydrologic histories (i.e., dry, wet/dry transition, and saturated wet zones) of a restored coastal plain wetland. We measured soil nutrient concentrations, redox status, greenhouse gas concentrations, and characterized soil microbial communities using amplicon sequencing. By simulating acute differences in hydrologic states, the addition of plants, and maintenance of soil structure, we were able to link microbial-scale changes to ecosystem-level processes.

## **Methods**

### *Study site*

We collected soil samples from the Timberlake Observatory for Wetland Restoration located in the Albemarle Peninsula in Tyrell County, North Carolina

(35°54'22" N 76°09'25" W; Fig. 2.1). Previously described by Ardón et al., 2010 and Morse et al., 2012, the field site was previously used for agriculture and is a part of the Great Dismal Swamp Mitigation Bank, LLC which is a 1,700 ha wetland consisting of 420 ha of mature forested wetland, 787 ha of forested wetland, 57.2 ha of drained shrub-scrub, and 440 ha of agricultural fields restored to wetland habitat in 2007 (Ardón et al., 2013, 2010). A major portion of the restoration effort was to remove drainage ditches and plant 750,000 saplings including *Taxodium distichm*, *Nyssa* spp., *Salix nigra*, *Fraxinus pennsylvania*, and *Quercus* spp. (Morse et al., 2012). A more recent survey indicates that the dominant plant species at the site is *Juncus effusus* L. along with *Euthamia caroliniana* (L.) Greene ex Porter & Britton, *Solidago fistulosa* Mill., and *Scirpus cyperinus* (L.) Kunth (Hopfensperger et al., 2014). The site is connected to the Albemarle Sound via the Little Alligator River, and the site's position in the landscape increases the potential for saltwater intrusion to occur. In addition, salinity in the sound ranges from 0-7 psu and up to 12 psu during drought years (Ardón et al. 2013). Even though there is little elevation change (-1 m to 2 m) across the restored wetland, there is a hydrologic gradient, which is driven by the position of the water table and represents upland dry, saturated wet, and transition dry/wet sites (Hopfensperger et al., 2014).

### *Mesocosm experimental design*

We used a mesocosm approach to assess the changes in the soil microbial community, redox status, and greenhouse gas (GHG) production due to hydrologic changes and vegetation. We set up a mesocosm experiment using soil blocks collected from three sites within the Timberlake Observatory for Wetland Restoration field site.

Soils were collected from the restored (12 years post-restoration) portion of the site that was previously used as agricultural fields for several decades prior to restoration (Ardón et al., 2010). We collected soils that represented three different hydrologic zones on the inflow side of the site at the following coordinates: 35°53'45.3"N 76°09'57.5"W (dry), 35°53'44.8"N 76°09'57.1"W (dry/wet transition or interim), and 35°53'44.3"N 76°09'56.0"W (wet). Six intact soil blocks (25 cm × 25 cm × 20 cm deep) were cut out from each of the three sites using landscaping knives and shovels. Soil history was determined by water table levels at the time of collection (dry = 20 cm, interim = 10 cm, and wet = 0 cm below surface level). Soil blocks were contained in dark plastic containers of the same dimensions as the soil blocks (Fig. 2.1). To manipulate hydrology within the mesocosm, vinyl tubing was inserted 3 cm from the bottom of the mesocosm container on each side and connected to a 1 L water bottle (Fig. 2.1). Water levels inside the mesocosm were maintained by filling the 1 L bottle to the desired height using rain water collected from a cistern. To manipulate the presence of vegetation, the mesocosm was divided in half and separated by root screen (20 µm stainless steel mesh). On one side plants were allowed to grow during the experiment, while the 'no plant' side was maintained by careful removal of above- and belowground plant biomass. Finally, 4" schedule 40 polyvinyl chloride (PVC) collars were inserted 5 cm below the surface as a sampling base for GHG chambers (described in subsection *GHG concentrations*). The mesocosm experiment was housed at the East Carolina University West Research Campus (Greenville, NC) under a covered hoop house with shade cloth which prevented precipitation and allowed 60% light into the hoop house. Soils were collected April 1, 2016, prepared on May 29, 2016, and experimental

mesocosm sampling started on June 13, 2016 and ended on August 11, 2016. Temperatures ranged from  $22.7^{\circ}\text{C} \pm 1.5$  to  $30.8^{\circ}\text{C} \pm 1.4$  during the experimental sampling period.

Two weeks after installing PVC collars and setting up the plant treatment, we started hydrologic treatments. Hydrologic manipulation occurred over eight weeks to allow for multiple dry/wet transitions for the interim treatment. Mesocosms exposed to wet conditions were flooded by overhead watering and maintained using water reservoirs filled to maximum container height (18 cm). Mesocosms exposed to dry conditions were maintained at a 5 cm water level. The dry/wet (interim) treatments fluctuated between flooded and dry conditions, as described above, every two weeks starting with a wet treatment and ending with a dry treatment. We measured soil redox status and microbial community composition at the beginning and end of the 8-week experiment. In addition, we measured GHG fluxes every two weeks starting two weeks after initiating hydrologic treatments. Finally, at the end of the eight week experiment, we collected soils for physiochemical analyses: soil moisture, pH, total carbon, total nitrogen, extractable ammonium and nitrate, phosphorus, potassium, magnesium, sulfur, iron, manganese, and organic matter concentrations (described in subsection *Soil Physiochemical Characteristics*).

#### *Soil redox status*

We measured soil redox status at the beginning and end of the hydrologic experiment using Indicator of Reduction in Soils (IRIS) tubes (InMass Technologies; (Jenkinson and Franzmeier, 2006) (Fig. S2.1A). The IRIS tubes are constructed from

1/2" schedule 40 PVC pipe coated in iron oxide (Fe (III)) paint (Rabenhorst, 2008). When exposed to oxidative conditions, Fe(III) is visible as an orange-red paint; but when exposed to anoxic conditions, Fe(III) is reduced to Fe(II) which dissolves in solution and appears as a clearing (white) on the tube (Jenkinson and Franzmeier, 2006; Rabenhorst, 2008). At the beginning of the experiment, two IRIS tubes (12 cm depth) were installed in each mesocosm: one on the plant side and one on the bare soil side. The IRIS tubes were incubated in mesocosm conditions for two weeks before removal and analysis. After we removed the IRIS tube, a non-coated PVC pipe was used to fill the hole. Two weeks prior to the end of the experiment, the non-coated PVC pipe was removed and replaced with a new IRIS tube to measure soil redox status at the end of the experiment.

We quantified the surface area of Fe(III) paint removed from IRIS tubes using ImageJ software (v1.48, (Schneider et al., 2012)). First, we imaged the entire tube by taking four pictures and then stitched the photo into a composite using GIMP2 (v2.8.14, <https://gimp.org/>) photo editing software. Next, we identified areas of artificial paint removal, that is scratches from installing or removing tubes, and manually filled these pixels. Then, using ImageJ software (v1.48, (Schneider et al., 2012)), we converted all colored pixels to black. We compared the number of white pixels to total pixels to determine the percent of paint removed. Interpretation of redox status is based on the percent paint removed from a 10 cm section of tubing and summarized as follows: 0% not reducing, 1-5% probably not reducing, 5-10% possibly reducing, 10-25% and >25% definitely reducing (Rabenhorst, 2008).

### *Greenhouse gas (GHG) concentrations*

We examined the effects of hydrology and vegetation on GHG production. We measured GHG concentrations on June 13, 2016, two weeks after hydrologic treatments were established, and then every two weeks until August 11, 2016 for a total of five sampling events. The GHG collection chambers were 20 cm in height with a diameter of 8.25 cm and constructed from clear acrylic tubing. Since GHG samples were captured using clear chambers versus opaque chambers, GHG measurements represent total GHG fluxes and not just soil respiration due to microbial activity. Chambers were sealed on one end with silicon and a pipe cap with 33 mm septa installed as gas sampling port. At the time of sampling, chambers were placed on top of preinstalled PVC collars and the seal taped to prevent diffusion from the seam (Hoffmann et al., 2018). We collected gas samples every 30 minutes for a total of four time points. To collect gas samples, we used a needle attached to a 20 mL syringe, mixed headspace gas three times by pulling and depressing the plunger, and then collected 20 mL of sample. The collected gas sample was equally distributed between two 3 mL glass Exetainer® vials (Labco, Lampeter, Wales, UK) fitted with screw top and dual layer septa. Samples were stored upside down at room temperature in a dark location and were analyzed within 96 hours of collection. We analyzed GHG concentrations using a Shimadzu gas chromatograph (GC-2014) fitted with an electron capture detector to detect nitrous oxide and flame ionization detector with methanizer to measure methane and carbon dioxide. Calibration standards for June 13 and June 28, 2016 contained 0, 120, 240, 360, 480, and CO<sub>2</sub> ppm; 0, 1, 2, 3, 4, and 5 CH<sub>4</sub> ppm; and 0, 0.2, 0.4, 0.6, 0.8, and 1 N<sub>2</sub>O ppm. Calibration standards for July 11, Jul 25, and

August 11, 2016 contained 0, 120, 480, 1200, 2400, and 3000 CO<sub>2</sub> ppm; 0, 1, 4, 20, 40, and 50 CH<sub>4</sub> ppm; and 0, 0.2, 0.8, 20, 40, and 50 N<sub>2</sub>O ppm. If a sample measured above the calibration curve, we diluted the sample and reanalyzed it.

We used the linear change in concentration and the ideal gas law to calculate GHG fluxes (Millar et al., 2018). However, upon curation of analyzed gas samples for GHG flux calculations, we identified that 30-50% of samples from no plant treatments were not linear and that 50-75% of those samples represented wet treatments. Due to reduced ability in determining the effects of hydrology and plants on GHG rates by removing these samples from further analyses, we chose an alternate approach to analyzing gas samples. We determined the concentration of CH<sub>4</sub>, CO<sub>2</sub>, and N<sub>2</sub>O in each sample for the first sampling time point which occurred at the first 30 minute collection interval.

#### *Bacterial and archaeal community analyses*

We assessed the soil microbial community composition at the beginning of the experiment ('start' based on soils collected from the IRIS tube installation) and at the end of the experiment ('final' based on soils collected during destructive sampling). We collected 'final' soil samples using a standard soil probe (3 cm diameter, 10 cm deep) from the same location that we collected GHGs samples. We extracted genomic DNA from soils using the Qiagen DNeasy PowerSoil Kit and diluted DNA to 20 ng µl<sup>-1</sup>. This genomic DNA was used as template in PCR reactions and used barcoded primers (bacterial/archaeal 515FB/806R primer set) originally developed by the Earth

Microbiome Project (Caporaso et al., 2012) to target the V4 region of the bacterial 16S subunit of the ribosomal RNA gene (Apprill et al., 2015; Caporaso et al., 2012; Parada et al., 2016). For each sample, three 50  $\mu\text{L}$  PCR libraries were prepared by combining 35.75  $\mu\text{L}$  molecular grade water, 5  $\mu\text{L}$  Amplitaq Gold 360 10x buffer, 5  $\mu\text{L}$   $\text{MgCl}_2$  (25 mM), 1  $\mu\text{L}$  dNTPs (40mM total, 10mM each), 0.25  $\mu\text{L}$  Amplitaq Gold 360 polymerase, 1  $\mu\text{L}$  515 forward barcoded primer (10  $\mu\text{M}$ ), 1  $\mu\text{L}$  806 reverse primer (10  $\mu\text{M}$ ), and 1  $\mu\text{L}$  DNA template (10 ng  $\mu\text{L}^{-1}$ ). Thermocycler conditions for PCR reactions were as follows: initial denaturation (94 °C, 3 minutes); 30 cycles of 94°C for 45 seconds, 50 °C for 30 seconds, 72 °C for 90 seconds; final elongation (72 °C, 10 minutes). The triplicate 50  $\mu\text{L}$  PCR libraries were combined and then cleaned using the AMPure XP magnetic bead protocol (Axygen, Union City, California, USA). Cleaned PCR product were quantified using QuantIT dsDNA BR assay (Thermo Scientific, Waltham, Massachusetts, USA) and diluted to a concentration of 10 ng  $\mu\text{L}^{-1}$  before pooling libraries in equimolar concentration of 5 ng  $\mu\text{L}^{-1}$ . We sequenced the pooled libraries using the Illumina MiSeq platform using paired end reads (Illumina Reagent Kit v2, 500 reaction kit) at the Indiana University Center for Genomics and Bioinformatics Sequencing Facility.

Sequences were processed using the mothur (v1.42.0) (Schloss et al., 2009) (Schloss et al. 2009) MiSeq pipeline (Kozich et al., 2013). We assembled contigs from the paired end reads, quality trimmed using a moving average quality score (minimum quality score 35), aligned sequences to the SILVA rRNA database (v132) (Quast et al., 2013), and removed chimeric sequences using the VSEARCH algorithm (Rognes et al., 2016). We created operational taxonomic units (OTUs) by first splitting sequences based on taxonomic class and then binning into OTUs based on 97% sequence

similarity. Taxonomic identity was assigned using the SILVA rRNA database (v132) (Quast et al., 2013).

### *Soil physiochemical characteristics*

Soil properties were determined from soils collected during the destructive sampling of mesocosms at the end of the experimental duration. We collected six soil cores (3 cm diameter, 10 cm depth) from each side of the box (i.e., plant and no plant) and combined cores collected from one side into a composite sample (i.e., one plant composite and one no plant composite), passed soils through a 4 mm sieve, and homogenized samples prior to subsampling for soil analyses. For each sample, we measured gravimetric soil moisture by drying 20-30 g of field-moist soil at 105 °C for at least 24 hours. Approximately 5 g of field-moist soil was extracted with 45 ml of 2 M KCl, and extractable ammonium ( $\text{NH}_4^+$ ) and nitrate ( $\text{NO}_3^-$ ) ions were colorimetrically measured using a SmartChem 200 auto analyzer (Unity Scientific Milford, Massachusetts, USA) at the East Carolina University Environmental Research Laboratory. To determine total carbon and total nitrogen (TC, TN), a subsample of air-dried soil was finely ground and sieved through a 500  $\mu\text{m}$  mesh, and analyzed using an elemental analyzer (2400 CHNS Analyzer; Perkin Elmer; Waltham, Massachusetts, USA) at the Environmental and Agricultural Testing Service Laboratory, Department of Crop and Soil Sciences, North Carolina State University). A second subsample of air-dried soil was sent to Waters Agricultural Laboratories, Inc. (Warsaw, NC) and analyzed

for pH, phosphorus, potassium, magnesium, sulfur, manganese, iron, and humic matter, using standard Mehlich III methods (Mehlich, 1984; Mylavarapu et al., 2014).

### *Statistical analyses*

All statistical analyses were performed in the R statistical environment (RStudio v1.2.5001, Rv3.6.1) (R Core Team, 2019). Prior to multivariate statistical analyses, we normalized sample-to-sample variation in sequence depth by taking the relative abundance of each OTU and dividing by the total number of OTUs for each soil community. We examined beta diversity by visualizing bacterial community responses to hydrologic history (field conditions) and hydrologic treatment (manipulated dry/wet treatments) using principal coordinates of analysis (PCoA) of bacterial community composition based on Bray-Curtis dissimilarity. We used permutational multivariate analysis of variance (PERMANOVA) to determine differences between bacterial communities among hydrologic history, hydrologic treatment, and plant presence. Hypothesis testing using PERMANOVA was performed using the *vegan::adonis* function (Oksanen, 2015). Unique taxa representing each hydrologic history were determined by Dufrene-Legendre indicator species analysis using the *labdsv::indval* function (Roberts, 2016). Finally, soil parameters were compared against bacterial community patterns (based on Bray-Curtis dissimilarity) using *vegan::envfit* function (Oksanen, 2015). Soil parameters with  $p < 0.05$  were represented on the PCoA plot as vectors scaled by their correlation to microbial community patterns.

We constructed linear mixed effects models with sampling plot and sampling date as random effects to determine the importance of the fixed effects of hydrologic history (field conditions), hydrologic treatment (contemporary dry/wet treatments), and plant presence on GHG concentrations using the *lme4* R package (Bates et al., 2015). Then, we used AICc model comparisons, which adjust for small sample size, to determine which simplest combination of fixed effects (hydrologic history, hydrologic treatment, and plant presence) is needed to explain the most variation in GHG concentrations (Gorsky et al., 2019; Hurvich and Tsai, 1993). We compared individual fixed effects and the combination of those fixed effects. We did not use the interaction between the fixed effects hydrologic history and hydrologic treatment because we only had a sample size of  $n=2$  for each group. Lastly, to determine the proportion of variance explained by fixed effects (marginal) and the complete model (conditional), we used the *MuMIn* R package (Barton, 2019; Gorsky et al., 2019). The CH<sub>4</sub>, CO<sub>2</sub>, and N<sub>2</sub>O concentrations were log transformed to better meet normality assumptions prior to running mixed effects models. To assess microbial community structure and function relationships, we examined the relationship between individual GHG concentration to microbial community Bray-Curtis dissimilarity matrix using distance-based partial least squares regression in the *dbstats* R package (Boj et al., 2017). Finally, we used Mantel R statistic function in the *vegan* R package (Oksanen, 2015) to examine the relationship between the soil properties (redox, moisture %, pH, ammonium, total soil C, phosphorus ppm, potassium ppm, magnesium ppm, sulfur ppm, and humic matter percent) and microbial community composition. Only soil properties with a correlation of <50% were used in this analysis.

## Results

### *Characterization of soil physical-chemical properties*

There was little variability in soil properties across main effects (hydrologic history, hydrologic treatment, plant presence). However, there were notable differences in soil moisture between plant treatments within dry and wet hydrologic treatments. In addition,  $\text{NO}_3^-$  concentrations were below detection limits in samples with plants, but were measurable in samples without plants ( $0.01 \pm 0.0005$  to  $0.25 \pm 0.38 \text{ NO}_3^- \text{ mg L}^{-1}$ ) (Table 2.1). Soil redox status as measured by IRIS tube analysis revealed that soils experiencing dry and interim treatments (0% iron oxide paint removed) were not reducing, while soils in wet treatments were reducing (average 40%, range 27-67% paint removed). In wet treatments, plant presence decreased soil redox status to a lesser degree (average 38%, range 27%-60% paint removed) than when plants were absent, but soils were still considered reducing (Fig. 2.2, Fig. S2.1).

### *Plant and soil redox effects on GHG concentrations*

#### *Methane ( $\text{CH}_4$ )*

Within no-plant treatments, wet ( $19.9 \pm 42.0 \text{ mg CH}_4\text{-C m}^{-2}$ , average  $\pm$  SD) and interim ( $6.5 \pm 25.4 \text{ mg CH}_4\text{-C m}^{-2}$ ) hydrologic treatments produced the highest  $\text{CH}_4$  concentrations and the greatest variability between samples compared to dry treatments ( $0.22 \pm 0.93$ ) (Fig. 2.4). However, treatments with plants produced the lowest

CH<sub>4</sub> concentrations across wet, dry, and interim hydrologic treatments ( $0.64 \pm 0.47$ ,  $0.17 \pm 0.16$ ,  $0.60 \pm 0.85$  mg CH<sub>4</sub>-C m<sup>-2</sup>, respectively) (Fig. 2.4). The model with hydrologic history, hydrologic treatment, and plant presence explained the most variation in CH<sub>4</sub> concentrations based on  $\Delta$ AICc score of 0 and AICc weight of 0.45 (Table S2.1). The full model explained 32% of variation, while the fixed effect of hydrologic treatment explained 21% of the variation and plant and hydrologic history only explained 4% and 6%, respectively (Table S2.1).

### *Carbon dioxide (CO<sub>2</sub>)*

Within no plant treatments, dry ( $104.7 \pm 37.4$  mg CO<sub>2</sub>-C m<sup>-2</sup>), interim ( $58.1 \pm 30.6$  mg CO<sub>2</sub>-C m<sup>-2</sup>), and wet ( $42.3 \pm 18.5$  mg CO<sub>2</sub>-C m<sup>-2</sup>) hydrologic treatments produced the highest CO<sub>2</sub> concentrations compared to treatments with plants ( $35.1 \pm 19.2$ ,  $29.5 \pm 15.0$ ,  $24.9 \pm 0.6$  mg CH<sub>4</sub>-C m<sup>-2</sup>, respectively) (Fig. 2.5). The model with the interaction of hydrologic treatment and plant explained the most variation in CO<sub>2</sub> concentrations based on a  $\Delta$ AICc score of 0 and AICc weight of 0.93 (Table S2.1). The fixed effect of plant explained 32% of the variation and hydrologic treatment explained 15% of variation while the interaction explained 52% of variation (Table S2.1).

### *Nitrous oxide (N<sub>2</sub>O)*

The N<sub>2</sub>O concentrations were near zero in all hydrologic and plant treatments (range: 0.05-0.15 mg N<sub>2</sub>O-N m<sup>-2</sup>) (Fig. 2.6). The model with hydrologic treatment and

plant explained the most variation in N<sub>2</sub>O concentrations based on  $\Delta$ AICc score of 0 and AICc weight of 0.53 (Table S2.1). The full model explained only 14% of variation, while the fixed effect of plant explained 10% of variation and hydrologic treatment explained 3% of variation (Table S2.1).

### *Relationship between soil redox conditions and GHG concentrations*

We used linear regression to examine the relationship between soil redox status and GHG concentrations. CH<sub>4</sub> had weak but significant positive relationship to redox status ( $R^2=0.26$ ,  $p=0.001$ ). This relationship improved after removing a wet/no plant sample that had unusually high CH<sub>4</sub> concentrations ( $R^2= 0.45$ ,  $p<0.001$ ). In addition, CO<sub>2</sub> concentrations had a weak but significant negative relationship with redox conditions ( $R^2=0.19$ ,  $p=0.005$ ), and N<sub>2</sub>O concentrations were not significantly related to redox conditions ( $R^2=0.01$ ,  $p=0.25$ ).

### *Patterns in microbial community composition*

Sequencing efforts returned a total of 1,570,135 reads and 35,897 operational taxonomic units (OTUs) before removing low abundance sequences occurring less than 10 times or 0.01% in all samples. After removing low abundance sequences, 1,505,797 reads representing 7,026 OTUs were retained after filtering. Within OTUs prior to filtering, 15,582 of those OTUs occurred once and 5,536 occurred twice in all samples.

All samples were rarefied to 23,528 reads since this was the lowest read count among all samples.

Bacterial and archaeal community composition clustered by hydrologic treatment within hydrologic history. Hydrologic history (along PCoA axis 1) explained 24.5% of variation in microbial community composition while hydrologic treatment (along PCoA axis 2) explained 10.6% of variation (Fig. 2.7). The PERMANOVA results indicate that hydrologic history ( $R^2=0.305$ ,  $p=0.001$ ) and hydrologic treatment ( $R^2=0.110$ ,  $p=0.002$ ) explained variation in microbial community patterns (Table S2.2). In addition, sulfur concentrations were correlated to soil microbial communities from the wet hydrologic history, pH levels were correlated to microbial communities from the interim hydrologic history; and total soil C and manganese concentrations were correlated to microbial communities from the dry hydrologic history. Also, overall patterns in microbial composition and soil properties were significantly correlated (Mantel  $r= 0.32$ ,  $p= 0.001$ ).

Indicator species analysis of the top 2.5% OTUs (by relative abundance at a significance level of  $p\leq 0.01$ ) revealed that 33 OTUs, 21 OTUs, and 39 OTUs represented dry, interim, and wet hydrologic histories, respectively. The bacterial phyla Acidobacteria (Gp1, Gp2, Gp3, and Gp6) (24%) and Proteobacteria (Alpha-, Beta-, Delta-, and Gammaproteobacteria) (30%) represented communities from dry hydrologic histories, while the bacterial phyla Acidobacteria (Gp1, Gp10, Gp3, and Gp7) (33%) and Proteobacteria (Alpha-, Beta-, and Deltaproteobacteria) (29%) represented communities from interim hydrologic histories. Soils from wet hydrologic histories were represented by Acidobacteria (Gp1, Gp2, Gp3) (38%) and Proteobacteria (Alpha-, Delta-, and Gammaproteobacteria) (21%). Finally, microbial taxa putatively associated with methane

cycling including the archaeal genera *Methanobacterium* and the bacterial genera *Methylocystis* and *Syntrophobacter* were unique to microbial communities from wet hydrologic histories.

### *Relationships between GHG concentrations, microbial community composition, and soil properties*

Microbial community composition explained more of the variation in GHG concentrations than do soil properties. Distance-based partial least squares regression revealed that microbial community composition explained 51.3%, 54.8%, and 48.6%, of variation in concentrations of CH<sub>4</sub>, CO<sub>2</sub>, and N<sub>2</sub>O, respectively, based on components 1 and 2. However, distance-based partial least squares regression revealed that patterns in soil properties only explained 30.0%, 31.6%, and 17.9%, of variation in concentrations of CH<sub>4</sub>, CO<sub>2</sub>, and N<sub>2</sub>O, respectively, based on components 1 and 2.

## **Discussion**

This study revealed that initial hydrologic conditions (compared to manipulated hydrology) strongly influenced microbial community composition more than function. Mesocosm soils for this study were collected from wet, dry, and interim hydrologic histories from a restored wetland. This difference in hydrologic history resulted in distinct microbial community patterns with wet hydrology being the most distinct compared to microbial communities from the dry and interim hydrology. Specifically, dry hydrologic histories were represented by taxa in the genera *Gaiella*, which are classified

as strict aerobes (Albuquerque et al., 2011). Wet hydrologic histories were uniquely identified by bacterial and archaeal taxa putatively associated with methanogenesis, methanotrophy, and iron reduction. These microbial processes occur in low redox/low oxygen systems (Burgin et al., 2011). Microbes that are facultative anaerobes can shift between aerobic and anaerobic respiration based on soil redox conditions, therefore they can metabolically shift during dynamic soil hydrologic conditions. However, obligate anaerobes such as methanogens are sensitive to soil oxygen concentrations and desiccation (Fetzer et al., 1993). For example, in a study of peat bog layers, oxic subsurface layers contained more methanotrophs than methanogens which were found only in anoxic layers near the bottom of the bog (Lew and Glińska-Lewczuk, 2018). This suggests that hydrology is a strong determinant of oxygen availability in soils and that wet hydrologic histories best support microbial communities involved in anaerobic processes.

Plant and hydrologic treatment strongly affected microbial function, despite hydrologic history acting as a robust environmental filter on microbial community composition. Plants can influence GHG rates by consuming CO<sub>2</sub> during photosynthesis, releasing CO<sub>2</sub> during respiration, aerating soils in contact with roots, and releasing labile C from roots which can stimulate microbial activity (Carmichael et al., 2014; Chanton, 2005; Luan and Wu, 2014). In the current study, soil redox status as visualized with IRIS tubes indicated that oxidative conditions existed near plant roots. This result suggests that plants are transporting oxygen belowground into soils. Regardless of hydrologic history, CH<sub>4</sub> concentrations were highest and CO<sub>2</sub> concentrations were lowest in soils experiencing the wet hydrologic treatment. However, soil undergoing

fluctuating hydrologic treatments had similar GHG concentrations to soils experiencing dry hydrologic treatments. As such, the GHG concentrations were lower in all hydrologic treatments with plants. The reduction in CH<sub>4</sub> with plant presence is likely due oxygen radiation from plant roots providing methanotrophs with needed oxygen for methane consumption, thereby decreasing methane emissions (Chanton, 2005; Truu et al., 2009). The reduction in CO<sub>2</sub> emissions in the presence of plants is likely due to plant photosynthesis and plant uptake of atmospheric CO<sub>2</sub> from within the collection chamber (Luan and Wu, 2014). This suggests that plants are important mediators of GHG production in wetland soils. These results reveal that fluctuating soil moisture levels can decrease CH<sub>4</sub> emissions even within soils from wet hydrologic histories. Therefore, both hydrology of soils and plant presence are two important considerations when planning wetland restoration with the goal of enhancing soil C storage.

Results of this study highlight the importance of considering plant contributions to GHG emissions. Many studies investigating GHG emissions use opaque chambers to decrease heating of the headspace; however, these chambers can bias measurements of CH<sub>4</sub> emissions (Günther et al., 2014; Luan and Wu, 2014). Estimates of GHG emissions that do not include plant inputs can underestimate the C storage potential of wetlands. For example, a previous study estimates the C storage potential of wetlands by subtracting CO<sub>2</sub> sequestered from the atmosphere from CH<sub>4</sub> released from soils to determine that the world's wetlands sequester ~118 g-C m<sup>-2</sup> year<sup>-1</sup> (Mitsch et al., 2013). However, it is unclear if the studies used to estimate this value considered local soil hydrology and whether plants were present or not. According to our study and others (Günther et al., 2014; Luan and Wu, 2014), plant inclusion and

plant species considerations in most cases would decrease the total estimation of CH<sub>4</sub> emissions from wetlands. These findings suggest that to improve estimations of C storage in wetlands, plant presence and hydrologic status should be considered in order to understand wetlands' potential to be a C sink.

Further, increasing extreme weather events cause changes in duration of decreased or excessive rainfall, which will alter microbial ecosystem functions. Changes in precipitation regimes could directly alter soil hydrology or plant abundance and composition. Results from this study reveal that the longer the duration of hydrologic change, the more dramatic the change in ecosystem functions. These results can be used to infer what might happen during an extreme drought event. One potential scenario is that during early summer a saturated non-tidal coastal plain wetland experiences decreased rainfall to the degree that the first meter of soil completely dries out and kills all vegetation. This may temporarily decrease methane emissions, but if in the following month the same area then becomes saturated again methane emissions could increase due to the lack of vegetation. However, if the duration of drying alters the microbial community structure, then methane production may be decreased upon re-flooding since obligate anaerobes will not persist under dry, aerated conditions. This warrants future studies to more closely examine the temporal component of when changes in hydrology permanently alter microbial community structure and lead to unexpected changes in ecosystem functions.

## Figures and Tables

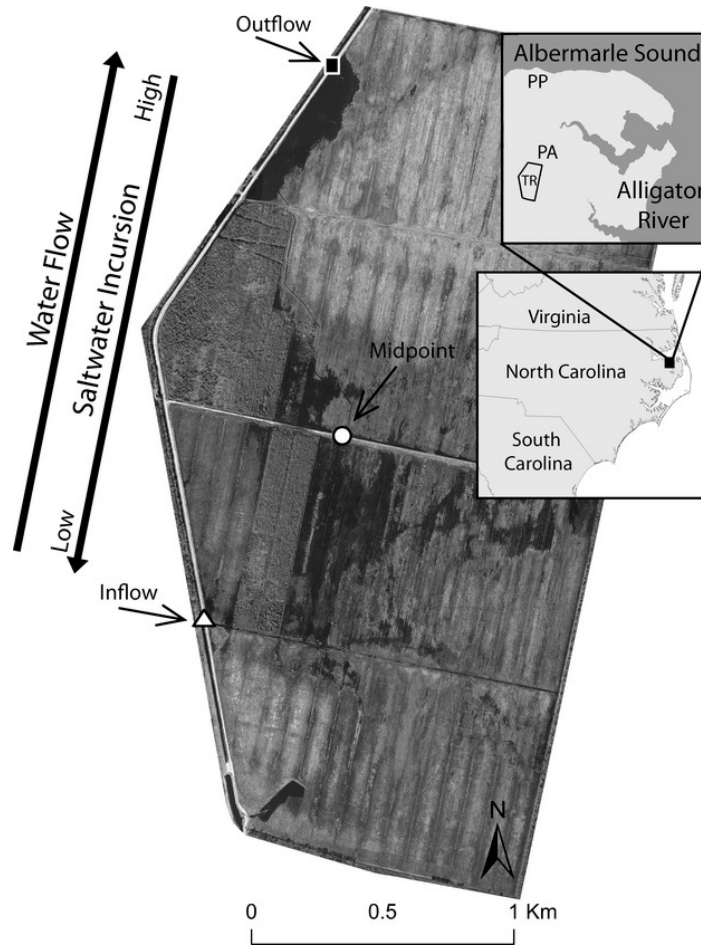


**Figure 2.1.** Timberlake Observatory for Wetland Restoration. (Modified from Ardón et al., 2013)

**Figure 2.2.** Mesocosm setup. Top: Left side of box represents plant treatment, and right side represents no plant treatment. There is a stainless mesh divider between each side. PVC collars permanently placed in mesocosm for GHG sampling. 1 liter bottle attached to each side of the mesocosm used to maintain water levels. Middle: Example of a wet treatment mesocosm with IRIS tubes installed. Bottom: Example of mesocosm with prepared for GHG sampling.



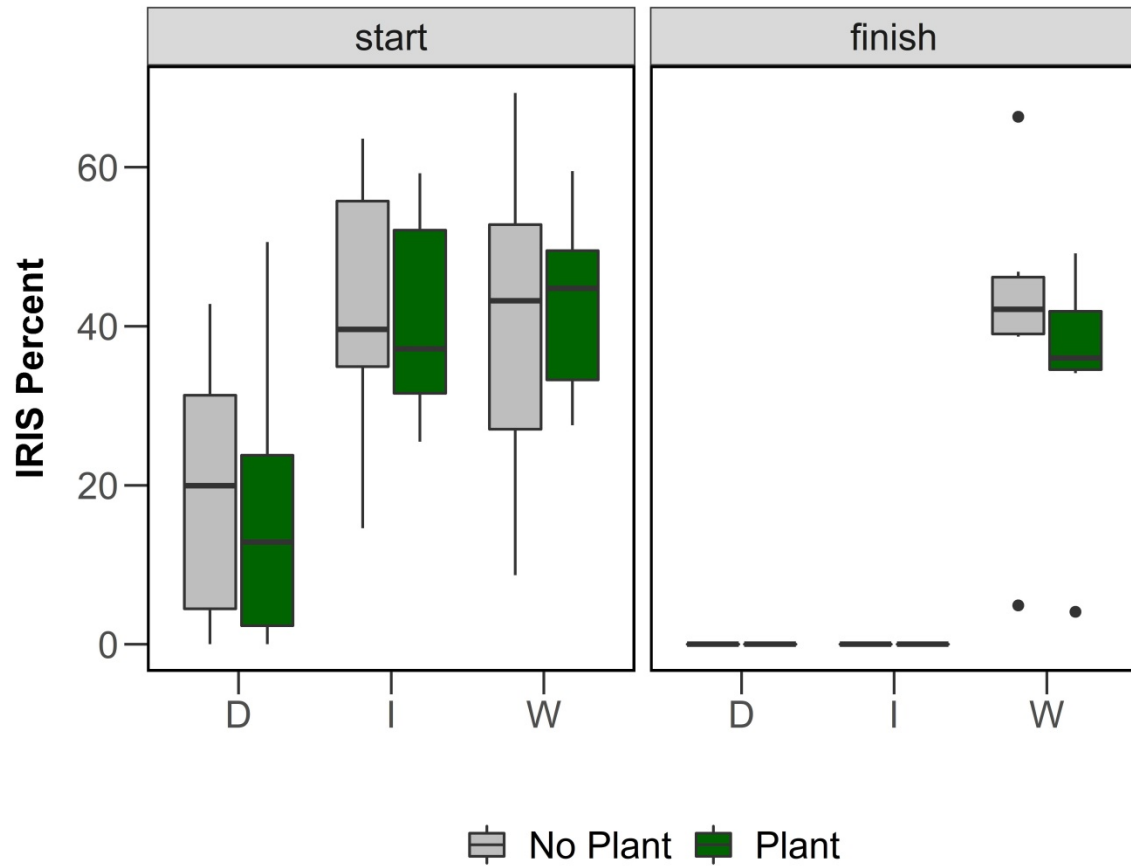


**Figure 2.3.** Boxplots of percent paint removed from IRIS tubes at start of experiment and the end of experiment. Note: At start of experiment plants were at seedling stand and fully mature by the end of experiment. D= dry, I=interim, W= wet. Gray= no plant, Dark green= plant present.

**Table 2.1.** Soil properties. Mean  $\pm$  SD by hydrologic treatment and plant status. Abbreviations: MDL = Below detection limit, ppm = parts per million

	Dry		Interim		Wet	
	No Plant	Plant	No Plant	Plant	No Plant	Plant
Moisture %	39 $\pm$ 0.31	14 $\pm$ 0.03	19 $\pm$ 0.16	13 $\pm$ 0.02	29 $\pm$ 0.23	62 $\pm$ 0.07
pH	5.31 $\pm$ 0.11	5.31 $\pm$ 0.09	5.4 $\pm$ 0.16	5.35 $\pm$ 0.1	5.55 $\pm$ 0.15	5.41 $\pm$ 0.17
NH <sub>4</sub> <sup>+</sup> mg/L	0.39 $\pm$ 0.07	0.27 $\pm$ 0.04	0.26 $\pm$ 0.1	0.19 $\pm$ 0.02	0.77 $\pm$ 0.76	0.39 $\pm$ 0.42
NO <sub>3</sub> <sup>-</sup> mg/L	0.08 $\pm$ 0.07	MDL	0.25 $\pm$ 0.38	MDL	0.01 $\pm$ 0.0005	MDL
C%	4.63 $\pm$ 0.78	4.63 $\pm$ 0.81	4.48 $\pm$ 0.32	4.37 $\pm$ 0.52	4.91 $\pm$ 0.92	4.68 $\pm$ 0.74
N%	0.22 $\pm$ 0.03	0.22 $\pm$ 0.03	0.22 $\pm$ 0.01	0.21 $\pm$ 0.03	0.24 $\pm$ 0.04	0.23 $\pm$ 0.03
P ppm	21 $\pm$ 4.14	20.41 $\pm$ 4.4	23.58 $\pm$ 8.87	22.83 $\pm$ 8.37	23.16 $\pm$ 5.98	23 $\pm$ 5.79
K ppm	33.66 $\pm$ 5.97	30.25 $\pm$ 10.31	39.5 $\pm$ 11.44	26.75 $\pm$ 3.04	46.16 $\pm$ 16.02	34.25 $\pm$ 10.78
Mg ppm	77.58 $\pm$ 6.46	74.66 $\pm$ 11.43	86 $\pm$ 22.33	78.66 $\pm$ 16.47	89.25 $\pm$ 16.85	79.41 $\pm$ 18.8
S ppm	15.75 $\pm$ 1.94	15.33 $\pm$ 2.29	13.25 $\pm$ 1.25	12.16 $\pm$ 0.4	11.33 $\pm$ 1.21	11.5 $\pm$ 1
Fe ppm	252.66 $\pm$ 14.45	243.66 $\pm$ 17.06	275.33 $\pm$ 27.07	251.16 $\pm$ 37.6	306.83 $\pm$ 22.52	280.66 $\pm$ 40.71
Mn ppm	3.91 $\pm$ 1.15	3.41 $\pm$ 0.97	4.33 $\pm$ 1.16	4.58 $\pm$ 1.31	5.83 $\pm$ 1.32	5.58 $\pm$ 2.05
Humic Matter%	2.35 $\pm$ 0.19	2.17 $\pm$ 0.14	2.04 $\pm$ 0.29	2.28 $\pm$ 0.22	1.98 $\pm$ 0.422	1.96 $\pm$ 0.43

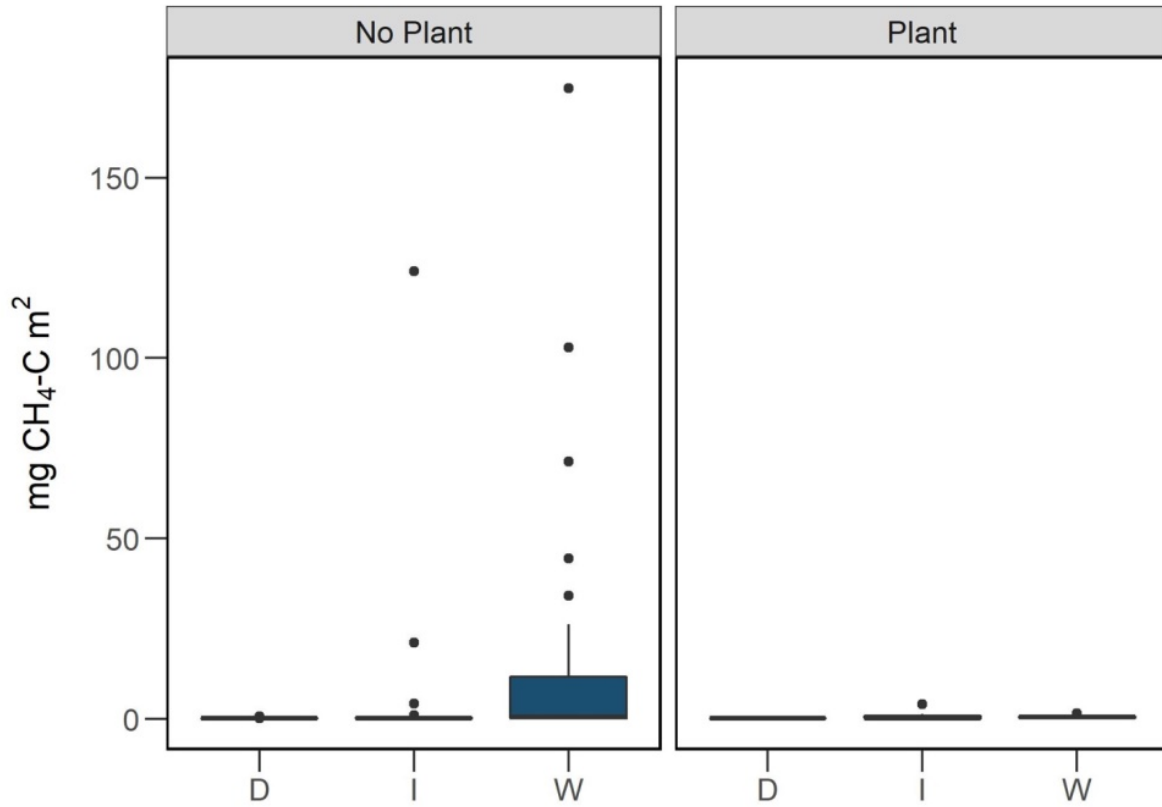


**Figure 2.4.** Boxplots of CH<sub>4</sub> concentrations by hydrologic treatment. Plot on left represents samples in no plant treatment and right represents plant treatment. D=dry, I= interim, W= wet.

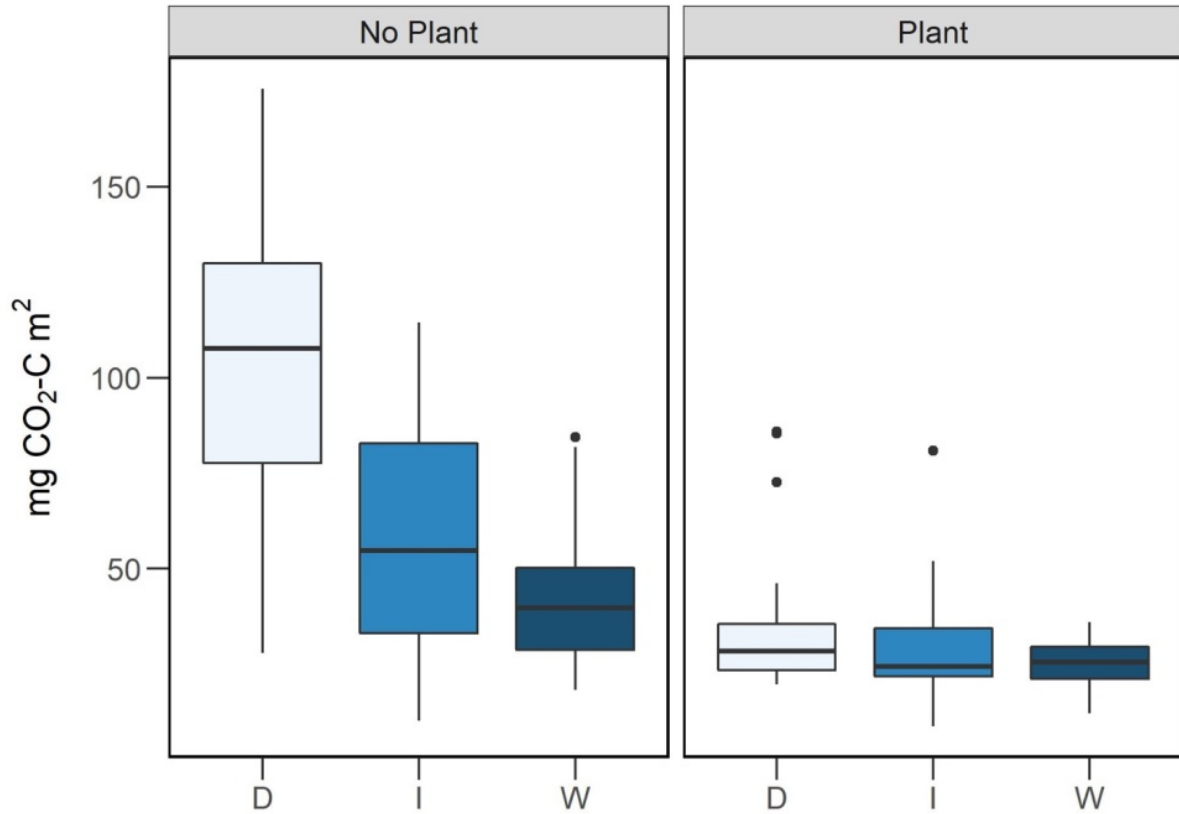


**Figure 2.5.** Boxplots of CO<sub>2</sub> concentrations by hydrologic treatment. Plot on left represents samples in no plant treatment and right represents plant treatment. D=dry, I= interim, W= wet.

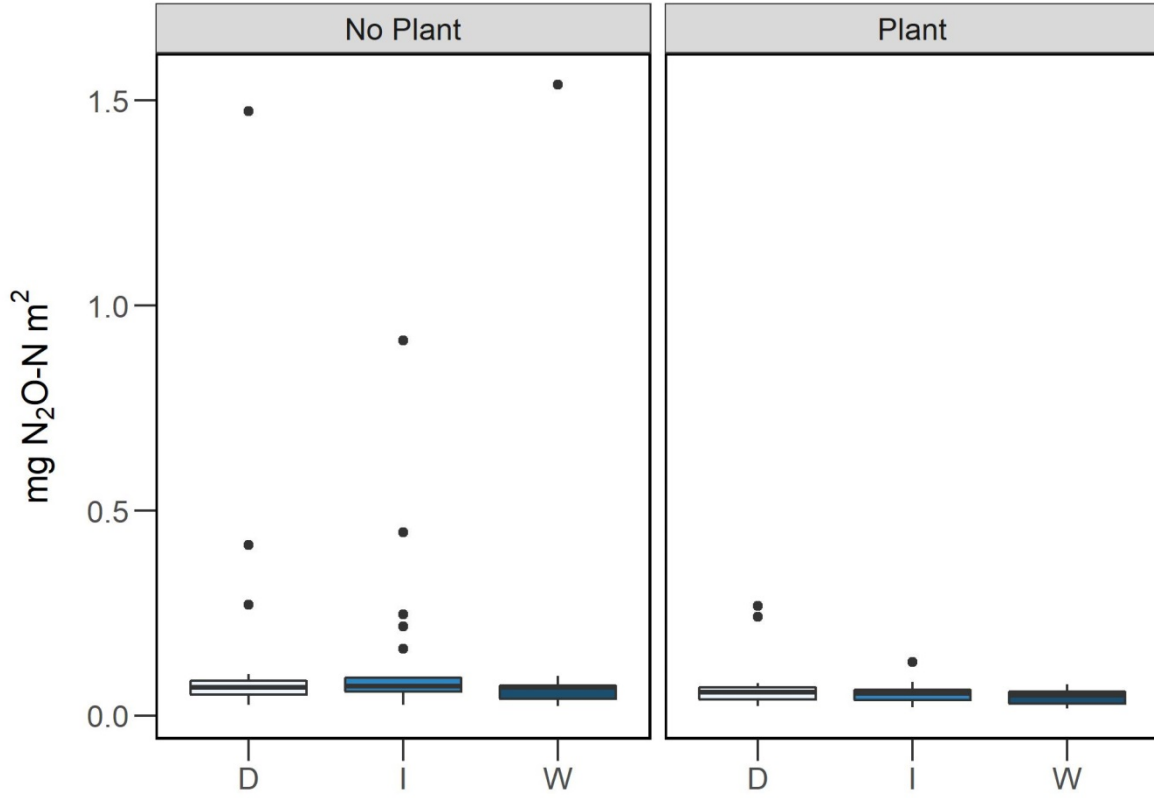


**Figure 2.6.** Boxplots of N<sub>2</sub>O concentrations by hydrology treatment. Plot on left represents samples in no plant treatment and right represents plant treatment. D=dry, I= interim, W= wet.

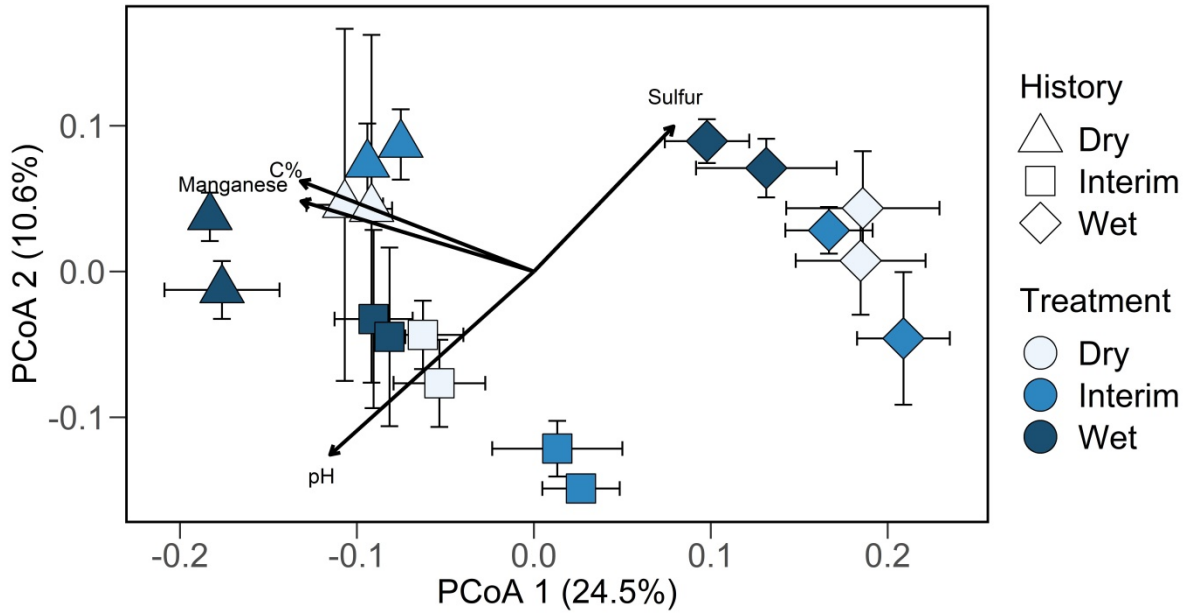


**Figure 2.7.** Ordination plot of PCoA analyses of bacterial and archaeal community composition based on Bray-Curtis dissimilarity matrix. Colors refer to hydrologic treatments white = dry, blue = interim, dark blue = wet. Shapes refer to hydrologic history of the sample: triangle = dry, square = interim, diamond = wet.

## Supplemental Figures and Tables

**Figure S2.1.** Indicator of Reduction in Soils (IRIS) tubes. Representative IRIS tubes collected from the dry hydrologic treatment without plants (A.) and without plants (B), wet treatment without plants (C), in wet treatment with plants (D).

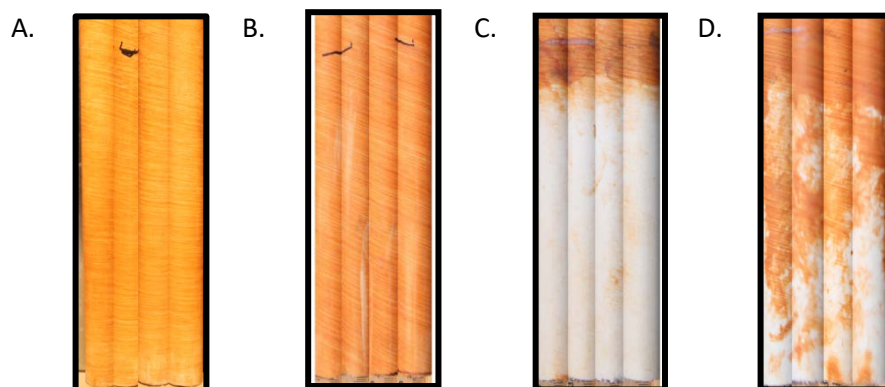


**Table S2.1.** Summary of mixed effects models to explain variation in greenhouse gas concentrations ( $\text{CH}_4$ ,  $\text{CO}_2$ ,  $\text{N}_2\text{O}$ ) due to hydrologic history, hydrologic treatment, and plant presence and random effects of sample plot and date. Fixed effects: H = hydrologic history (dry, interim, wet), T = hydrologic treatment, and P = plant.

Model	k	AICc	$\Delta\text{AICc}$	AICc Wt	$R^2$ Marg	$R^2$ Cond
$\text{CH}_4$						
P+T+H	9	455.64	0.00	0.45	0.32	0.60
P+T	7	457.25	1.61	0.20	0.26	0.60
T+H	8	457.63	1.98	0.17	0.28	0.60
Treatment	6	458.66	3.02	0.10	0.21	0.60
P*T	9	458.86	3.21	0.09	0.27	0.60
Plant	5	468.62	12.97	0.00	0.04	0.60
Null	4	468.84	13.20	0.00	-	0.60
P+H	7	469.19	13.54	0.00	0.10	0.60
History	6	469.61	13.96	0.00	0.06	0.60
P*T	9	470.51	14.87	0.00	0.27	0.60
$\text{CO}_2$						
P*T	9	184.92	0.00	0.93	0.52	0.60
P+T+H	9	191.00	6.08	0.04	0.50	0.60

P+T	7	191.95	7.03	0.03	0.48	0.60
Plant	5	210.43	25.51	0.00	0.32	0.60
H+P	7	212.05	27.13	0.00	0.35	0.60
H*P	9	215.29	30.37	0.00	0.36	0.60
Treatment	6	228.06	43.13	0.00	0.15	0.60
H+T	8	230.74	45.82	0.00	0.17	0.60
Null	4	233.27	48.35	0.00	-	0.60
History	6	236.25	51.33	0.00	0.02	0.60
<b>N<sub>2</sub>O</b>						
P+T	7	290.27	0.00	0.53	0.14	0.22
Plant	5	291.59	1.32	0.27	0.10	0.19
T*P	9	293.95	3.68	0.08	0.14	0.23
P+T+H	9	294.17	3.91	0.07	0.14	0.23
H+P	7	295.39	5.12	0.04	0.11	0.19
P*H	9	299.90	9.63	0.00	0.11	0.20
Treatment	6	305.97	15.70	0.00	0.03	0.14
Null	4	306.12	15.85	0.00	-	0.14
H+T	8	309.92	19.65	0.00	0.03	0.14
History	6	310.00	19.73	0.00	0.00	0.14

**Table S2.2.** Summary PERMANOVA comparing microbial community composition due to main effects (plant, hydrologic history, hydrologic treatment) and interaction between plant x history and plant x treatment. Bolded text indicates significant differences.

Main Effect	SumSq	F-value	R <sup>2</sup>	P-value
Plant	0.034	0.698	0.102	0.824
<b>History</b>	<b>0.743</b>	<b>7.562</b>	<b>0.305</b>	<b>0.001</b>
<b>Treatment</b>	<b>0.256</b>	<b>2.605</b>	<b>0.110</b>	<b>0.002</b>
Plant x History	0.066	0.667	0.027	0.942
Plant x Treatment	0.059	0.598	0.024	0.986

**Table S2.3.** Summary of bacterial and archaeal (OTUs) representative of hydrologic history based on indicator species analysis. These are the top OTUs (>2.5% relative abundance) that are significantly ( $p \leq 0.01$ ) associated with dry, interim, and wet hydrologic histories.

OTU_ID	Cluster	IndVal	Prob	Classification Domain; Phylum; Class; Order; Family; Genus
Otu00082	dry	0.675	0.001	Archaea; Thaumarchaeota; Nitrososphaerales; Nitrososphaeraceae; Nitrososphaera; Nitrososphaera
Otu00225	dry	0.475	0.008	Bacteria; Acidobacteria; Acidobacteria Gp1;
Otu00048	dry	0.426	0.006	Bacteria; Acidobacteria; Acidobacteria Gp2;
Otu00081	dry	0.502	0.001	Bacteria; Acidobacteria; Acidobacteria Gp3;
Otu00010	dry	0.433	0.001	Bacteria; Acidobacteria; Acidobacteria Gp6;
Otu00014	dry	0.443	0.007	Bacteria; Acidobacteria; Acidobacteria Gp6;
Otu00055	dry	0.413	0.009	Bacteria; Acidobacteria; Acidobacteria Gp6;
Otu00111	dry	0.551	0.002	Bacteria; Acidobacteria; Acidobacteria Gp6;
Otu00151	dry	0.552	0.002	Bacteria; Acidobacteria; Acidobacteria Gp6;
Otu00096	dry	0.535	0.001	Bacteria; Actinobacteria; Actinobacteria;
Otu00163	dry	0.506	0.002	Bacteria; Actinobacteria; Actinobacteria; Actinomycetales;
Otu00090	dry	0.476	0.001	Bacteria; Actinobacteria; Actinobacteria; Gaiellales; Gaiellaceae; Gaiella
Otu00101	dry	0.418	0.003	Bacteria; Actinobacteria; Actinobacteria; Gaiellales; Gaiellaceae; Gaiella
Otu00035	dry	0.497	0.001	Bacteria;
Otu00128	dry	0.498	0.002	Bacteria;
Otu00175	dry	0.487	0.001	Bacteria;
Otu00176	dry	0.398	0.01	Bacteria;
Otu00114	dry	0.517	0.001	Bacteria; Bacteroidetes; Sphingobacteriia; Sphingobacteriales; Chitinophagaceae; Chitinophagaceae
Otu00071	dry	0.443	0.002	Bacteria; Bacteroidetes; Sphingobacteriia; Sphingobacteriales; Chitinophagaceae; Terrimonas
Otu00274	dry	0.449	0.009	Bacteria; Firmicutes; Bacilli; Bacillales; Bacillaceae 1; Bacillaceae 1
Otu00250	dry	0.501	0.002	Bacteria; Planctomycetes; Planctomycetia; Planctomycetales; Planctomycetaceae; Planctomycetaceae
Otu00001	dry	0.381	0.007	Bacteria; Proteobacteria; Alphaproteobacteria; Rhizobiales;
Otu00040	dry	0.423	0.002	Bacteria; Proteobacteria; Alphaproteobacteria; Rhizobiales;
Otu00161	dry	0.438	0.004	Bacteria; Proteobacteria; Alphaproteobacteria; Rhodospirillales;
Otu00104	dry	0.546	0.001	Bacteria; Proteobacteria; Alphaproteobacteria; Sphingomonadales; Sphingomonadaceae;
Otu00042	dry	0.528	0.001	Bacteria; Proteobacteria; Betaproteobacteria;

Otu00049	dry	0.535	0.001	Bacteria; Proteobacteria; Betaproteobacteria;
Otu00169	dry	0.440	0.007	Bacteria; Proteobacteria; Deltaproteobacteria; Myxococcales; Myxococcales; Myxococcales
Otu00153	dry	0.766	0.001	Bacteria; Proteobacteria; Gammaproteobacteria;
Otu00170	dry	0.659	0.001	Bacteria; Proteobacteria; Gammaproteobacteria;
Otu00198	dry	0.708	0.001	Bacteria; Proteobacteria;
Otu00186	dry	0.554	0.004	Bacteria; Verrucomicrobia; Spartobacteria;
Otu00242	dry	0.471	0.001	Bacteria; Verrucomicrobia; Subdivision3;
Otu00018	interim	0.466	0.001	Bacteria; Acidobacteria; Acidobacteria Gp1;
Otu00058	interim	0.412	0.005	Bacteria; Acidobacteria; Acidobacteria Gp1;
Otu00106	interim	0.619	0.001	Bacteria; Acidobacteria; Acidobacteria Gp10;
Otu00056	interim	0.459	0.003	Bacteria; Acidobacteria; Acidobacteria Gp3;
Otu00092	interim	0.515	0.001	Bacteria; Acidobacteria; Acidobacteria Gp3;
Otu00122	interim	0.468	0.001	Bacteria; Acidobacteria; Acidobacteria Gp3;
Otu00112	interim	0.457	0.001	Bacteria; Acidobacteria; Acidobacteria Gp7;
Otu00032	interim	0.481	0.002	Bacteria;
Otu00057	interim	0.485	0.006	Bacteria;
Otu00311	interim	0.729	0.001	Bacteria;
Otu00221	interim	0.522	0.001	Bacteria; Chloroflexi; Ktedonobacteria; Ktedonobacterales; Ktedonobacterales; Ktedonobacterales
Otu00118	interim	0.436	0.006	Bacteria; Chloroflexi; Ktedonobacteria; Ktedonobacteria; Ktedonobacteria; Ktedonobacteria
Otu00059	interim	0.462	0.002	Bacteria; Planctomycetes; Planctomycetia; Planctomycetales; Planctomycetaceae;
Otu00087	interim	0.426	0.001	Bacteria; Planctomycetes; Planctomycetia; Planctomycetales; Planctomycetaceae;
Otu00174	interim	0.447	0.006	Bacteria; Planctomycetes; Planctomycetia; Planctomycetales; Planctomycetaceae;
Otu00017	interim	0.400	0.001	Bacteria; Proteobacteria; Alphaproteobacteria; Rhizobiales;
Otu00148	interim	0.460	0.002	Bacteria; Proteobacteria; Alphaproteobacteria; Rhizobiales;
Otu00164	interim	0.560	0.006	Bacteria; Proteobacteria; Betaproteobacteria;
Otu00166	interim	0.477	0.001	Bacteria; Proteobacteria; Betaproteobacteria;
Otu00072	interim	0.482	0.001	Bacteria; Proteobacteria; Deltaproteobacteria;
Otu00137	interim	0.543	0.005	Bacteria; Proteobacteria; Deltaproteobacteria; Desulfuromonadales; Geobacteraceae; Geobacter
Otu00291	wet	0.932	0.001	Archaea; Euryarchaeota; Methanobacteria; Methanobacteriales; Methanobacteriaceae; Methanobacterium
Otu00068	wet	0.712	0.001	Bacteria; Acidobacteria; Acidobacteria Gp1;

Otu00171	wet	0.441	0.006	Bacteria; Acidobacteria; Acidobacteria Gp1;
Otu00231	wet	0.504	0.005	Bacteria; Acidobacteria; Acidobacteria Gp1;
Otu00238	wet	0.678	0.001	Bacteria; Acidobacteria; Acidobacteria Gp1;
Otu00003	wet	0.563	0.001	Bacteria; Acidobacteria; Acidobacteria Gp1;
Otu00008	wet	0.482	0.001	Bacteria; Acidobacteria; Acidobacteria Gp1;
Otu00012	wet	0.669	0.001	Bacteria; Acidobacteria; Acidobacteria Gp1;
Otu00063	wet	0.551	0.001	Bacteria; Acidobacteria; Acidobacteria Gp1;
Otu00124	wet	0.735	0.001	Bacteria; Acidobacteria; Acidobacteria Gp1;
Otu00140	wet	0.628	0.001	Bacteria; Acidobacteria; Acidobacteria Gp1;
Otu00187	wet	0.861	0.001	Bacteria; Acidobacteria; Acidobacteria Gp1;
Otu00303	wet	0.491	0.001	Bacteria; Acidobacteria; Acidobacteria Gp1;
Otu00060	wet	0.455	0.009	Bacteria; Acidobacteria; Acidobacteria Gp2;
Otu00180	wet	0.624	0.001	Bacteria; Acidobacteria; Acidobacteria Gp2;
Otu00033	wet	0.413	0.01	Bacteria; Acidobacteria; Acidobacteria Gp3;
Otu00088	wet	0.424	0.01	Bacteria; Actinobacteria; Actinobacteria;
Otu00191	wet	0.415	0.004	Bacteria; Actinobacteria; Actinobacteria; Actinomycetales;
Otu00044	wet	0.438	0.001	Bacteria; Actinobacteria; Actinobacteria; Actinomycetales; Thermomonosporaceae; Actinoallomurus
Otu00025	wet	0.484	0.001	Bacteria; Actinobacteria; Actinobacteria; Solirubrobacterales;
Otu00075	wet	0.627	0.001	Bacteria;
Otu00113	wet	0.563	0.001	Bacteria;
Otu00117	wet	0.723	0.001	Bacteria;
Otu00165	wet	0.626	0.001	Bacteria;
Otu00177	wet	0.523	0.006	Bacteria;
Otu00211	wet	0.846	0.001	Bacteria;
Otu00220	wet	0.570	0.002	Bacteria;
Otu00105	wet	0.588	0.001	Bacteria; Chloroflexi;
Otu00070	wet	0.461	0.001	Bacteria; Proteobacteria; Alphaproteobacteria; Alphaproteobacteria incertae sedis; Rhizomicrobium; Rhizomicrobium
Otu00052	wet	0.426	0.002	Bacteria; Proteobacteria; Alphaproteobacteria;
Otu00099	wet	0.428	0.006	Bacteria; Proteobacteria; Alphaproteobacteria; Rhizobiales; Hyphomicrobiaceae; Rhodomicrobium
Otu00119	wet	0.657	0.001	Bacteria; Proteobacteria; Alphaproteobacteria; Rhizobiales; Methylocystaceae; Methylocystis
Otu00036	wet	0.421	0.008	Bacteria; Proteobacteria; Alphaproteobacteria; Rhizobiales; Roseiarcaceae; Roseiarcus
Otu00080	wet	0.670	0.002	Bacteria; Proteobacteria; Deltaproteobacteria; Desulfuromonadales; Geobacteraceae;

				Geobacter
Otu00192	wet	0.508	0.006	Bacteria; Proteobacteria; Deltaproteobacteria; Desulfuromonadales; Geobacteraceae; Geobacter
Otu00189	wet	0.641	0.001	Bacteria; Proteobacteria; Deltaproteobacteria; Syntrophobacterales; Syntrophobacteraceae; Syntrophobacter
Otu00181	wet	0.615	0.001	Bacteria; Proteobacteria; Gammaproteobacteria;
Otu00149	wet	0.631	0.001	Bacteria; Verrucomicrobia; Subdivision3;
Otu00183	wet	0.839	0.001	Bacteria; Verrucomicrobia; Subdivision3;

## References

- Albuquerque, L., França, L., Rainey, F.A., Schumann, P., Nobre, M.F., Da Costa, M.S., 2011. *Gaiella occulta* gen. nov., sp. nov., a novel representative of a deep branching phylogenetic lineage within the class Actinobacteria and proposal of Gaiellaceae fam. nov. and Gaiellales ord. nov. *Syst. Appl. Microbiol.* 34, 595–599. <https://doi.org/10.1016/j.syapm.2011.07.001>
- Apprill, A., McNally, S., Parsons, R., Weber, L., 2015. Minor revision to V4 region SSU rRNA 806R gene primer greatly increases detection of SAR11 bacterioplankton. *Aquat. Microb. Ecol.* 75, 129–137. <https://doi.org/10.3354/ame01753>
- Ardón, M., Morse, J.L., Colman, B.P., Bernhardt, E.S., 2013. Drought-induced saltwater incursion leads to increased wetland nitrogen export. *Glob. Chang. Biol.* 19, 2976–2985. <https://doi.org/10.1111/gcb.12287>
- Ardón, M., Morse, J.L., Doyle, M.W., Bernhardt, E.S., 2010. The Water Quality Consequences of Restoring Wetland Hydrology to a Large Agricultural Watershed in the Southeastern Coastal Plain. *Ecosystems* 13, 1060–1078. <https://doi.org/10.1007/s10021-010-9374-x>
- Barton, K., 2019. Package “MuMIn.”
- Bates, D., Machler, M., Bolker, B., Walker, S., 2015. Fitting Linear Mixed-Effects Models Using lme4. *J. Stat. Softw.* 67, 1–48. <https://doi.org/10.18637/jss.v067.i01>
- Boj, E., Caballe, A., Delicado, P., Fortiana, J., 2017. Package ‘dbstats.’
- Burgin, A.J., Yang, W.H., Hamilton, S.K., Silver, W.L., 2011. Beyond carbon and nitrogen: how the microbial energy economy couples elemental cycles in diverse ecosystems. *Front. Ecol. Environ.* 9, 44–52. <https://doi.org/10.1890/090227>
- Caporaso, J.G., Lauber, C.L., Walters, W. a, Berg-Lyons, D., Huntley, J., Fierer, N., Owens, S.M., Betley, J., Fraser, L., Bauer, M., Gormley, N., Gilbert, J. a, Smith, G., Knight, R., 2012. Ultra-high-throughput microbial community analysis on the Illumina HiSeq and MiSeq platforms. *ISME J.* 6, 1621–1624. <https://doi.org/10.1038/ismej.2012.8>
- Carmichael, M.J., Bernhardt, E.S., Bräuer, S.L., Smith, W.K., 2014. The role of vegetation in methane flux to the atmosphere: should vegetation be included as a distinct category in the global methane budget? *Biogeochemistry* 119, 1–24. <https://doi.org/10.1007/s10533-014-9974-1>
- Chanton, J.P., 2005. The effect of gas transport on the isotope signature of methane in wetlands. *Org. Geochem.* 36, 753–768. <https://doi.org/10.1016/j.orggeochem.2004.10.007>
- Conrad, R., 2009. The global methane cycle: recent advances in understanding the microbial processes involved. *Environ. Microbiol. Rep.* 1, 285–292. <https://doi.org/10.1111/j.1758-2229.2009.00038.x>

- Davidson, N.C., Fluet-Chouinard, E., Finlayson, C.M., 2018. Global extent and distribution of wetlands: Trends and issues. *Mar. Freshw. Res.* 69, 620–627. <https://doi.org/10.1071/MF17019>
- Fetzer, S., Bak, F., Conrad, R., 1993. Sensitivity of methanogenic bacteria from paddy soil to oxygen and desiccation. *FEMS Microbiol. Ecol.* 12, 107–115. <https://doi.org/10.1111/j.1574-6941.1993.tb00022.x>
- Gorsky, A.L., Racanelli, G.A., Belvin, A.C., Chambers, R.M., 2019. Greenhouse gas flux from stormwater ponds in southeastern Virginia (USA). *Anthropocene* 28. <https://doi.org/10.1016/j.ancene.2019.100218>
- Günther, A., Jurasinski, G., Huth, V., Glatzel, S., 2014. Opaque closed chambers underestimate methane fluxes of *Phragmites australis* (Cav.) Trin. ex Steud. *Environ. Monit. Assess.* 186, 2151–2158. <https://doi.org/10.1007/s10661-013-3524-5>
- Hoffmann, M., Pehle, N., Huth, V., Jurisch, N., Sommer, M., Augustin, J., 2018. A simple method to assess the impact of sealing, headspace mixing and pressure vent on airtightness of manually closed chambers. *J. Plant Nutr. Soil Sci.* 181, 36–40. <https://doi.org/10.1002/jpln.201600299>
- Hopfensperger, K.N., Burgin, A.J., Schoepfer, V.A., Helton, A.M., 2014. Impacts of Saltwater Incursion on Plant Communities, Anaerobic Microbial Metabolism, and Resulting Relationships in a Restored Freshwater Wetland. *Ecosystems* 17, 792–807. <https://doi.org/10.1007/s10021-014-9760-x>
- Hu, Q., Cai, J., Yao, B., Wu, Q., Wang, Y., Xu, X., 2015. Plant-mediated methane and nitrous oxide fluxes from a carex meadow in Poyang Lake during drawdown periods. *Plant Soil.* <https://doi.org/10.1007/s11104-015-2733-9>
- Hurvich, C., Tsai, C., 1993. A CORRECTED AKAIKE INFORMATION ON CRITERION FOR VECTOR AUTOREGRESSIVE MODEL SELECTION. *J. Time Ser. Anal.* 14, 271–279.
- Jenkinson, B.J., Franzmeier, D.P., 2006. Development and Evaluation of Iron-Coated Tubes that Indicate Reduction in Soils. *Soil Sci. Soc. Am. J.* 70, 183–191. <https://doi.org/10.2136/sssaj2004.0323>
- Kim, S.Y., Lee, S.H., Freeman, C., Fenner, N., Kang, H., 2008. Comparative analysis of soil microbial communities and their responses to the short-term drought in bog, fen, and riparian wetlands. *Soil Biol. Biochem.* 40, 2874–2880. <https://doi.org/10.1016/j.soilbio.2008.08.004>
- Kozich, J.J., Westcott, S.L., Baxter, N.T., Highlander, S.K., Schloss, P.D., 2013. Development of a dual-index sequencing strategy and curation pipeline for analyzing amplicon sequence data on the miseq illumina sequencing platform. *Appl. Environ. Microbiol.* 79, 5112–5120. <https://doi.org/10.1128/AEM.01043-13>

- Kuzyakov, Y., 2010. Soil Biology & Biochemistry Priming effects : Interactions between living and dead organic matter. *Soil Biol. Biochem.* 42, 1363–1371. <https://doi.org/10.1016/j.soilbio.2010.04.003>
- Lennon, J.T., Jones, S.E., 2011. Microbial seed banks: The ecological and evolutionary implications of dormancy. *Nat. Rev. Microbiol.* 9, 119–130. <https://doi.org/10.1038/nrmicro2504>
- Lew, S., Glińska-Lewczuk, K., 2018. Environmental controls on the abundance of methanotrophs and methanogens in peat bog lakes. *Sci. Total Environ.* 645, 1201–1211. <https://doi.org/10.1016/j.scitotenv.2018.07.141>
- Luan, J., Wu, J., 2014. Gross photosynthesis explains the “artificial bias” of methane fluxes by static chamber (opaque versus transparent) at the hummocks in a boreal peatland. *Environ. Res. Lett.* 9. <https://doi.org/10.1088/1748-9326/9/10/105005>
- McDonald, I.R., Murrell, J.C., 1997. The Methanol Dehydrogenase Structural Gene *mxnA* and Its Use as a Functional Gene Probe for Methanotrophs and Methylotrophs. *FEMS Microbiol. Lett.* 156, 205–210.
- Mehlich, A., 1984. Mehlich 3 Soil Test Extractant: A Modification of Mehlich 2 Extractant. *Commun. Soil Sci. Plant Anal.* 15, 1409–1416. <https://doi.org/10.1080/00103628409367568>
- Mentzer, J.L., Goodman, R.M., Balsler, T.C., 2006. Microbial response over time to hydrologic and fertilization treatments in a simulated wet prairie. *Plant Soil* 284, 85–100. <https://doi.org/10.1007/s11104-006-0032-1>
- Millar, N., Urrea, A., Kahmark, K., Shcherbak, I., Robertson, G.P., Ortiz-Monasterio, I., 2018. Nitrous oxide (N<sub>2</sub>O) flux responds exponentially to nitrogen fertilizer in irrigated wheat in the Yaqui Valley, Mexico. *Agric. Ecosyst. Environ.* 261, 125–132. <https://doi.org/10.1016/j.agee.2018.04.003>
- Mitsch, W.J., Bernal, B., Nahlik, A.M., Mander, Ü., Zhang, L., Anderson, C.J., Jørgensen, S.E., Brix, H., 2013. Wetlands, carbon, and climate change. *Landsc. Ecol.* 28, 583–597. <https://doi.org/10.1007/s10980-012-9758-8>
- Mitsch, W.J., Gosslink, J.G., 2007. *Wetlands*, 4th ed. John Wiley & Sons, Hoboken.
- Morse, J.L., Ardón, M., Bernhardt, E.S., 2012. Greenhouse gas fluxes in southeastern U.S. coastal plain wetlands under contrasting land uses. *Ecol. Appl.* 22, 264–280. <https://doi.org/10.1890/11-0527.1>
- Mylavarapu, R., Obreza, T., Morgan, K., Hochmuth, G., Nair, V., Wright, A., 2014. Extraction of Soil Nutrients Using Mehlich-3 Reagent for Acid-Mineral Soils of Florida. *Univ. Florida. Inst. Food Agric. Sci.* 1–7.
- Nygaard, B., Ejrnæs, R., 2009. The impact of hydrology and nutrients on species composition and richness: Evidence from a microcosm experiment. *Wetlands* 29, 187–195. <https://doi.org/10.1672/08-13.1>

- Oksanen, J., 2015. Vegan : ecological diversity 1, 1–12.  
<https://doi.org/10.1029/2006JF000545>
- Parada, A.E., Needham, D.M., Fuhrman, J.A., 2016. Every base matters: Assessing small subunit rRNA primers for marine microbiomes with mock communities, time series and global field samples. *Environ. Microbiol.* 18, 1403–1414.  
<https://doi.org/10.1111/1462-2920.13023>
- Peralta, Ariane L, Ludmer, S., Matthews, J.W., Kent, A.D., 2014. Bacterial community response to changes in soil redox potential along a moisture gradient in restored wetlands. *Ecol. Eng.* 73, 246–253. <https://doi.org/10.1016/j.ecoleng.2014.09.047>
- Peralta, Ariane L., Stuart, D., Kent, A.D., Lennon, J.T., 2014. A social-ecological framework for “micromanaging” microbial services. *Front. Ecol. Environ.* 12, 524–531.  
<https://doi.org/10.1890/130308>
- Philippot, L., Raaijmakers, J.M., Lemanceau, P., Van Der Putten, W.H., 2013. Going back to the roots: The microbial ecology of the rhizosphere. *Nat. Rev. Microbiol.* 11, 789–799. <https://doi.org/10.1038/nrmicro3109>
- Quast, C., Pruesse, E., Yilmaz, P., Gerken, J., Schweer, T., Yarza, P., Peplies, J., Glöckner, F.O., 2013. The SILVA ribosomal RNA gene database project: Improved data processing and web-based tools. *Nucleic Acids Res.* 41, 590–596.  
<https://doi.org/10.1093/nar/gks1219>
- R Core Team, 2019. R: A language and environment for statistical computing. R Found. Stat. Comput. Vienna, Austria.
- Rabenhorst, M.C., 2008. Protocol for Using and Interpreting IRIS Tubes. *Soil Surv. Horizons* 49, 74–77.
- Roberts, D., 2016. Package ‘labdsv .’
- Rocca, J.D., Hall, E.K., Lennon, J.T., Evans, S.E., Waldrop, M.P., Cotner, J.B., Nemergut, D.R., Graham, E.B., Wallenstein, M.D., 2015. Relationships between protein-encoding gene abundance and corresponding process are commonly assumed yet rarely observed. *ISME J.* 9, 1693–9.  
<https://doi.org/10.1038/ismej.2014.252>
- Rognes, T., Flouri, T., Nichols, B., Quince, C., Mahé, F., 2016. VSEARCH: a versatile open source tool for metagenomics. *PeerJ* 4, e2584.  
<https://doi.org/10.7717/peerj.2584>
- Schloss, P.D., Westcott, S.L., Ryabin, T., Hall, J.R., Hartmann, M., Hollister, E.B., Lesniewski, R. a., Oakley, B.B., Parks, D.H., Robinson, C.J., Sahl, J.W., Stres, B., Thallinger, G.G., Van Horn, D.J., Weber, C.F., 2009. Introducing mothur: Open-source, platform-independent, community-supported software for describing and comparing microbial communities. *Appl. Environ. Microbiol.* 75, 7537–7541.  
<https://doi.org/10.1128/AEM.01541-09>

- Schneider, C.A., Rasband, W.S., Eliceiri, K.W., 2012. NIH Image to ImageJ: 25 years of image analysis. *Nat. Methods* 9, 671–675. <https://doi.org/10.1038/nmeth.2089>
- Sundberg, C., Jenny, J.S., Tonderski, K., Lindgren, P.E., 2007. Overland flow systems for treatment of landfill leachates-Potential nitrification and structure of the ammonia-oxidising bacterial community during a growing season. *Soil Biol. Biochem.* 39, 127–138. <https://doi.org/10.1016/j.soilbio.2006.06.016>
- Truu, M., Juhanson, J., Truu, J., 2009. Microbial biomass, activity and community composition in constructed wetlands. *Sci. Total Environ.* 407, 3958–3971. <https://doi.org/10.1016/j.scitotenv.2008.11.036>

# CHAPTER 3: LONG-TERM NUTRIENT ENRICHMENT OF AN OLIGOTROPH-DOMINATED WETLAND INCREASES BACTERIAL DIVERSITY IN BULK SOILS AND PLANT RHIZOSPHERES

In Review at  
*mSphere*, 2020

## Abstract

In nutrient-limited conditions, plants rely on rhizosphere microbial members to facilitate nutrient acquisition, and in return plants provide carbon resources to these root-associated microorganisms. However, atmospheric nutrient deposition can affect plant-microbe relationships by changing soil bacterial composition and by decreasing cooperation between microbial taxa and plants. To examine how long-term nutrient addition shapes rhizosphere community composition, we compared traits associated with bacterial (fast growing copiotrophs, slow growing oligotrophs) and plant (C3 forb, C4 grass) communities residing in a nutrient poor wetland ecosystem. Results revealed that oligotrophic taxa dominated soil bacterial communities and that fertilization increased the presence of oligotrophs in bulk and rhizosphere communities. Additionally, bacterial species diversity was greatest in fertilized soils, particularly in bulk soils. Nutrient enrichment (fertilized vs. unfertilized) and plant association (bulk vs. rhizosphere) determined bacterial community composition; bacterial community structure associated with plant functional group (grass vs. forb) was similar within treatments but differed between fertilization treatments. The core forb microbiome consisted of 602 unique taxa, and the core grass microbiome consisted of 372 unique taxa. Forb rhizospheres were enriched in potentially disease suppressive bacterial taxa and grass rhizospheres were enriched in bacterial taxa associated with complex carbon

decomposition. Results from this study demonstrate that fertilization serves as a strong environmental filter on the soil microbiome, which leads to distinct rhizosphere communities and can shift plant effects of the rhizosphere microbiome. These taxonomic shifts within plant rhizospheres could have implications for plant health and ecosystem functions associated with carbon and nitrogen cycling.

### **Importance**

Over the last century, humans have substantially altered nitrogen and phosphorus cycling. Use of fertilizer and burning of fossil fuels and biomass have increased nitrogen and phosphorous deposition, which results in unintended fertilization of historically low-nutrient ecosystems. With increased nutrient availability, plant biodiversity is expected to decline and bacterial communities are anticipated to increase in abundance of copiotrophic taxa. Here, we address how bacterial communities associated with different plant functional types (forb, grass) shift due to long-term nutrient enrichment. Unlike other studies, results revealed an increase in bacterial diversity, particularly, of oligotrophic bacteria in fertilized plots. We observed that nutrient addition strongly determines forb and grass rhizosphere composition, which could indicate different metabolic preferences in the bacterial communities. This study highlights how long-term fertilization of oligotroph-dominated wetlands could alter the metabolism of rhizosphere bacterial communities in unexpected ways.

## Introduction

The soil microbiome is critical for plant health, fitness, and diversity, especially in nutrient-limited environments (Jach-Smith and Jackson, 2018; Regus et al., 2017; Van Der Heijden et al., 2008; Weese et al., 2014). In particular, within the rhizosphere plants provide carbon (C) resources to soil microorganisms in exchange for nutrients such as nitrogen (N) and phosphorus (P). However, nutrient enrichment has been documented to disrupt plant-microbe mutualisms (Weese et al., 2014). Over the last century, agricultural fertilization and the burning of fossil fuels and biomass have indirectly led to nutrient deposition onto historically low-nutrient ecosystems (Fowler et al., 2013; Galloway et al., 2004; Guignard et al., 2017; Wang et al., 2015). Nutrient enrichment generally causes decreased plant species diversity (Harpole et al., 2016; Wallis De Vries and Bobbink, 2017) sometimes as a shift in plant functional types with an increase in grass biomass and loss of forb diversity (Dickson and Foster, 2011; Song et al., 2011; Stevens et al., 2006). Fertilization has also been shown to decrease soil microbial diversity across cropland, grassland, forest, and tundra ecosystems (Wang et al., 2018; Zeng et al., 2016; Zhou et al., 2017). Despite patterns that have emerged from these bulk soil studies, it is less clear how changes in soil microbial diversity due to nutrient additions influence rhizosphere microbial community assembly and diversity. We address this knowledge gap by comparing changes in rhizosphere bacterial community composition of a grass and forb within a long-term fertilization experiment.

Both bulk soil matrix (i.e., not in contact with plant roots) properties and plant identity influences rhizosphere microbial communities. The bulk soil matrix is the reservoir of microbial diversity from which rhizosphere-associated microbial

communities are selected; therefore, shifts in bulk soil microbial communities affect rhizosphere assemblages (Bulgarelli et al., 2013; de Ridder-Duine et al., 2005; Mendes et al., 2014). In many cases N, N and P, and N-P-K fertilization decreases soil bacterial diversity (Wang et al., 2018; Zeng et al., 2016; Zhou et al., 2017). Additionally, nutrient enrichment selects for more copiotrophic (i.e., fast-growing, r-strategists) microbial heterotrophs that preferentially metabolize labile C sources versus oligotrophic (i.e., slow-growing, K-strategist) microbial species, which can metabolize complex C sources (Fierer et al., 2007; Goldfarb et al., 2011; Leff et al., 2015; Roller et al., 2016). A molecular marker to identify life history strategy (i.e., copiotroph or oligotroph) is rRNA (*rrn*) gene copy number (Klappenbach et al., 2000; Roller et al., 2016; Stevenson and Schmidt, 2004; Yano et al., 2013). Bacterial taxa are estimated to contain 1-15 rRNA gene copies, with faster growing taxa containing higher gene copies than slower growing taxa (Fierer et al., 2007; Klappenbach et al., 2000; Roller et al., 2016; Stevenson and Schmidt, 2004; Stoddard et al., 2015; Yano et al., 2013). Specifically, bacterial growth rate is limited by transcription rates of rRNA, such that growth rate is estimated to double with doubling of rRNA gene copy number. Further, several studies indicate fertilization increases the abundance of copiotrophic bacterial groups within Actinobacteria, Alphaproteobacteria, and Gammaproteobacteria and decreases abundance in oligotrophic bacterial groups within Acidobacteria, Nitrospirae, Planctomycetes, and Deltaproteobacteria of bulk soils (Francioli et al., 2016; Ho et al., 2017; Leff et al., 2015; Wang et al., 2018). Additionally, copiotrophic taxa within Alpha-, Beta-, and Gamma- Proteobacteria, Actinobacteria, Firmicutes and Bacteroidetes are

dominant members of some rhizosphere communities (Bulgarelli et al., 2013; Matthews et al., 2019; Zarraonaindia et al., 2015).

While the bulk soil environment is the primary source of rhizosphere diversity, plant species also influence rhizosphere bacterial community assembly due to variation in rhizodeposition (Lundberg et al., 2012; Matthews et al., 2019; Uroz et al., 2010; Zarraonaindia et al., 2015). Rhizodeposits include nutrients, exudates, root cells, and mucilage released by plant roots (Philippot et al., 2013a). Plants allocate 5-20% of photosynthetically fixed C belowground (Haichar et al., 2014; Hütsch et al., 2002; Jones et al., 2004). Some estimates suggest up to 40% of fixed C is translocated belowground (Jones et al., 2009), and grasses are suggested to be near that upper limit with ~30% of fixed C allocated belowground (Kuzyakov and Domanski, 2000). These rhizodeposits also include root exudates which are composed of sugars, organic acids, phenolic compounds, and amino acids (Bertin et al., 2003; Bulgarelli et al., 2013; Dakora and Phillips, 2002; Van Der Heijden et al., 2008). Differences in plant physiology influencing the quantity and composition of root exudates can affect rhizosphere bacterial community composition. For example, C<sub>4</sub> grasses have higher photosynthetic rates (i.e., fix more C) and greater root biomass allocation compared to C<sub>3</sub> plants, resulting in a greater quantity of root exudates (Kellogg, 2013; Schmitt and Edwards, 1981). C<sub>3</sub> plant root exudates can contain a greater variety of organic acids and amino acids along with the sugars mannose, maltose, and ribose compared to C<sub>4</sub> plant root exudates, which can contain several sugar alcohols (i.e., inositol, erythritol, and ribitol) (Vranova et al., 2013). However, N fertilization has been shown to increase C assimilation in plants but decrease belowground allocation of assimilated C while increasing total C into soils

as rhizodeposits (Kuzyakov et al., 2002; Kuzyakov and Domanski, 2000). Prior studies revealed that root exudation of organic C can be higher in both low-nutrient scenarios (Wu et al., 2012; Yin et al., 2013) and high nutrient scenarios (Phillips et al., 2009; Uselman et al., 2000). Further, differences in soil nutrient status can change the composition (i.e., carbohydrates, organic acids, and amino acid concentrations) of root exudates (Carvalhais et al., 2011; Wu et al., 2012). Thus, fertilization and plant specific rhizodeposition patterns of C3 forbs and C4 grasses are predicted to differentially affect rhizosphere bacterial community structure.

In this study, we address the following question: To what extent does long-term fertilization (N-P-K) of bulk soil shift rhizosphere bacterial communities of two plant species representing distinct functional types (i.e., a C3 forb and a C4 grass)? First, we hypothesize that nutrient addition will decrease bacterial species diversity and increase the abundance of copiotrophic taxa in all soils, especially rhizosphere soils due to increased availability of labile C from root exudates. We expect that fertilization will stimulate microbial activity of faster growing copiotrophic species, which could out compete slower growing oligotrophic species and result in decreased bacterial diversity. This effect is predicted to be amplified within plant rhizospheres due to the availability of labile C substrates in root exudates, which should preferentially select for copiotrophic bacteria. Second, we hypothesize that fertilization will be the primary factor determining differences in rhizosphere communities and plant identity will secondarily influence the rhizosphere community. If bulk soil is the reservoir for the rhizosphere community, then fertilization will determine rhizosphere bacterial diversity and community composition more strongly. In addition, plant type can also affect rhizosphere communities due to

differences in root exudate composition; however, fertilization effects will constrain rhizosphere effects. As a result, plant species are expected to associate with unique core microbiomes that differ between fertilization treatments.

To test these hypotheses, bulk and rhizosphere soils were sampled from two plant species (grass, forb) from fertilized and unfertilized plots at a long-term disturbance and fertilization experiment (established in 2003). Bacterial communities were identified using 16S rRNA amplicon sequencing which allowed binning of bacterial taxa as copiotrophic or oligotrophic by estimating the average rRNA (*rrn*) gene copy number. By evaluating differences in taxonomic information and 16S rRNA gene copy numbers of bulk and rhizosphere soils of two plant species with associated soil properties (i.e., ammonium, nitrate, soil pH, carbon, and moisture), we provide insight to biotic and abiotic processes that are contributing to rhizosphere bacterial community assembly.

## **Methods**

### *Study site and experimental design*

A long-term experimental site established in 2003 to test the effects of fertilization, mowing, and the interaction on wetland plant communities. The site is located at East Carolina University's West Research Campus in Greenville, North Carolina, USA (35.6298N, -77.4836W). A description of the study site and experimental design can be found in Goodwillie and Franch (2006) and is summarized here. This site is classified as a jurisdictional wetland but historically described as a mosaic of wet pine

flatwood habitat, pine savanna, and hardwood communities. Soils were characterized as fine, kaolinitic, thermic Typic Paleaquults (Coxville series) with a fine sandy loam texture which are ultisols that are acidic and moderate to poorly drained soil types (<https://soilseries.sc.egov.usda.gov/osdname.aspx>). The annual mean temperature is 17.2 °C and annual precipitation is 176 cm (<https://www.climate.gov/maps-data/dataset/>). Treatments are replicated on eight 20×30 m blocks, and the N-P-K 10-10-10 pellet fertilizer is applied 3× per year (February, June, and October) for a total annual supplementation of 45.4 kg ha<sup>-1</sup> for each nutrient. Plots are mowed by bush-hog and raked annually to simulate a fire disturbance (Goodwillie and Franch, 2006).

We compared rhizosphere and bulk soil microbiomes in mowed unfertilized and fertilized plots, where herbaceous species dominated. Soil samples were collected at mowed/unfertilized and mowed/fertilized plots in four out of eight replicate blocks to decrease variability due to hydrology. Half the site is located adjacent to a ditch (drier soils) compared to away from the ditch, where soil conditions are wetter. Since this hydrologic gradient has resulted in distinct plant communities (C. Goodwillie M.W. McCoy and A. L. Peralta, submitted for publication), we collected samples from the wetter plots (away from the drainage ditch).

#### *Bulk and rhizosphere soil sampling*

We collected soil samples on September 29, 2015, approximately three months after last fertilization treatment. Due to annual mowing and raking in sample plots, there was limited biomass accumulated in the organic horizon. We focused soil sampling and

analysis on the mineral horizon. For a single composite bulk soil sample, we collected two soil cores (12 cm depth, 3.1 cm diameter) near each of the three permanently installed 1 m<sup>2</sup> quadrats used for annual plant surveys. Each composite bulk soil sample was homogenized, passed through a 4 mm sieve, and any plant material removed before further analysis. At each plot, rhizosphere soils were collected from the C3 forb *Euthamia caroliniana* (L.) Greene ex Porter & Britton and C4 grass *Andropogon virginicus* L. Rhizosphere soils were a composite of three root systems of the same species. Roots were gently dislodged from soil and neighboring roots and placed in a paper bag. After vigorous shaking, soil in the bag was processed for abiotic analysis. The roots were placed into 50 mL centrifuge tubes with 30 mL sterilized Nanopure® water and shaken at 100 RPM for 1 hour. Washed roots were removed, and the rhizosphere soil and water mixture was freeze-dried to remove water. Freeze-dried rhizosphere samples were stored at -80 °C until DNA extraction.

#### *Soil chemical and physical characteristics*

We measured gravimetric soil moisture by drying 20-30 g of field-moist soil at 105 °C for 24 hours. We calculated percent moisture as the difference in weight of moist and dried soils divided by the oven-dried soil weight. Oven-dried samples were ground and measured for pH by mixing a 1:1 (soil:water) solution. A subsample of oven-dried soil was sieved with a 500 µm mesh and analyzed for total carbon and total nitrogen (TC, TN) using an elemental analyzer (2400 CHNS Analyzer; Perkin Elmer; Waltham, Massachusetts, USA) at the Environmental and Agricultural Testing Service laboratory

(Department of Crop and Soil Sciences at NC State). Approximately 5 g of field moist soil was extracted with 45 mL of 2 M KCl, and available ammonium ( $\text{NH}_4^+$ ) and nitrate ( $\text{NO}_3^-$ ) ions were colorimetrically measured using a SmartChem 200 auto analyzer (Unity Scientific Milford, Massachusetts, USA) at the East Carolina University Environmental Resources Laboratory.

### *Bacterial community analyses*

We extracted DNA from soils using the Qiagen DNeasy PowerSoil Kit. We used this DNA as template in PCR reactions using barcoded primers (bacterial 515FB/806R) originally developed by the Earth Microbiome Project to target the V4 region of the bacterial 16S subunit of the ribosomal RNA gene (Caporaso et al., 2012). For each sample, three 50  $\mu\text{L}$  PCR libraries were prepared by combining 30.75  $\mu\text{L}$  molecular grade water, 5  $\mu\text{L}$  Perfect Taq 10x buffer, 10  $\mu\text{L}$  Perfect Taq 5x buffer, 1  $\mu\text{L}$  dNTPs (40 mM total, 10 mM each), 0.25  $\mu\text{L}$  Perfect Taq polymerase, 1  $\mu\text{L}$  forward barcoded primer (10  $\mu\text{M}$ ), 1  $\mu\text{L}$  reverse primer (10  $\mu\text{M}$ ), and 1  $\mu\text{L}$  DNA template (10 ng  $\mu\text{L}^{-1}$ ). Thermocycler conditions for PCR reactions were as follows: initial denaturation (94 °C for 3 minutes); 30 cycles of 94 °C for 45 seconds, 50 °C for 30 seconds, 72 °C for 90 seconds; final elongation (72 °C, 10 minutes). Triplicate PCR reactions were combined and cleaned using the AMPure XP magnetic bead protocol (Axygen, Union City, California, USA). Cleaned PCR product were quantified using QuantIT dsDNA BR assay (Thermo Scientific, Waltham, Massachusetts, USA) and diluted to a concentration of 10 ng  $\mu\text{L}^{-1}$  before pooling libraries in equimolar concentration of 5 ng

$\mu\text{L}^{-1}$ . We sequenced pooled libraries using the Illumina MiSeq platform using paired end reads (Illumina Reagent Kit v2, 500 reaction kit) at the Indiana University Center for Genomics and Bioinformatics Sequencing Facility. Sequences were processed using mothur (v1.40.1) (Schloss et al., 2009) MiSeq pipeline (Kozich et al., 2013). We assembled contigs from the paired end reads, quality trimmed using a moving average quality score (minimum quality score 35), aligned sequences to the SILVA rRNA database (v128) (Quast et al., 2013), and removed chimeric sequences using the VSEARCH algorithm (Rognes et al., 2016). We created operational taxonomic units (OTUs) by first splitting sequences based on taxonomic class and then binning into OTUs based on 97% sequence similarity. The SILVA rRNA database (v128) (Quast et al., 2013) was then used to assign taxonomic designations to OTUs.

Samples were rarefied to the sample with the lowest read count (43,811) and resampled. We used *vegan::diversity* (Oksanen, 2015) to calculate bacterial species diversity as Shannon diversity index ( $H'$ ) because it accounts for species abundance and evenness and rare species (Kim et al., 2017; Shannon, 1948). We estimated bacterial richness using Chao1 species richness because it is non-parametric and also considers rare species (Chao, 1984; Kim et al., 2017). Chao1 OTU richness using *vegan::estimate* (Oksanen, 2015). We assigned gene copy number to each OTU using RDP classifier (v2.12) (Wang et al., 2007) integrated with the *rrn* operon database developed by the Schimdt Laboratory at the Michigan Microbiome Project, University of Michigan (Roller et al., 2016; Stoddard et al., 2015). Higher gene copy numbers ( $\geq 5$ ) represent the copiotrophic lifestyle and lower gene copy numbers ( $< 5$ ) represent the oligotrophic lifestyle (Fierer et al., 2007; Klappenbach et al., 2000; Roller and Schmidt,

2015). The number of copiotrophs and oligotrophs were summed for each soil sample to calculate the copiotroph to oligotroph ratio within a soil bacterial community.

### *Statistical analyses*

All statistical analyses were performed in the R statistical environment (RStudio v1.1.383, Rv3.4.0) (R Core Team, 2019). We used two-way model of analysis of variance (ANOVA) to compare main effects of soil source and fertilization treatment and the interaction to test for differences in OTU diversity and richness, copiotroph to oligotroph ratios, and soil parameters (soil pH, total carbon, extractable ammonium and nitrate total nitrogen, soil moisture). Significant interactions were compared with Tukey's post-hoc analysis using the *agricolae::HSD.test* R function (de Mendiburu, 2019). We examined diversity by visualizing bacterial community responses to fertilization and rhizosphere association using principal coordinates of analysis (PCoA) based on Bray-Curtis dissimilarity. We used permutational multivariate analysis of variance (PERMANOVA) to test for differences in bacterial community composition among treatments and within treatment using pairwise comparisons. Hypothesis testing using PERMANOVA was performed using the *vegan::adonis* function (Oksanen, 2015). We examined the relationship between soil parameters and bacterial Bray-Curtis dissimilarity patterns using the *vegan::envfit* function (Oksanen, 2015). Soil parameters with  $p < 0.05$  were represented on the PCoA plot as vectors scaled by strength of correlation. We performed Dufrene-Legendre indicator species analysis using the

*labdsv::indval* function (Roberts, 2016) to identify specific community members that represented each soil source and fertilization treatment combination.

## Results

Soil source and fertilization distinguishes soil properties. The main effect of fertilization was significantly different in the soil physiochemical property of pH ( $p=0.02$ ); and the main effect of soil source (bulk vs. rhizosphere) was significantly different in the soil physiochemical properties of pH ( $p < 0.001$ ), nitrate ( $p<0.0001$ ), C percent ( $p=0.03$ ), and N percent ( $p=0.04$ ; Table S3.1). Rhizosphere soils were more similar to each other in soil properties than to bulk soils (Table 3.1, Tukey HSD,  $p<0.05$ ). Specifically, bulk soil had lower total C and N, and nitrate concentrations than for rhizospheres with grass rhizospheres having the highest values (Table 3.1, Tukey HSD,  $p<0.05$ ). Soil pH was lowest in rhizosphere soils compared to bulk soils but higher in fertilized soils compared to unfertilized soils within soil sources (Table 3.1, Tukey HSD,  $p<0.05$ ).

Fertilization increased soil bacterial diversity in bulk and rhizosphere soils. Chao1 bacterial richness ( $p<0.0001$ ) and Shannon H' diversity ( $p<0.0001$ ) were higher in fertilized soils compared to unfertilized soils (Table S3.2, Fig. 3.1A). In addition, the main effect of soil source influenced bacterial diversity; bulk soil bacterial diversity was significantly higher than rhizosphere soil diversity (Tukey HSD,  $p<0.05$ , Table S3.2, Fig. 3.1B). Finally, results revealed a positive relationship between Shannon H' diversity and pH, where pH explained 71% ( $p=0.0003$ ) and 32% ( $p=0.03$ ) of the variation in bacterial

diversity in unfertilized and fertilized treatments, respectively, across all soil sources (Fig. 3.1C).

Copiotroph to oligotroph ratios indicated oligotroph-dominated bacterial communities. Across all samples we detected 9 to 30 copiotrophic and 82 to 190 oligotrophic taxa at the class level. This resulted in copiotroph to oligotroph ratios of < 0.2 within all treatment combinations. Nutrient additions significantly decreased the ratio of copiotrophs to oligotrophs in bulk soils compared to rhizosphere soils (Tukey's HSD,  $p < 0.05$ ; Table S3.3; Fig. 3.2). Finally, there was no relationship between bacterial Shannon H' diversity and copiotroph to oligotroph ratio ( $R^2 = -0.006$ ,  $p = 0.4$ ) (Fig. S3.1).

Fertilization treatment and soil source influenced bacterial community composition. Specifically, fertilization treatment (along PCoA axis 1) explained 31.6% of variation in bacterial community composition, while soil source (primarily bulk vs. rhizosphere) separated bacterial composition (along PCoA axis 2) and explained 22.5% of bacterial community variation (Fig. 3.3). Main effects of soil source (PERMANOVA  $R^2 = 0.23$ ,  $P = 0.001$ ) and fertilization treatment (PERMANOVA  $R^2 = 0.281$ ,  $P = 0.001$ ) influenced bacterial community composition (Table S3.4A). According to pairwise comparisons, rhizosphere bacterial community composition was similar between grass and forb rhizosphere samples within fertilization treatments (Table S3.4B). When examining relationships between community composition and soil characteristics, higher soil pH and moisture were correlated to fertilized bulk soils (Fig. 3.3). Further, higher concentrations of soil C and N were correlated with rhizosphere community composition (Fig. 3.3).

Different bacterial taxa (OTUs) represented fertilization treatments and plant species. We compared bacterial community taxonomic shifts in unfertilized and fertilized bulk soils and then grass and forb rhizospheres, concluding with differences in microbiome structure between the two plant species. Within bulk soil samples, important indicator species for bacterial communities within unfertilized plots were from the class Alphaproteobacteria with 1 OTU from the order Rhizobiales and 2 OTUs from Rhodospirillales and 3 OTUs from the class Spartobacteria (Table S3.5). In contrast, fertilized bulk soils were best represented by members of the class Actinobacteria with 1 OTU from the order Actinomycetales and 2 OTUs from the order Solirubrobacterales. While OTUs within Rhizobiales were identified as indicator species for bacterial communities in unfertilized bulk soils, this order was in greatest relative abundance compared to other orders within both fertilization treatments (Fig. S3.2).

Comparisons of rhizosphere bacterial OTU presence/absence data revealed that forb (1,249 OTUs) and grass (1,019 OTUs) rhizospheres have distinct but overlapping microbiomes. Of the 1,621 total OTUs found in rhizosphere soils, 647 are broadly-distributed and are observed in all plant rhizospheres and bulk soils regardless of treatment. Therefore, less than half of the forb (48%) and grass (37%) rhizosphere members were unique to that plant functional type, and broadly-distributed OTUs dominate plant microbiomes especially in grasses.

Of OTUs that were only represented in the grass microbiome (n=372), only 22 bacterial families are represented at > 0.075% relative abundance. Within those top OTUs, unfertilized grass rhizospheres were enriched in 9 families while fertilized plots were enriched in 19 families (Fig. 3.4). Indicator species for unfertilized grass

rhizospheres included 2 OTUs, one in the genus *Singulisphaera* and family Planctomycetaceae (IndVal = 0.38,  $P=0.026$ ) and an unclassified Spartobacteria OTU (IndVal = 0.44,  $P=0.008$ ; Table S3.5). Indicator species for fertilized grass rhizospheres included two OTUs, one in the genus *Planctomyces* and family Planctomycetaceae (IndVal = 0.42,  $P=0.011$ ) and one in the genus *Actinoallomurus* and family Thermomonosporaceae (IndVal = 0.36,  $P=0.045$ ; Table S3.5).

Of the OTUs that were only represented in the forb microbiome ( $n=602$ ), only 21 bacterial families are represented at  $> 0.1\%$  relative abundance. Within those top OTUs, unfertilized forb rhizospheres were enriched in 10 families while fertilized plots were enriched in 16 families (Fig. 3.5). Indicator species included two OTUs, Acidobacteria Gp1 (IndVal=0.42,  $P=0.02$ ), and an unclassified Proteobacteria (IndVal=0.46,  $P=0.033$ ; Table S3.5). Indicator species included an OTU in Acidobacteria Gp1 (IndVal= 0.34,  $P=0.041$ ) class and an unclassified bacterial OTU (IndVal=0.60,  $P=0.017$ ; Table S3.5).

## Discussion

In this study, nutrient addition increased bacterial species diversity ( $H'$ ) and richness in bulk and rhizosphere soils. These results were similar to O'Brien et al. (O'Brien et al., 2016) but contrary to our prediction and the results of other studies (Wang et al., 2018; Zeng et al., 2016; Zhou et al., 2017). Overall, bulk soils had the greatest bacterial diversity and highest pH values when compared to rhizosphere soils. Since pH is known to be a strong driver of bacterial diversity which can have a positive relationship to pH (Fierer and Jackson, 2006; Rousk et al., 2010), this increase in

diversity may, in part, be due to the greater bulk soil pH compared to rhizosphere soil. The difference in pH between soil types is possibly due to organic acids in plant root exudates released into the rhizosphere (Dakora and Phillips, 2002), however, we did not analyze the composition of root exudates. Additionally, pH tended to be lower in unfertilized treatments, and diversity was more strongly related to pH in unfertilized soils compared to fertilized soils. This may be due to sensitivity of bacteria to acidic soils (Fierer and Jackson, 2006). The increase in bacterial diversity is likely the result of soil pH and niche differentiation due to fertilization increasing nutrient availability and rhizodeposition by plants, which introduces organic C resources for heterotrophs (Bulgarelli et al., 2013; Lundberg et al., 2012). In dilution to extinction experiments, decreases in microbial diversity can result in loss of microbial functional diversity (Philippot et al., 2013b; Trivedi et al., 2019). Therefore, increases in microbial diversity could result in increased microbial functional diversity, which could increase C cycling and promote N mining particularly in plant rhizospheres (Weidner et al., 2015).

Bacterial taxa identified in rhizosphere samples are putatively involved in nutrient cycling and disease suppressive functions. For example, fertilized forb rhizospheres were enriched in taxa from the family Streptomycetaceae, of which many produce antibiotics (Kinkel et al., 2012) and Sphingomonadaceae, which include taxa with disease suppression potential against fungal pathogens (Chapelle et al., 2015) (Fig. 3.5). This increase in disease suppressive bacterial taxa suggest a potential increase in plant pathogenic taxa within fertilized rhizospheres; however, this study did not specifically address disease suppression in soils. In contrast, fertilized grass rhizospheres were enriched with taxa putatively involved in N<sub>2</sub>-fixation

(Acetobacteraceae) (Saravanan et al., 2008) and also Chitiniphagaceae and Conexibacteraceae, which have been implicated in decomposition of recalcitrant C sources (Deng et al., 2015; Seki et al., 2019) (Fig. 3.4). Bacterial taxa in the Xanthomonadaceae family, which have previously been found in environments containing glyphosate (Newman et al., 2016), and Caulobacteraceae, which grows optimally on pesticides (Lingens et al., 1985), are also more abundant in fertilized grass rhizospheres (Fig. 3.4). Since fertilization increased bacterial diversity and shifted composition, it is possible that fertilization has stimulated root exudation. The relative increase in complex C degrading bacterial taxa in the grass rhizosphere could be due to greater inputs of phenolics and terpenoids used as allelochemicals by the plant as revealed in past studies (Inderjit and Duke, 2003; Rice, 1972). These differences in bacterial composition between the two plants species could be due to differences in composition of root exudates released into the rhizosphere (Haichar et al., 2014), however, we did not analyze the composition of root exudates in the present study. Together, results suggest that nutrient addition enriches forb rhizospheres with putatively disease suppressive bacteria and grass rhizospheres with taxa capable of decomposing complex C sources.

Within bulk soil bacterial members, putative nitrogen cycling taxa in the order Rhizobiales were enriched across all fertilization treatments (Anderson et al., 2011; Rilling et al., 2018). This is not surprising considering the limited amount of nitrogen in both unfertilized and fertilized soils at the study site. Despite the increase in taxa capable of N<sub>2</sub>-fixation in fertilized rhizospheres, these bacteria will acquire soil N if it is available (Da Costa and Passaglia, 2015). Therefore, these taxa may be less

cooperative with plant associates than the same taxa from unfertilized soils thereby decreasing plant benefit (Ai et al., 2015; Weese et al., 2014). This was not specifically tested in this study but could be an important future research topic.

Contrary to our prediction, bulk soils had a higher copiotroph to oligotroph ratio (based on *rrn* gene copy number) than rhizospheres. Characteristic of the copiotrophic life history strategy is the ability to rapidly decompose labile C sources, therefore we expected that C rich root exudates in the rhizosphere would support higher proportions of copiotrophic species (Bulgarelli et al., 2013). Additionally, fertilization did not increase the relative abundance of copiotrophic taxa. Rather, the observed copiotroph to oligotroph ratios were low in all samples with unfertilized bulk soils having the greatest proportion (22%) and unfertilized grass rhizospheres having the lowest (13%) copiotroph to oligotroph ratios. We suggest that the dominance of oligotrophs reflects the low-nutrient history of this wetland (Ho et al., 2017; Song et al., 2016), which is in contrast to agricultural systems that undergo regular fertilization at rates intended to support high nutrient requirements for enhanced crop production (e.g., corn).

These results are in contrast to our first hypothesis and in agreement with our second hypothesis. Analyses of bacterial diversity and copiotroph to oligotroph ratios revealed an increase in bacterial diversity in response to fertilization and dominance of oligotrophs across all treatments within the study wetland. The low-nutrient history of the study site is likely the primary factor shaping bacterial community composition within the wetland. In agreement with our second hypothesis, comparisons of bulk and rhizosphere bacterial communities revealed that rhizospheres were more similar to each other than to bulk soil bacterial communities within fertilization treatments. Core plant

microbiomes were predominantly composed of broadly-distributed taxa; therefore, changes in bulk soil bacterial composition due to nutrient enrichment can directly alter plant microbiome composition and indirectly diminish benefits to plants if nutrient enrichment selects for more competitive bacterial taxa. These results highlight the importance of bulk soils as reservoirs of diversity for plant rhizospheres, which could have further implications for agricultural plant species in maintaining beneficial microbial communities.

Overall, this study revealed that long-term fertilization of oligotroph-dominated soils in low-nutrient wetlands increases bacterial species diversity. This increase in bacterial diversity has the potential to result in increased C and nutrient cycling that could lead to declines of wetland C storage potential. Nutrient enrichment also differentially alters plant rhizosphere composition in a way that suggests metabolic changes within soil bacterial communities. These metabolic changes could indirectly impact plant species diversity by providing an advantage to one species versus another through disease suppression or by increasing plant available N through promotion of soil organic matter decomposition. If indirect fertilization supports rhizosphere bacterial communities that can enhance recalcitrant or labile C decomposition, wetland C storage potential could decline. Based on this study, bacterial taxonomic characterization sheds light on fertilization effects on plant-bacterial relationships. As such, nutrient enrichment effects on the metabolic diversity of bacterial communities could be even more pronounced and warrants further investigation.

## **Acknowledgments**

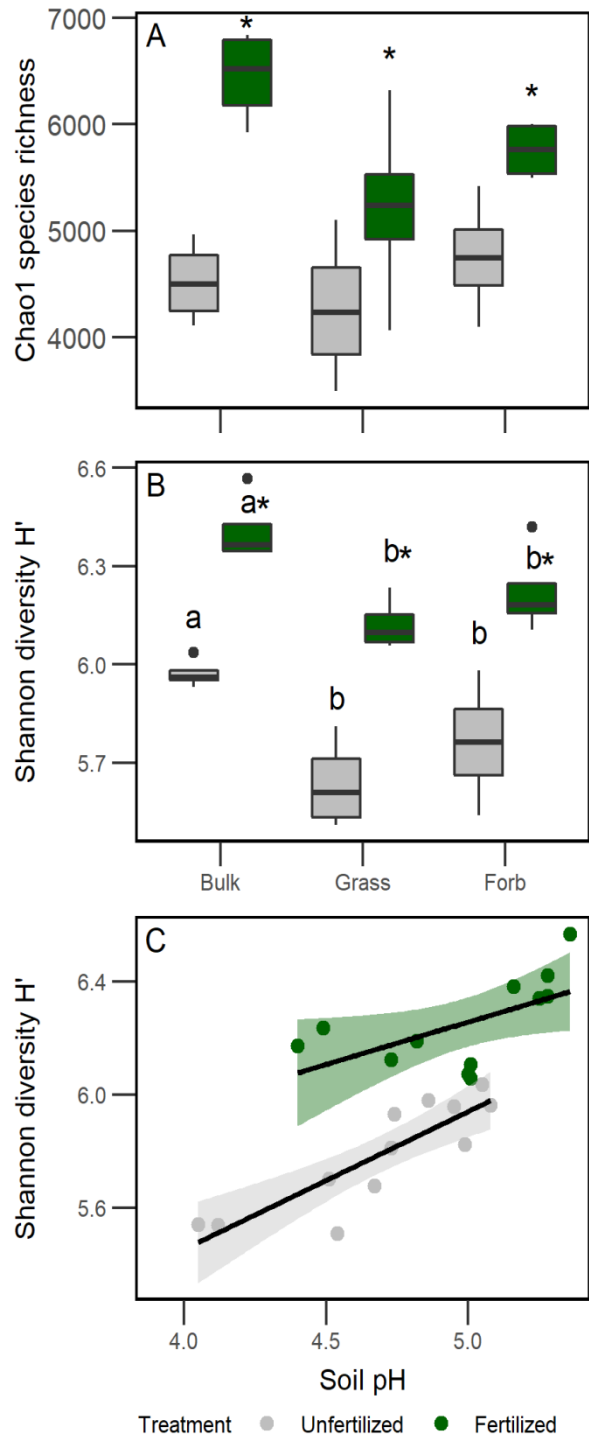
We thank M. Beamon, C. Eakins, J. LeCrone, J. Stiller, and S. Wilkinson for laboratory and field assistance. We thank J. Gill and the East Carolina University grounds crew for their efforts in maintaining the long-term ecological experiment. This work was supported by the National Science Foundation (GRFP to RBB and DEB 1845845 to ALP) and East Carolina University. We also thank two anonymous reviewers for their suggestions that greatly improved this manuscript. All code and data used in this study can be found in a public GitHub repository ([https://github.com/PeraltaLab/WRC15\\_Rhizo](https://github.com/PeraltaLab/WRC15_Rhizo)) and the NCBI SRA (BioProject PRJNA599142).

## Figures and Tables

**Table 3.1.** (A) Soil physiochemical properties after 12 years of fertilization and mowing disturbance. Average (mean  $\pm$  SD) soil properties (temperature, gravimetric moisture, pH, extractable nitrate and ammonium concentrations, total soil C and N, and C:N ratio) across unfertilized and fertilized plots and among soil sources (bulk, forb rhizosphere, and grass rhizosphere). Fertilization main effect that is significantly differently (ANOVA  $p < 0.05$ ) is bolded. Letters represent significant differences between soil sources (Tukey's HSD  $p < 0.05$ ).

	Unfertilized			Fertilized		
	Bulk	Forb	Grass	Bulk	Forb	Grass
Temperature °C	23.3 $\pm$ 0.4	-	-	22.8 $\pm$ 0.6	-	-
Moisture (%)	19.53 $\pm$ 0.39	19.18 $\pm$ 0.13	19.18 $\pm$ 0.10	19.45 $\pm$ 0.26	19.18 $\pm$ 0.15	19.15 $\pm$ 0.10 <b>b</b>
<b>pH</b>	<b>5.17 <math>\pm</math> 0.15 <i>a</i></b>	<b>4.62 <math>\pm</math> 0.39 <i>b</i></b>	<b>4.50 <math>\pm</math> 0.31 <i>b</i></b>	<b>5.38 <math>\pm</math> 0.08 <i>a</i></b>	<b>4.88 <math>\pm</math> 0.37 <i>b</i></b>	<b>4.81 <math>\pm</math> 0.25 <i>b</i></b>
<b>NO<sub>3</sub><sup>-</sup>-N (<math>\mu</math>g/g dry soil)</b>	0.31 $\pm$ 0.26 <b><i>b</i></b>	0.97 $\pm$ 0.28 <b><i>ab</i></b>	1.83 $\pm$ 0.55 <b><i>a</i></b>	0.41 $\pm$ 0.28 <b><i>b</i></b>	0.92 $\pm$ 0.42 <b><i>ab</i></b>	0.97 $\pm$ 0.25 <b><i>a</i></b>
NH <sub>4</sub> <sup>+</sup> -N ( $\mu$ g/g dry soil)	2.51 $\pm$ 0.71	2.37 $\pm$ 0.14	2.45 $\pm$ 0.90	2.64 $\pm$ 0.95	2.89 $\pm$ 0.65	2.53 $\pm$ 0.82
<b>Total C (%)</b>	3.52 $\pm$ 0.86 <b><i>a</i></b>	5.00 $\pm$ 1.02 <b><i>ab</i></b>	5.24 $\pm$ 1.03 <b><i>b</i></b>	3.81 $\pm$ 0.59 <b><i>a</i></b>	4.20 $\pm$ 0.46 <b><i>ab</i></b>	5.82 $\pm$ 2.71 <b><i>b</i></b>
<b>Total N (%)</b>	0.20 $\pm$ 0.05 <b><i>a</i></b>	0.27 $\pm$ 0.06 <b><i>ab</i></b>	0.29 $\pm$ 0.06 <b><i>b</i></b>	0.22 $\pm$ 0.03 <b><i>a</i></b>	0.24 $\pm$ 0.02 <b><i>ab</i></b>	0.33 $\pm$ 0.15 <b><i>b</i></b>
Soil C:N (wt:wt)	17.84 $\pm$ 1.21	18.91 $\pm$ 0.35	18.13 $\pm$ 1.02	17.31 $\pm$ 1.47	17.86 $\pm$ 0.38	17.62 $\pm$ 0.49

**Figure 3.1.** Bacterial diversity patterns according to soil source, fertilization, and soil pH. Boxplots of bacterial diversity for Chao1 richness (A) and Shannon H' diversity index (B) associated with soil source (bulk, grass rhizosphere, forb rhizosphere) and fertilization treatment. Linear regression of soil pH and bacterial community Shannon H' diversity by fertilization treatment with 95% confidence intervals (C); Fertilized:  $R^2=0.32$ ,  $p=0.03$ , Unfertilized:  $R^2=0.71$ ,  $p=0.0003$ . Colors indicate fertilization treatment (gray = unfertilized, green = fertilized) at mowed plots. Asterisks (\*) indicate significant differences between fertilization treatments and letters represent significant differences between soil sources (Tukey's HSD,  $p < 0.05$ ).



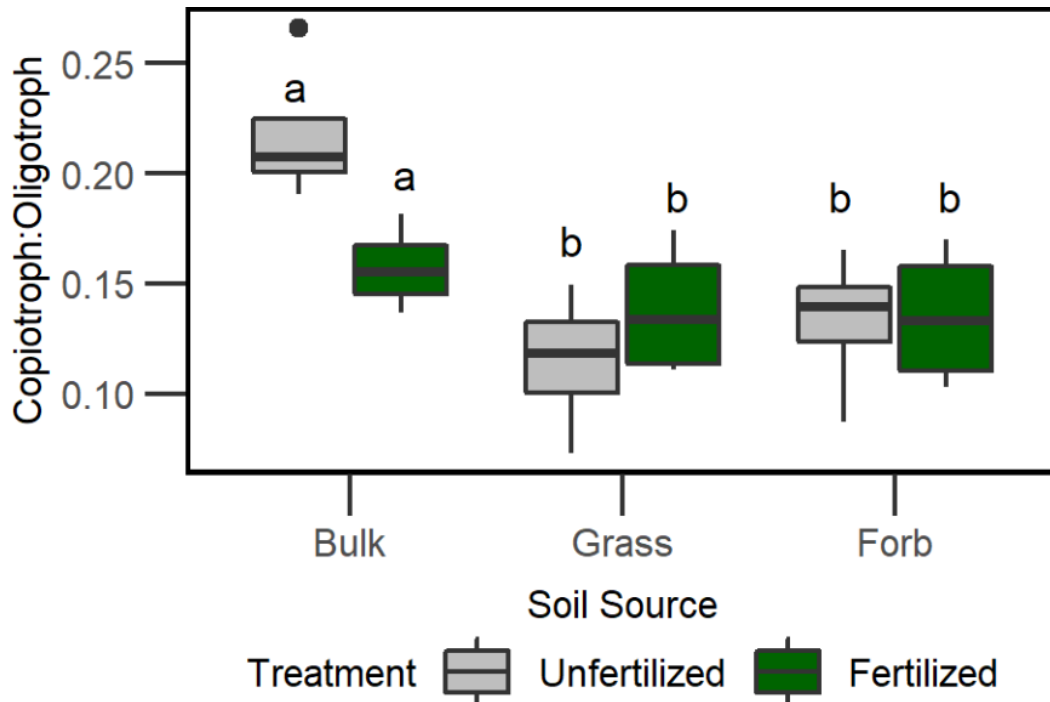


**Figure 3.2.** Comparison of bacterial life history traits. Boxplots of copiotroph to oligotroph ratios (based on 16S rRNA sequences) according to soil sources (bulk, grass rhizosphere, forb rhizosphere) and fertilization treatment. Boxplots are colored according to fertilization treatment (gray = unfertilized, green = fertilized). Letters indicate significant differences among soil sources (Tukey's HSD,  $p < 0.05$ ).

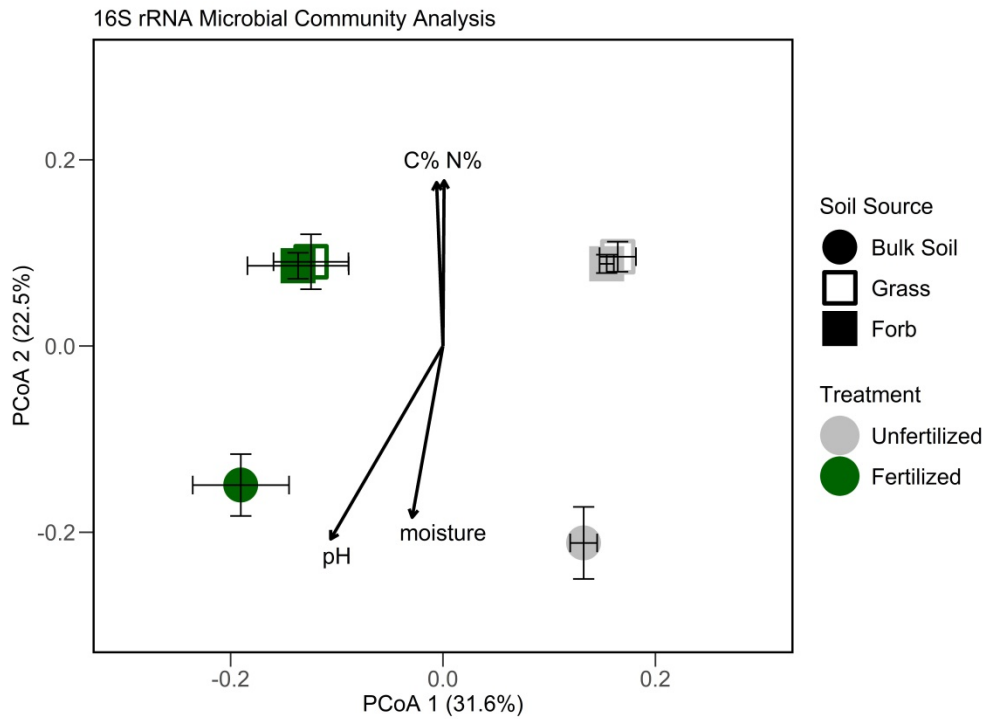


**Figure 3.3.** Ordination based on Principal Coordinates Analysis depicting bacterial community composition. Colors represent fertilization treatment (gray = unfertilized, green = fertilized) and symbols represent soil source (bulk soil = circle, grass rhizosphere = open square, forb rhizosphere = filled square). Vectors represent soil factors that are correlated to patterns in bacterial community composition ( $p < 0.05$ ) (pH = soil pH, moisture = soil gravimetric moisture percent, C% = total soil carbon, N% = total soil nitrogen).

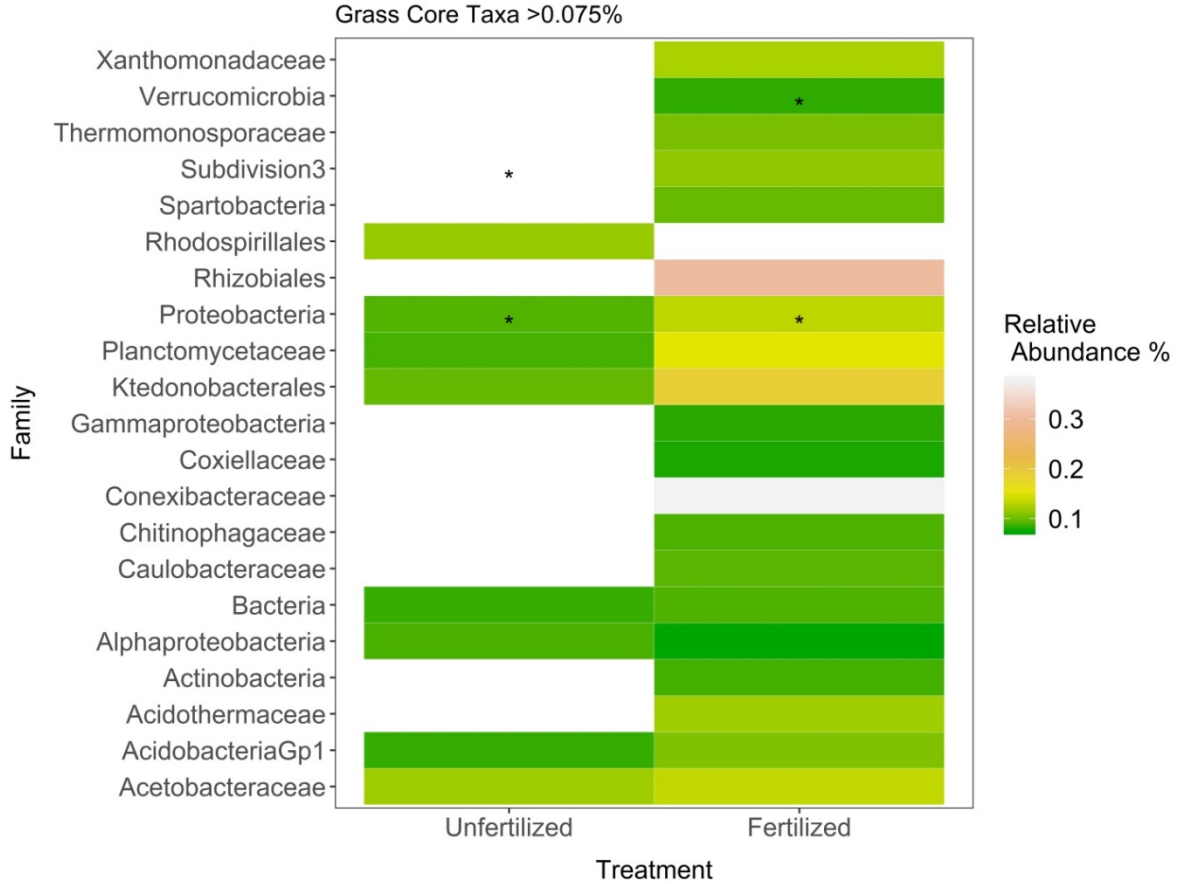


**Figure 3.4.** Comparisons of top OTU relative abundances (>0.075%) at the family level between fertilization treatments for grass rhizosphere bacterial communities. Asterisk (\*) represents indicator species present within family (Table S3.5). Colors indicate relative abundance increases from cool to warm (green yellow, orange, and red). White boxes indicate taxa present at <0.075% relative abundance.

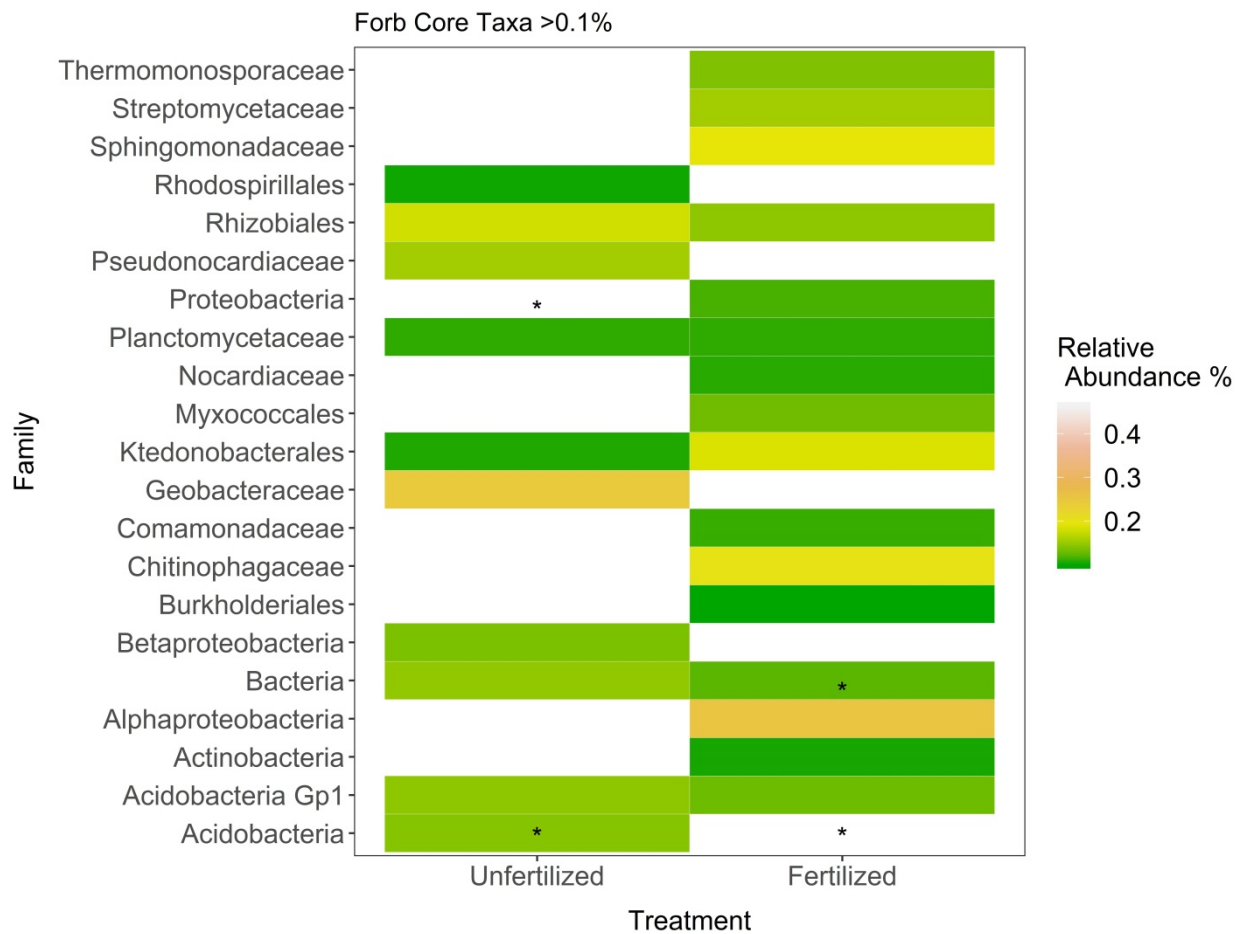


**Figure 3.5.** Comparisons of top OTU relative abundances (>0.1%) at the family level between fertilization treatments for forb rhizosphere bacterial communities. Asterisk (\*) represents indicator species present within family (Table S3.5). Colors indicate relative abundance increases from cool to warm (green yellow, orange, and red). White boxes indicate taxa present at <0.1% relative abundance.

## Supplemental Figures and Tables

**Table S3.1.** Summary of two-way ANOVA comparing soil properties among soil source (bulk, grass rhizosphere, forb rhizosphere) and fertilization treatments.

	Fertilization		Source		Fertilization x Source	
	F-value	P-value	F-value	P-value	F-value	P-value
Moisture (%)	0.04	0.85	2.71	0.09	0.12	0.89
<b>pH</b>	<b>6.43</b>	<b>0.02</b>	<b>5.83</b>	<b>0.01</b>	0.02	0.98
<b>NO<sub>3</sub><sup>-</sup>-N (µg/g dry soil)</b>	2.31	0.15	<b>11.52</b>	<b>0.001</b>	<b>3.95</b>	<b>0.04</b>
NH <sub>4</sub> <sup>+</sup> -N (µg/g dry soil)	0.08	0.77	0.07	0.93	0.52	0.60
<b>Total C (%)</b>	0.06	0.81	<b>3.96</b>	<b>0.04</b>	0.48	0.63
<b>Total N (%)</b>	0.001	0.97	<b>4.21</b>	<b>0.03</b>	0.26	0.78
Soil C:N (wt:wt)	1.13	0.30	0.78	0.47	1.47	0.26

**Table S3.2.** Summary of two-way ANOVA comparing bacterial community Chao1 richness (A) and Shannon H' diversity (B) metrics among soil source and fertilization treatments. Source represents bulk, grass rhizosphere, and forb rhizosphere and treatment represents fertilized and unfertilized mowed treatments. Main effects that were significantly different (ANOVA  $p < 0.05$ ) are bolded.

(A) Chao1 richness

Main Effect	SumSq	MeanSq	NumDF	F-value	Pr(>F)
Source	2323441	1161721	2	3.40	0.056
<b>Fertilization</b>	10062645	10062645	1	29.476	<b>&lt;0.0001</b>
Source x Fertilization	202762	101381	2	1.79	0.195

(B) Shannon diversity

Main Effect	SumSq	MeanSq	NumDF	F-value	Pr(>F)
<b>Source</b>	0.399	0.199	2	12.901	<b>0.0003</b>
<b>Fertilization</b>	1.278	1.278	1	82.705	<b>&lt;0.0001</b>
Source x Fertilization	0.003	0.015	2	0.082	0.922

**Table S3.3.** Summary of two-way ANOVA comparing bacterial community copiotroph to oligotroph ratio among soil source and fertilization treatments.

Main Effect	SumSq	MeanSq	NumDF	F-value	Pr(>F)
<b>Source</b>	0.757	0.379	2	7.257	<b>0.005</b>
Fertilization	0.007	0.007	1	0.136	0.717
Source x Fertilization	0.939	0.142	2	2.716	0.093

**Table S3.4.** Summary of PERMANOVA main effects (soil source and fertilization treatment) and interaction (A) and pairwise PERMANOVA comparisons of soil sources (bulk, grass rhizosphere, forb rhizosphere) within fertilization treatments (B).

(A) Main Effects

	SumSq	F-value	R <sup>2</sup>	P-value
<b>Source</b>	0.466	4.924	0.234	0.001
<b>Fertilization</b>	0.558	11.80	0.281	0.001
Source x Fertilization	0.114	1.202	0.057	0.257

(B) Pairwise PERMANOVA within fertilization treatments

Soil Sources	Unfertilized				Fertilized			
	SumSq	F-value	R <sup>2</sup>	P-value	SumSq	F-value	R <sup>2</sup>	P-value
<b>Bulk x Forb</b>	0.214	4.839	0.446	<b>0.033</b>	0.189	2.987	0.332	<b>0.024</b>
<b>Bulk x Grass</b>	0.215	5.123	0.461	<b>0.034</b>	0.169	3.011	0.334	<b>0.036</b>
Forb x Grass	0.035	0.819	0.120	0.557	0.072	1.223	0.169	0.186

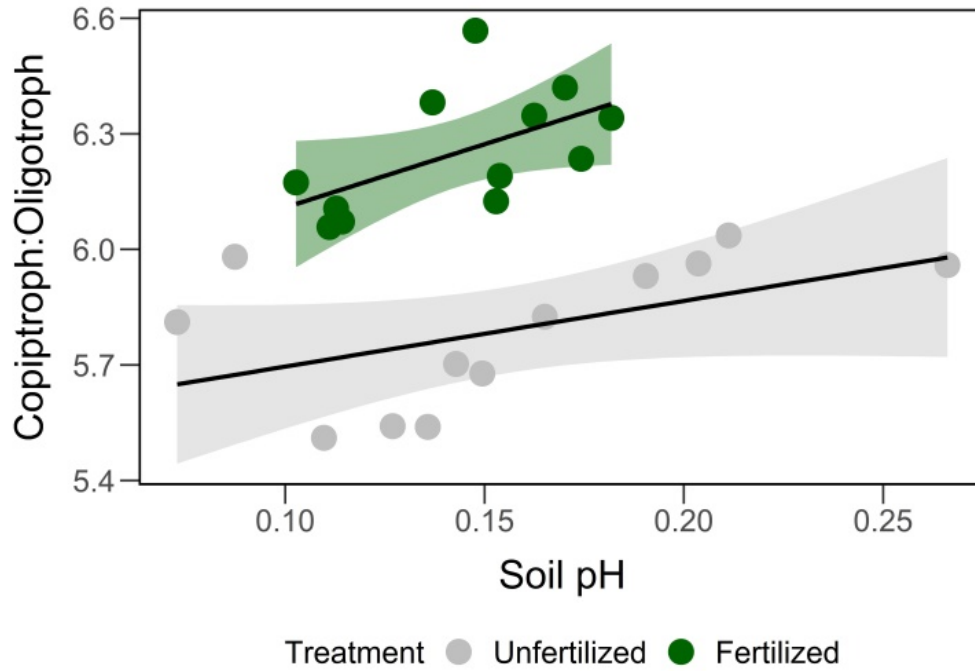


**Figure S3.1:** Linear regression of copiotroph to oligotroph ratio and Shannon diversity  $H'$  by fertilization treatment. Gray confidence bands represent 95% confidence intervals. Fertilized:  $R^2=-0.01$ ,  $p=0.38$ ; Unfertilized:  $R^2=0.14$ ,  $p=0.13$ .

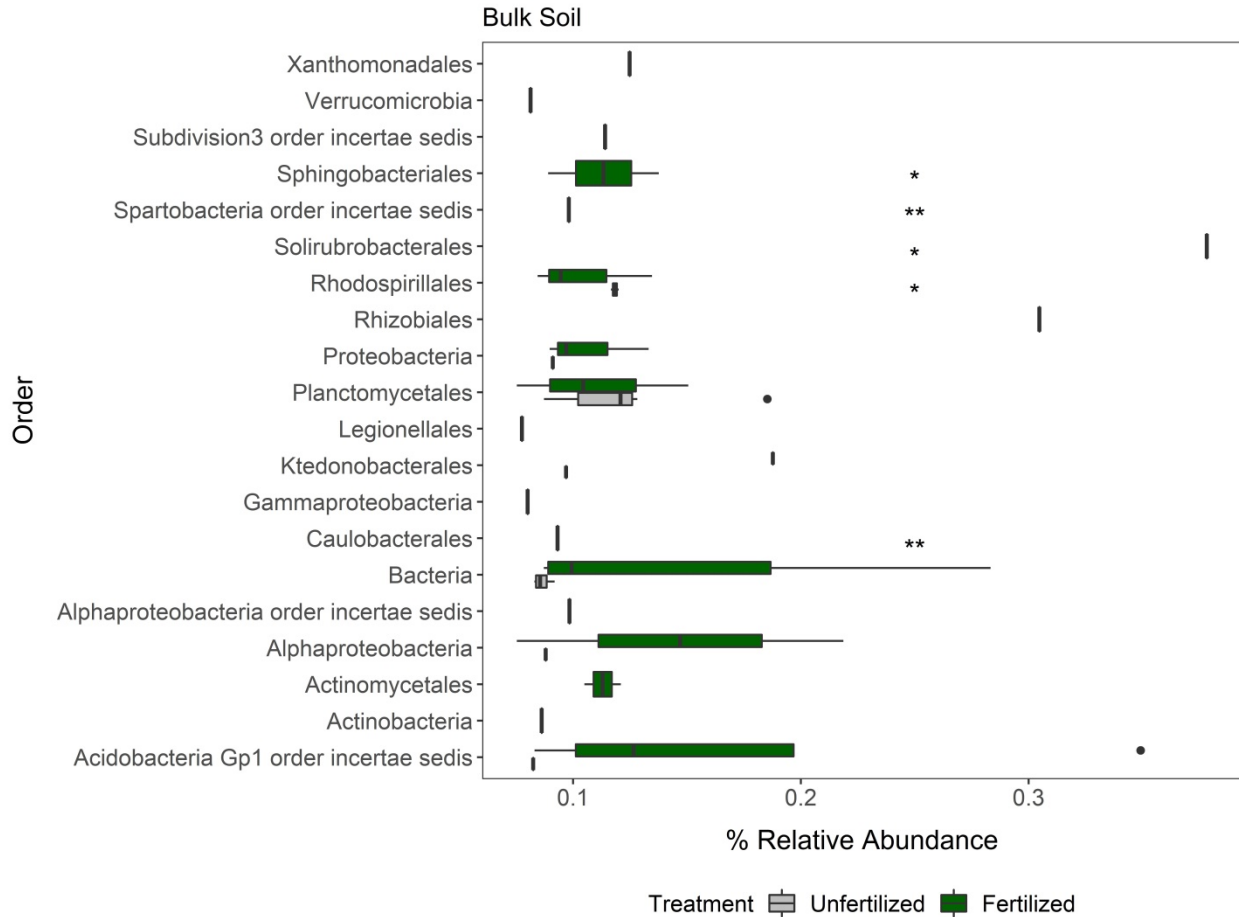


**Figure S3.2:** Comparisons of bulk soil top OTU relative abundances (>1%) grouped by Order. Single asterisk (\*) = indicator taxa for unfertilized treatment and double asterisk (\*\*) = indicator taxa for fertilized plots (Table S5). Boxplots are colored according to fertilization treatment (gray = unfertilized, green = fertilized).

**Table S3.5:** Summary of bacterial taxa (OTUs) characteristic to each soil source and fertilization treatment based on indicator species analysis. Listed are the top OTUs that are significantly associated with each soil source and fertilization treatment group.

OTU	Cluster	IndVal	Prob	Classification Phylum; Class; Order; Family; Genus
Otu0001 6	fertilized bulk	0.716	0.028	Actinobacteria; Actinobacteria; Solirubrobacterales; Solirubrobacterales; Solirubrobacterales
Otu0000 5	fertilized bulk	0.697	0.038	Actinobacteria; Actinobacteria; Solirubrobacterales; Solirubrobacterales; Solirubrobacterales
Otu0001 3	fertilized bulk	0.640	0.030	Actinobacteria; Actinobacteria; Actinomycetales; Thermomonosporaceae; Actinoallomurus
Otu0000 1	unfertilized bulk	0.592	0.022	Proteobacteria; Alphaproteobacteria; Rhizobiales; Rhizobiales ; Rhizobiales
Otu0003 9	unfertilized bulk	0.763	0.030	Proteobacteria; Alphaproteobacteria; Rhodospirillales; Rhodospirillales; Rhodospirillales
Otu0002 9	unfertilized bulk	0.713	0.034	Proteobacteria; Alphaproteobacteria; Rhodospirillales; Rhodospirillales; Rhodospirillales
Otu0006 4	unfertilized bulk	0.768	0.034	Proteobacteria; Alphaproteobacteria; Rhodospirillales; Rhodospirillales; Rhodospirillales
Otu0001 8	unfertilized bulk	0.723	0.030	Verrucomicrobia; Spartobacteria; Spartobacteria_order_incertae_sedis; Spartobacteria_family_incertae_sedis; Spartobacteria_genera_incertae_sedis
Otu0001 0	unfertilized bulk	0.642	0.033	Verrucomicrobia; Spartobacteria; Spartobacteria_order_incertae_sedis; Spartobacteria_family_incertae_sedis; Spartobacteria_genera_incertae_sedis
Otu0000 3	unfertilized bulk	0.706	0.035	Verrucomicrobia; Spartobacteria; Spartobacteria_order_incertae_sedis; Spartobacteria_family_incertae_sedis; Spartobacteria_genera_incertae_sedis
Otu0002 6	fertilized forb	0.341	0.041	Acidobacteria; Acidobacteria_Gp1; Acidobacteria_Gp1_order_incertae_sedis; Acidobacteria_Gp1_family_incertae_sedis ; Gp1
Otu0002	fertilized	0.595	0.017	Bacteria ; Bacteria ; Bacteria ; Bacteria ;

3	forb			Bacteria
Otu0004 4	unfertilized forb	0.418	0.020	Acidobacteria; Acidobacteria_Gp1; Acidobacteria_Gp1_order_incertae_sedis; Acidobacteria_Gp1_family_incertae_sedis ; Gp1
Otu0003 4	unfertilized forb	0.455	0.033	Proteobacteria; Proteobacteria ; Proteobacteria ; Proteobacteria ; Proteobacteria
Otu0002 7	fertilized grass	0.415	0.011	Planctomycetes; Planctomycetacia; Planctomycetales; Planctomycetaceae; Planctomyces
Otu0001 3	fertilized grass	0.358	0.045	Actinobacteria; Actinobacteria; Actinomycetales; Thermomonosporaceae; Actinoallomurus
Otu0002 4	unfertilized grass	0.384	0.026	Planctomycetes; Planctomycetacia; Planctomycetales; Planctomycetaceae; Singulisphaera
Otu0000 3	unfertilized grass	0.441	0.008	Verrucomicrobia; Spartobacteria; Spartobacteria_order_incertae_sedis; Spartobacteria_family_incertae_sedis; Spartobacteria_genera_incertae_sedis

## References

- Ai, C., Liang, G., Sun, J., Wang, X., He, P., Zhou, W., He, X., 2015. Reduced dependence of rhizosphere microbiome on plant-derived carbon in 32-year long-term inorganic and organic fertilized soils. *Soil Biol. Biochem.* 80, 70–78. <https://doi.org/10.1016/j.soilbio.2014.09.028>
- Anderson, C.R., Condron, L.M., Clough, T.J., Fiers, M., Stewart, A., Hill, R.A., Sherlock, R.R., 2011. Biochar induced soil microbial community change: Implications for biogeochemical cycling of carbon, nitrogen and phosphorus. *Pedobiologia (Jena)*. 54, 309–320. <https://doi.org/10.1016/j.pedobi.2011.07.005>
- Bertin, C., Yang, X., Weston, L.A., 2003. The role of root exudates and allelochemicals in the rhizosphere. *Plant Soil* 256, 67–83. <https://doi.org/10.1023/A:1026290508166>
- Bulgarelli, D., Schlaeppi, K., Spaepen, S., Ver Loren van Themaat, E., Schulze-Lefert, P., 2013. Structure and functions of the bacterial microbiota of plants. *Annu. Rev. Plant Biol.* 64, 807–38. <https://doi.org/10.1146/annurev-arplant-050312-120106>
- Caporaso, J.G., Lauber, C.L., Walters, W. a, Berg-Lyons, D., Huntley, J., Fierer, N., Owens, S.M., Betley, J., Fraser, L., Bauer, M., Gormley, N., Gilbert, J. a, Smith, G., Knight, R., 2012. Ultra-high-throughput microbial community analysis on the Illumina HiSeq and MiSeq platforms. *ISME J.* 6, 1621–1624. <https://doi.org/10.1038/ismej.2012.8>
- Carvalhais, L.C., Dennis, P.G., Fedoseyenko, D., Hajirezaei, M.R., Borriss, R., Von Wirén, N., 2011. Root exudation of sugars, amino acids, and organic acids by maize as affected by nitrogen, phosphorus, potassium, and iron deficiency. *J. Plant Nutr. Soil Sci.* 174, 3–11. <https://doi.org/10.1002/jpln.201000085>
- Chao, A., 1984. Board of the Foundation of the Scandinavian Journal of Statistics Nonparametric Estimation of the Number of Classes in a Population Author ( s ): Anne Chao Source : *Scandinavian Journal of Statistics* , Vol . 11 , No . 4 ( 1984 ) , pp . 265-270 Published by. *Scand. J. Stat.* 11, 265–270.
- Chapelle, E., Mendes, R., Bakker, P.A.H.M., Raaijmakers, J.M., 2015. Fungal invasion of the rhizosphere microbiome 10, 265–268. <https://doi.org/10.1038/ismej.2015.82>
- Da Costa, P.B., Passaglia, L.M.P., 2015. How Fertilization Affects the Selection of Plant Growth Promoting Rhizobacteria by Host Plants. *Biol. Nitrogen Fixat.* 2–2, 967–974. <https://doi.org/10.1002/9781119053095.ch95>
- Dakora, F.D., Phillips, D.A., 2002. Root exudates as mediators of mineral acquisition in low-nutrient environments. *Plant Soil* 245, 35–47. <https://doi.org/10.1023/A:1020809400075>
- de Mendiburu, F., 2019. R Package ‘ agricolae . ’
- de Ridder-Duine, A.S., Kowalchuk, G.A., Klein Gunnewiek, P.J.A., Smant, W., Van Veen, J.A., De Boer, W., 2005. Rhizosphere bacterial community composition in

- natural stands of *Carex arenaria* (sand sedge) is determined by bulk soil community composition. *Soil Biol. Biochem.* 37, 349–357.  
<https://doi.org/10.1016/j.soilbio.2004.08.005>
- Deng, J., Gu, Y., Zhang, J., Xue, K., Qin, Y., Yuan, M., Yin, H., He, Z., Wu, L., Schuur, E.A.G., Tiedje, J.M., Zhou, J., 2015. Shifts of tundra bacterial and archaeal communities along a permafrost thaw gradient in Alaska. *Mol. Ecol.* 24, 222–234.  
<https://doi.org/10.1111/mec.13015>
- Dickson, T.L., Foster, B.L., 2011. Fertilization decreases plant biodiversity even when light is not limiting. *Ecol. Lett.* 14, 380–388. <https://doi.org/10.1111/j.1461-0248.2011.01599.x>
- Fierer, N., Bradford, M.A., Jackson, R.B., 2007. Toward an Ecological Classification of Soil Bacteria. *Ecology* 88, 1354–1364. <https://doi.org/10.1890/05-1839>
- Fierer, N., Jackson, R.B., 2006. The diversity and biogeography of soil bacterial communities. *Proc. Natl. Acad. Sci. U. S. A.* 103, 626–631.  
<https://doi.org/10.1073/pnas.0507535103>
- Fowler, D., Coyle, M., Skiba, U., Sutton, M.A., Cape, J.N., Reis, S., Sheppard, L.J., Jenkins, A., Grizzetti, B., Galloway, J.N., Vitousek, P., Leach, A., Bouwman, A.F., Butterbach-Bahl, K., Dentener, F., Stevenson, D., Amann, M., Voss, M., 2013. The global nitrogen cycle in the Twentyfirst century. *Philos. Trans. R. Soc. B Biol. Sci.* 368. <https://doi.org/10.1098/rstb.2013.0164>
- Francioli, D., Schulz, E., Lentendu, G., Wubet, T., Buscot, F., Reitz, T., 2016. Mineral vs. organic amendments: Microbial community structure, activity and abundance of agriculturally relevant microbes are driven by long-term fertilization strategies. *Front. Microbiol.* 7, 1–16. <https://doi.org/10.3389/fmicb.2016.01446>
- Galloway, J.N., Dentener, F.J., Capone, D.G., Boyer, E.W., Howarth, R.W., Seitzinger, S.P., Asner, G.P., Cleveland, C.C., Green, P.A., Holland, E.A., Karl, D.M., Michaels, A.F., Porter, J.H., Townsend, A.R., Vörösmarty, C.J., 2004. Nitrogen cycles: Past, present, and future, *Biogeochemistry*. <https://doi.org/10.1007/s10533-004-0370-0>
- Goldfarb, K.C., Karaoz, U., Hanson, C.A., Santee, C.A., Bradford, M.A., Treseder, K.K., Wallenstein, M.D., Brodie, E.L., 2011. Differential growth responses of soil bacterial taxa to carbon substrates of varying chemical recalcitrance. *Front. Microbiol.* 2, 1–10.  
<https://doi.org/10.3389/fmicb.2011.00094>
- Goodwillie, C., Franch, W.R., 2006. An experimental study of the effects of nutrient addition and mowing on a ditched wetland plant community: Results of the first year. *J. North Carolina Acad. Sci.* 122, 106–117.
- Guignard, M.S., Leitch, A.R., Acquisti, C., Eizaguirre, C., Elser, J.J., Hessen, D.O., Jeyasingh, P.D., Neiman, M., Richardson, A.E., Soltis, P.S., Soltis, D.E., Stevens, C.J., Trimmer, M., Weider, L.J., Woodward, G., Leitch, I.J., 2017. Impacts of Nitrogen

- and Phosphorus: From Genomes to Natural Ecosystems and Agriculture. *Front. Ecol. Evol.* 5. <https://doi.org/10.3389/fevo.2017.00070>
- Haichar, F. el Z., Santaella, C., Heulin, T., Achouak, W., 2014. Root exudates mediated interactions belowground. *Soil Biol. Biochem.* 77, 69–80. <https://doi.org/10.1016/j.soilbio.2014.06.017>
- Harpole, W.S., Sullivan, L.L., Lind, E.M., Firn, J., Adler, P.B., Borer, E.T., Chase, J., Fay, P.A., Hautier, Y., Hillebrand, H., MacDougall, A.S., Seabloom, E.W., Williams, R., Bakker, J.D., Cadotte, M.W., Chaneton, E.J., Chu, C., Cleland, E.E., D'Antonio, C., Davies, K.F., Gruner, D.S., Hagenah, N., Kirkman, K., Knops, J.M.H., La Pierre, K.J., McCulley, R.L., Moore, J.L., Morgan, J.W., Prober, S.M., Risch, A.C., Schuetz, M., Stevens, C.J., Wragg, P.D., 2016. Addition of multiple limiting resources reduces grassland diversity. *Nature* 537, 93–96. <https://doi.org/10.1038/nature19324>
- Ho, A., Di Lonardo, D.P., Bodelier, P.L.E., 2017. Revisiting life strategy concepts in environmental microbial ecology. *FEMS Microbiol. Ecol.* 93. <https://doi.org/10.1093/femsec/fix006>
- Hütsch, B.W., Augustin, J., Merbach, W., 2002. Plant rhizodeposition an important source for carbon turnover in soils. *J. Plant Nutr. Soil Sci* 165, 397–407.
- Inderjit, Duke, S.O., 2003. Ecophysiological aspects of allelopathy. *Planta* 217, 529–539. <https://doi.org/10.1007/s00425-003-1054-z>
- Jach-Smith, L.C., Jackson, R.D., 2018. N addition undermines N supplied by arbuscular mycorrhizal fungi to native perennial grasses. *Soil Biol. Biochem.* 116, 148–157. <https://doi.org/10.1016/j.soilbio.2017.10.009>
- Jones, D.L., Hodge, A., Kuzyakov, Y., 2004. Plant and mycorrhizal regulation of rhizodeposition. *Tansley Review* 163:3 (September 2004). *New Phytol.* 163, 459–480. <https://doi.org/10.1111/j.1469-8137.2004.01130.x>
- Jones, D.L., Nguyen, C., Finlay, R.D., 2009. Carbon flow in the rhizosphere: Carbon trading at the soil-root interface. *Plant Soil* 321, 5–33. <https://doi.org/10.1007/s11104-009-9925-0>
- Kellogg, E.A., 2013. C4 photosynthesis. *Curr. Biol.* 23, R594–R599. <https://doi.org/10.1016/j.cub.2013.04.066>
- Kim, B.R., Shin, J., Guevarra, R.B., Lee, Jun Hyung, Kim, D.W., Seol, K.H., Lee, Ju Hoon, Kim, H.B., Isaacson, R.E., 2017. Deciphering diversity indices for a better understanding of microbial communities. *J. Microbiol. Biotechnol.* 27, 2089–2093. <https://doi.org/10.4014/jmb.1709.09027>
- Kinkel, L.L., Schlatter, D.C., Bakker, M.G., Arenz, B.E., 2012. *Streptomyces* competition and co-evolution in relation to plant disease suppression 163, 490–499.

- Klappenbach, J.A., Dunbar, J.M., Schmidt, T.M., 2000. rRNA operon copy number reflects ecological strategies of bacteria. *Appl. Environ. Microbiol.* 66, 1328–1333. <https://doi.org/10.1128/AEM.66.4.1328-1333.2000>
- Kozich, J.J., Westcott, S.L., Baxter, N.T., Highlander, S.K., Schloss, P.D., 2013. Development of a dual-index sequencing strategy and curation pipeline for analyzing amplicon sequence data on the miseq illumina sequencing platform. *Appl. Environ. Microbiol.* 79, 5112–5120. <https://doi.org/10.1128/AEM.01043-13>
- Kuzyakov, Y., Domanski, G., 2000. Carbon input by plants into the soil. *Review. J. Plant Nutr. Soil Sci.* 421–431.
- Kuzyakov, Y., Siniakina, S. V., Ruehlmann, J., Domanski, G., Stahr, K., 2002. Effect of nitrogen fertilisation on below-ground carbon allocation in lettuce. *J. Sci. Food Agric.* 82, 1432–1441. <https://doi.org/10.1002/jsfa.1202>
- Leff, J.W., Jones, S.E., Prober, S.M., Barberán, A., Borer, E.T., Firn, J.L., Harpole, W.S., Hobbie, S.E., Hofmockel, K.S., Knops, J.M.H., McCulley, R.L., La Pierre, K., Risch, A.C., Seabloom, E.W., Schütz, M., Steenbock, C., Stevens, C.J., Fierer, N., 2015. Consistent responses of soil microbial communities to elevated nutrient inputs in grasslands across the globe. *Proc. Natl. Acad. Sci.* 112, 10967–10972. <https://doi.org/10.1073/pnas.1508382112>
- Lingens, F., Blecher, R., Blecher, H., Blobel, F., Frohner, C., Gorisch, Helma, Gorisch, Helmut, Layh, A.N.D.G., 1985. *Phenylobacterium immobile* gen. nov. sp. nov. a Gram-Negative Bacterium That Degrades the Herbicide Chloridazon. *Int. J. Syst. BACTERIOLO* 26–39.
- Lundberg, D.S., Lebeis, S.L., Paredes, S.H., Yourstone, S., Gehring, J., Malfatti, S., Tremblay, J., Engelbrektson, A., Kunin, V., del Rio, T.G., Edgar, R.C., Eickhorst, T., Ley, R.E., Hugenholtz, P., Tringe, S.G., Dangl, J.L., 2012. Defining the core *Arabidopsis thaliana* root microbiome. *Nature* 488, 86–90. <https://doi.org/10.1038/nature11237>
- Matthews, A., Pierce, S., Hipperson, H., Raymond, B., 2019. Rhizobacterial Community Assembly Patterns Vary Between Crop Species. *Front. Microbiol.* 10, 1–13. <https://doi.org/10.3389/fmicb.2019.00581>
- Mendes, L.W., Kuramae, E.E., Navarrete, A.A., Van Veen, J.A., Tsai, S.M., 2014. Taxonomical and functional microbial community selection in soybean rhizosphere. *ISME J.* 8, 1577–1587. <https://doi.org/10.1038/ismej.2014.17>
- Newman, M.M., Hoilett, N., Lorenz, N., Dick, R.P., Liles, M.R., Ramsier, C., Kloepper, J.W., 2016. Glyphosate effects on soil rhizosphere-associated bacterial communities. *Sci. Total Environ.* 543, 155–160. <https://doi.org/10.1016/j.scitotenv.2015.11.008>
- O'Brien, S.L., Gibbons, S.M., Owens, S.M., Hampton-marcell, J., Johnston, E.R., Jastrow, J.D., Gilbert, J.A., Meyer, F., Antonopoulos, D.A., 2016. Spatial scale drives

- patterns in soil bacterial diversity 18, 2039–2051. <https://doi.org/10.1111/1462-2920.13231>
- Oksanen, J., 2015. Vegan : ecological diversity 1, 1–12. <https://doi.org/10.1029/2006JF000545>
- Philippot, L., Raaijmakers, J.M., Lemanceau, P., Van Der Putten, W.H., 2013a. Going back to the roots: The microbial ecology of the rhizosphere. *Nat. Rev. Microbiol.* 11, 789–799. <https://doi.org/10.1038/nrmicro3109>
- Philippot, L., Spor, A., Hénault, C., Bru, D., Bizouard, F., Jones, C.M., Sarr, A., Maron, P.A., 2013b. Loss in microbial diversity affects nitrogen cycling in soil. *ISME J.* 7, 1609–1619. <https://doi.org/10.1038/ismej.2013.34>
- Phillips, R.P., Bernhardt, E.S., Schlesinger, W.H., 2009. Elevated CO<sub>2</sub> increases root exudation from loblolly pine (*Pinus taeda*) seedlings as an N-mediated response. *Tree Physiol.* 29, 1513–1523. <https://doi.org/10.1093/treephys/tpp083>
- Quast, C., Pruesse, E., Yilmaz, P., Gerken, J., Schweer, T., Yarza, P., Peplies, J., Glöckner, F.O., 2013. The SILVA ribosomal RNA gene database project: Improved data processing and web-based tools. *Nucleic Acids Res.* 41, 590–596. <https://doi.org/10.1093/nar/gks1219>
- R Core Team, 2019. R: A language and environment for statistical computing. R Found. Stat. Comput. Vienna, Austria.
- Regus, J.U., Wendlandt, C.E., Bantay, R.M., Gano-Cohen, K.A., Gleason, N.J., Hollowell, A.C., O'Neill, M.R., Shahin, K.K., Sachs, J.L., 2017. Nitrogen deposition decreases the benefits of symbiosis in a native legume. *Plant Soil* 414, 159–170. <https://doi.org/10.1007/s11104-016-3114-8>
- Rice, E.L., 1972. Allelopathic Effects of *Andropogon Virginicus* and Its Persistence in Old Fields. *Am. J. Bot.* 59, 752–755. <https://doi.org/10.1002/j.1537-2197.1972.tb10148.x>
- Rilling, J.I., Acuña, J.J., Sadowsky, M.J., Jorquera, M.A., 2018. Putative nitrogen-fixing bacteria associated with the rhizosphere and root endosphere of wheat plants grown in an andisol from southern Chile. *Front. Microbiol.* 9, 1–13. <https://doi.org/10.3389/fmicb.2018.02710>
- Roberts, D., 2016. Package 'labdsv.'
- Rognes, T., Flouri, T., Nichols, B., Quince, C., Mahé, F., 2016. VSEARCH: a versatile open source tool for metagenomics. *PeerJ* 4, e2584. <https://doi.org/10.7717/peerj.2584>
- Roller, B.R.K., Schmidt, T.M., 2015. The physiology and ecological implications of efficient growth. *ISME J.* 9, 1481–1487. <https://doi.org/10.1038/ismej.2014.235>

- Roller, B.R.K., Stoddard, S.F., Schmidt, T.M., 2016. Exploiting rRNA operon copy number to investigate bacterial reproductive strategies. *Nat. Microbiol.* 1, 1–19. <https://doi.org/10.1038/nmicrobiol.2016.160>
- Rousk, J., Bååth, E., Brookes, P.C., Lauber, C.L., Lozupone, C., Caporaso, J.G., Knight, R., Fierer, N., 2010. Soil bacterial and fungal communities across a pH gradient in an arable soil. *ISME J.* 4, 1340–1351. <https://doi.org/10.1038/ismej.2010.58>
- Saravanan, V.S., Madhaiyan, M., Osborne, J., Thangaraju, M., Sa, T.M., 2008. Ecological occurrence of *Gluconacetobacter diazotrophicus* and nitrogen-fixing *Acetobacteraceae* members: Their possible role in plant growth promotion. *Microb. Ecol.* 55, 130–140. <https://doi.org/10.1007/s00248-007-9258-6>
- Schloss, P.D., Westcott, S.L., Ryabin, T., Hall, J.R., Hartmann, M., Hollister, E.B., Lesniewski, R. a., Oakley, B.B., Parks, D.H., Robinson, C.J., Sahl, J.W., Stres, B., Thallinger, G.G., Van Horn, D.J., Weber, C.F., 2009. Introducing mothur: Open-source, platform-independent, community-supported software for describing and comparing microbial communities. *Appl. Environ. Microbiol.* 75, 7537–7541. <https://doi.org/10.1128/AEM.01541-09>
- Schmitt, M.R., Edwards, G.E., 1981. Photosynthetic Capacity and Nitrogen Use Efficiency of Maize , Wheat , and Rice : A Comparison Between C 3 and C 4 Photosynthesis content in a trusted digital archive . We use information technology and tools to increase productivity and facilitate new fo. *J. Exp. Bot.* 32, 459–466.
- Seki, T., Matsumoto, A., Shimada, R., Inahashi, Y., 2019. *Conexibacter arvalis* sp . nov ., isolated from a cultivated field soil sample 2400–2404. <https://doi.org/10.1099/ijs.0.036095-0>
- Shannon, C.E., 1948. A Mathematical Theory of Communication. *Bell Syst. Tech. J.* 27, 379–423. <https://doi.org/10.1002/j.1538-7305.1948.tb01338.x>
- Song, L., Bao, X., Liu, X., Zhang, Y., Christie, P., Fangmeier, A., Zhang, F., 2011. Nitrogen enrichment enhances the dominance of grasses over forbs in a temperate steppe ecosystem. *Biogeosciences* 8, 2341–2350. <https://doi.org/10.5194/bg-8-2341-2011>
- Song, W., Kim, M., Tripathi, B.M., Kim, H., Adams, J.M., 2016. Predictable communities of soil bacteria in relation to nutrient concentration and successional stage in a laboratory culture experiment. *Environ. Microbiol.* 18, 1740–1753. <https://doi.org/10.1111/1462-2920.12879>
- Stevens, C.J., Dise, N.B., Gowing, D.J.G., Mountford, J.O., 2006. Loss of forb diversity in relation to nitrogen deposition in the UK: Regional trends and potential controls. *Glob. Chang. Biol.* 12, 1823–1833. <https://doi.org/10.1111/j.1365-2486.2006.01217.x>

- Stevenson, B.S., Schmidt, T.M., 2004. Life history implications of rRNA gene copy number in *Escherichia coli*. *Appl. Environ. Microbiol.* 70, 6670–6677. <https://doi.org/10.1128/AEM.70.11.6670-6677.2004>
- Stoddard, S.F., Smith, B.J., Hein, R., Roller, B.R.K., Schmidt, T.M., 2015. rrnDB: Improved tools for interpreting rRNA gene abundance in bacteria and archaea and a new foundation for future development. *Nucleic Acids Res.* 43, D593–D598. <https://doi.org/10.1093/nar/gku1201>
- Trivedi, C., Delgado-Baquerizo, M., Hamonts, K., Lai, K., Reich, P.B., Singh, B.K., 2019. Losses in microbial functional diversity reduce the rate of key soil processes. *Soil Biol. Biochem.* 135, 267–274. <https://doi.org/10.1016/j.soilbio.2019.05.008>
- Uroz, S., Buée, M., Murat, C., Frey-Klett, P., Martin, F., 2010. Pyrosequencing reveals a contrasted bacterial diversity between oak rhizosphere and surrounding soil. *Environ. Microbiol. Rep.* 2, 281–288. <https://doi.org/10.1111/j.1758-2229.2009.00117.x>
- Uselman, S.M., Qualls, R.G., Thomas, R.B., 2000. Effects of increased atmospheric CO<sub>2</sub>, temperature, and soil N availability on root exudation of dissolved organic carbon by a N-fixing tree (*Robinia pseudoacacia* L.). *Plant Soil* 222, 191–202. <https://doi.org/10.1023/A:1004705416108>
- Van Der Heijden, M.G.A., Bardgett, R.D., Van Straalen, N.M., 2008. The unseen majority: Soil microbes as drivers of plant diversity and productivity in terrestrial ecosystems. *Ecol. Lett.* <https://doi.org/10.1111/j.1461-0248.2007.01139.x>
- Vranova, V., Rejsek, K., Skene, K.R., Janous, D., Formanek, P., 2013. Methods of collection of plant root exudates in relation to plant metabolism and purpose: A review. *J. Plant Nutr. Soil Sci.* 176, 175–199. <https://doi.org/10.1002/jpln.201000360>
- WallisDeVries, M.F., Bobbink, R., 2017. Nitrogen deposition impacts on biodiversity in terrestrial ecosystems: Mechanisms and perspectives for restoration. *Biol. Conserv.* 212, 387–389. <https://doi.org/10.1016/j.biocon.2017.01.017>
- Wang, C., Liu, D., Bai, E., 2018. Decreasing soil microbial diversity is associated with decreasing microbial biomass under nitrogen addition. *Soil Biol. Biochem.* 120, 126–133. <https://doi.org/10.1016/j.soilbio.2018.02.003>
- Wang, Q., Garrity, G.M., Tiedje, J.M., Cole, J.R., 2007. Naïve Bayesian classifier for rapid assignment of rRNA sequences into the new bacterial taxonomy. *Appl. Environ. Microbiol.* 73, 5261–5267. <https://doi.org/10.1128/AEM.00062-07>
- Wang, R., Balkanski, Y., Boucher, O., Ciais, P., Peñuelas, J., Tao, S., 2015. Significant contribution of combustion-related emissions to the atmospheric phosphorus budget. *Nat. Geosci.* 8, 48–54. <https://doi.org/10.1038/ngeo2324>
- Weese, D.J., Heath, K.D., Dentinger, B.T.M., Lau, J.A., 2014. Long-term nitrogen addition causes the evolution of less-cooperative mutualists. *Evolution (N. Y.)*. 69, 631–642. <https://doi.org/10.1111/evo.12594>

- Weidner, S., Koller, R., Latz, E., Kowalchuk, G., Bonkowski, M., Scheu, S., Jousset, A., 2015. Bacterial diversity amplifies nutrient-based plant-soil feedbacks. *Funct. Ecol.* 29, 1341–1349. <https://doi.org/10.1111/1365-2435.12445>
- Wu, F.Y., Chung, A.K.C., Tam, N.F.Y., Wong, M.H., 2012. Root exudates of wetland plants influenced by nutrient status and types of plant cultivation. *Int. J. Phytoremediation* 14, 543–553. <https://doi.org/10.1080/15226514.2011.604691>
- Yano, K., Wada, T., Suzuki, S., Tagami, K., Matsumoto, T., Shiwa, Y., Ishige, T., Kawaguchi, Y., Masuda, K., Akanuma, G., Nanamiya, H., Niki, H., Yoshikawa, H., Kawamura, F., 2013. Multiple rRNA operons are essential for efficient cell growth and sporulation as well as outgrowth in *Bacillus subtilis*. *Microbiol. (United Kingdom)* 159, 2225–2236. <https://doi.org/10.1099/mic.0.067025-0>
- Yin, H., Li, Y., Xiao, J., Xu, Z., Cheng, X., Liu, Q., 2013. Enhanced root exudation stimulates soil nitrogen transformations in a subalpine coniferous forest under experimental warming. *Glob. Chang. Biol.* 19, 2158–2167. <https://doi.org/10.1111/gcb.12161>
- Zarraonaindia, I., Owens, S., Weisenhorn, P., West, K., Hampton-Marcell, J., Lax, S., Bokulich, N., Mills, D., Martin, G., Taghavi, S., Lelie, van der, D., Gilbert, J., 2015. The Soil Microbiome Influences Grapevine-Associated Microbiota. *MBio*. <https://doi.org/10.1128/mBio.02527-14.Editor>
- Zeng, J., Liu, X., Song, L., Lin, X., Zhang, H., Shen, C., Chu, H., 2016. Nitrogen fertilization directly affects soil bacterial diversity and indirectly affects bacterial community composition. *Soil Biol. Biochem.* 92, 41–49. <https://doi.org/10.1016/j.soilbio.2015.09.018>
- Zhou, J., Jiang, X., Wei, D., Zhao, B., Ma, M., Chen, S., Cao, F., Shen, D., Guan, D., Li, J., 2017. Consistent effects of nitrogen fertilization on soil bacterial communities in black soils for two crop seasons in China. *Sci. Rep.* 7, 1–10. <https://doi.org/10.1038/s41598-017-03539-6>

## CHAPTER 4: LONG-TERM NUTRIENT ENRICHMENT OF AN OLIGOTROPH-DOMINATED WETLAND SHIFTS MICROBIAL DIVERSITY AND INCREASES CARBON AND NITROGEN CYCLING

### Abstract

Wetlands represent ~7% of Earth's surface but store ~30% of the global carbon (C) stocks. However, ongoing human activities disrupt important wetland functions. Wetland C storage capacity is sensitive to nutrient enrichment from anthropogenic sources such as excess fertilizer use and fossil fuel combustion. Whether a wetland is a C sink or source is driven by rates of fungal and bacterial decomposition of soil organic matter. Plants can stimulate organic matter decomposition by supplying microbial communities with labile C in the form of rhizodeposits. Both plant species and fertilization can influence patterns of rhizodeposition. Therefore, understanding the extent that nutrient enrichment and plant-association influence microbial metabolism can provide insight into mechanisms that control C storage or loss. We hypothesized that fertilization strongly affects bacterial diversity, while plant-association would have a greater impact on fungal diversity. Due to labile C addition from rhizodeposits, we expect that rhizosphere communities will have greater metabolic potential than bulk soil communities; and microbial communities from fertilized plots will have greater metabolic potential compared to unfertilized plots. Using a long-term fertilization experiment, we examined how nutrient enrichment influenced microbial communities and C, nitrogen (N), and phosphorus (P) metabolic profiles of bulk and plant rhizosphere soils. Results indicate that bacterial diversity, but not fungal, increased with fertilization in both bulk and rhizosphere soils. Metabolic profiles of C, N, and P suggest that microbial communities from fertilized rhizosphere plots use a greater diversity of C, N, and P

substrates at a faster rate than microbial communities from unfertilized bulk soils. Together, these results indicate that fertilization increases bacterial diversity and enhances C and nutrient cycling, particularly, within fertilized plant rhizospheres. This study suggests that nutrient enrichment can alter C storage potential due to shifts in metabolic diversity of wetland microbial communities associated with plant rhizosphere soils.

## Introduction

Wetlands store a large portion of global carbon (C) stocks despite representing only 5-8% of terrestrial land surface (Mitsch et al., 2013). Wetland ecosystems are estimated to store 450 Pg C, or ~30%, of the estimated 1,500 Pg C found globally in soil organic C pools (Lal, 2008). However, wetlands, whether inland or coastal, can be vulnerable to C losses due to indirect nitrogen (N) and phosphorus (P) deposition from anthropogenic combustion processes and intensive agricultural practices. It is estimated that global atmospheric N deposition rates are ~112-116 Mton N yr<sup>-1</sup> (Peñuelas et al., 2012) and that atmospheric P deposition rates over terrestrial land surfaces are ~2.7 Tg P yr<sup>-1</sup> (Wang et al., 2015). This nonpoint source nutrient enrichment can boost plant photosynthesis but also enhance microbial soil organic matter (SOM) decomposition rates. When C mineralization rates are greater than C fixation rates, ecosystems shift from C sinks to sources. In particular, microbial activity within plant rhizospheres could be particularly responsive to fertilization effects since they are considered hotspots of (SOM) decomposition due to labile C sources in root exudates fueling microbial heterotrophic activity (Kuzyakov and Blagodatskaya, 2015; Philippot et al., 2013). Taken together, nutrient enrichment can lead to increases in primary production, increases in decomposition rates, and changes to SOM dynamics that can result in C gains or losses. Carbon gains are expected when increased primary production facilitates increased C storage via stabilization of newly incorporated biomass to SOM pools. Alternatively, C losses are expected when newly derived plant inputs to soils results in increased microbial respiration of existing and new SOM via mineralization is faster than C fixed via photosynthesis (Leff et al., 2015; Riggs et al., 2015). If nutrient additions

increase rates of SOM decomposition within plant rhizospheres and lead to net C losses, then estimates of wetland C storage potential could be overestimated.

Altered plant-microbe interactions can alter C cycling rates in different ways. Rhizodeposition by plant roots can induce a positive feedback (i.e., rhizosphere priming) in soils, where labile C from plant roots promote decomposition of existing SOM, which increases N availability to plants (Bengtson et al., 2012; Kuzyakov, 2010; Meier et al., 2017). Plants transfer C substrates to soil microorganisms through plant root exudates or by physical translocation of C between plant roots and mycorrhizal fungal hyphae to other microorganisms (Gorka et al., 2019). This increased availability of labile C sources is estimated to increase rhizosphere microbial activity by 2-20 times compared to microbial activity not associated with plant roots (i.e., bulk soil microbial activity) (Kuzyakov and Blagodatskaya, 2015). As such, it is estimated that rhizosphere priming can increase SOM decomposition from 27 to 245% with an average increase of 59% (Bengtson et al., 2012; Huo et al., 2017; Zhu et al., 2014). When soil N availability to plants is limiting, increased root exudation can stimulate heterotrophic microbial activity and N cycling (Phillips et al., 2009). Rhizosphere priming is estimated to enhance N mineralization by up to 62% in soils (Zhu et al., 2014). Thus, in chronically N-limited systems, like the Arctic tundra, fertilization may enhance rhizosphere priming in a way that promotes C mineralization and decreases soil C stocks (Bengtson et al., 2012; Nowinski et al., 2008).

Through differences in rhizodeposition profiles, plant identity can influence rhizosphere fungal (Hannula et al., 2019) and bacterial community assembly (Lundberg et al., 2012; Matthews et al., 2019; Uroz et al., 2010; Zarraonaindia et al., 2015). Since

rhizodeposits include root exudates which are composed of sugars, organic acids, phenolic compounds, and amino acids, the allocation of C to roots systems can determine microbial community composition (Bertin et al., 2003; Bulgarelli et al., 2013; Dakora and Phillips, 2002; Van Der Heijden et al., 2008). Vascular plant photosynthetic strategy can contribute to rhizodeposit variation. For example, it is estimated that plants allocate 5 to 40% of fixed C to belowground biomass (Haichar et al., 2014; Jones et al., 2009); and in particular, C4 grasses are estimated to allocate ~30% of fixed C to belowground biomass (Kuzyakov and Domanski, 2000). Also, C3 plant root exudates contain a greater variety of organic acids and amino acids along with the sugars mannose, maltose, and ribose compared to C4 plant root exudates, which are composed of several sugar alcohols (i.e., inositol, erythritol, and ribitol) (Vranova et al., 2013). In addition to plant functional types (i.e., C3 vs. C4), soil nutrient status can change the composition (i.e., carbohydrates, organic acids, and amino acid concentrations) of root exudates (Carvalhais et al., 2011; Wu et al., 2012). Further, N fertilization has been shown to decrease root exudation and belowground allocation of fixed C but also increases total microbial biomass C (Kuzyakov et al., 2002; Kuzyakov and Domanski, 2000; Phillips et al., 2009). Thus, fertilization and plant specific rhizodeposition patterns of C3 forbs and C4 grasses are predicted to differentially affect rhizosphere microbial community structure.

The ability of microbial communities to mineralize C is tightly coupled to the availability of nutrients, particularly N and P (Hill et al., 2017; Jennifer L. Soong et al., 2018). Studies investigating the effect of N fertilization on soil respiration have revealed mixed results; some studies reported increased soil respiration rates (Campbell et al.,

2010; Deng et al., 2015; Zhang et al., 2014) and others reported decreased soil respiration rates (Leff et al., 2015; Nguyen et al., 2018; Treseder, 2008) in response to N fertilization. However, due to the coupled nature of the elemental cycles (Hill et al., 2017; Jennifer L. Soong et al., 2018) measuring aggregate metabolic potential using an array of C, N, and P compounds could be particularly useful when examining how microbial community structure relates to nutrient cycling functions (Leff et al., 2015).

Fungal and bacterial soil communities both contribute to nutrient cycling and SOM decomposition in bulk soils and plant rhizospheres to varying degrees. Key differences between fungal and bacterial taxa that could contribute to differences in C and nutrient cycling are that fungi are multi-cellular, conduct decomposition at slower rates, and have higher average biomass C:N ratios (5-15) compared to bacteria (3-6) (Wallander et al., 2003). There is also evidence that fungi can promote bacterial growth by sharing resources such as plant-derived C, water, and N with bacteria (Gorka et al., 2019; Worrich et al., 2017). Therefore, simultaneous examination of bacterial and fungal community composition and metabolic capacity will contribute to novel insights into the context-dependent nutrient effects on plant-microbe associations. Thus, the overarching goal of this study is to examine how long-term nutrient enrichment influences both fungal and bacterial community composition and consequent C, N, and P (CNP) substrate usage and composition. This study could provide insight into mechanisms responsible for C storage or loss in nutrient-limited wetlands experiencing atmospheric nutrient enrichment.

Plant host species and plant functional types (i.e., forb and grass) tend to have a stronger influence on plant-fungal relationships than plant-bacterial relationships

(Bergelson et al., 2019; Hannula et al., 2019). In this study, we test the hypothesis that bacterial community diversity will increase and composition will group according to fertilization effects while fungal community diversity will increase and composition will group according to plant functional type. We also test the hypothesis that metabolic activity will be highest in rhizosphere soils exposed to fertilization compared to unfertilized treatments. Due to natural soil nutrient limitations at our study site, we predict that long-term fertilization will enhance plant activity in a way that increases C substrate abundance (via root exudation) thereby increasing microbial activity. Specifically, CNP usage and diversity is predicted to be greatest in rhizosphere soils due a greater variety of C sources available from root exudates compared to bulk soils. Finally, we test the hypothesis that both fungal and bacterial community composition will be positively correlated to metabolic activity. Fungal and bacterial species have been shown to share C sources, and this coupling of plant-fungal-bacterial associations could in part control soil C and N cycling. This study will provide insights into the effects of long-term fertilization on C cycling within bulk soils and plant rhizospheres of a historically low-nutrient wetland. We examine the link between fungal and bacterial community structure and how nutrient addition influences the utilization of CNP substrates in bulk soils and in the rhizospheres of a C<sub>4</sub> grass and C<sub>3</sub> forb. We use a combination of bacterial (16S rRNA) and fungal (ITS2) amplicon sequencing along with phenotypic microarrays (CNP substrate usage) to determine the diversity, composition, and metabolic diversity of soil microbial communities.

## Methods

### *Study site and experimental design*

A long-term experimental site was established in 2003 and designed to test the effects of fertilization, mowing, and the interaction on wetland plant communities. The site is located at East Carolina University's West Research Campus in Greenville, North Carolina, USA (35.6298N, -77.4836W). Site details are summarized here (and in Chapter 3). A full description can be found in Goodwillie and Franch (2006). Briefly, in 1962, the site was developed as a Voice of America receiving station, which included installation of several access roads and ditches. Historically, this wetland was described as a mosaic of wet pine flatwood habitat, pine savanna, and hardwood communities. Soils are poorly drained wetland soils characterized as fine, kaolinitic, thermic Typic Paleaquults (Coxville series) with a fine sandy loam texture making them acidic ultisols (<https://soilseries.sc.egov.usda.gov/osdname.aspx>). The annual mean temperature is 17.2 °C and annual precipitation is 176 cm (<https://www.climate.gov/maps-data/dataset/>) at this field site. Treatments are replicated on eight 20×30 m blocks, and the N-P-K 10-10-10 pellet fertilizer is applied 3× per year (February, June, and October) for a total annual supplementation of 45.4 kg ha<sup>-1</sup> for each nutrient. Plots are mowed by bush-hog and raked annually to simulate a fire disturbance (Goodwillie, McCoy, and Peralta, In revision; Goodwillie and Franch, 2006).

Soil samples were collected at mowed/unfertilized and mowed/fertilized plots in four (of eight) replicate blocks due to availability of herbaceous plant species and to decrease variability in plant communities. We collected samples from mowed plots

because unmowed plots were dominated by woody and shrubby plant species. The four experimental blocks adjacent to a drainage ditch experience drier soil conditions than the blocks further from the ditch, which represent relatively wetter soil conditions. This hydrologic gradient has resulted in distinct plant communities (Goodwillie, McCoy, and Peralta In revision). For this study, we collected samples from the wetter plots (away from the drainage ditch).

### *Bulk and rhizosphere soil sampling*

Soil samples were collected on November 13, 2018 approximately four months after the last fertilization treatment. For a single composite bulk soil sample, we collected two soil cores (12 cm depth, 3.1 cm diameter) near each of the three permanently installed 1 m<sup>2</sup> quadrats used for annual plant surveys. Annual mowing and raking prevent substantial litter accumulation in sample plots; therefore, soil cores represented the mineral soil horizon. Each composite bulk soil sample was homogenized by passing soils through a 4 mm sieve and removing plant material (>4 mm length) before further analysis. At each plot, rhizosphere soils were collected from the C3 forb *Euthamia caroliniana* (L.) Greene ex Porter & Britton and C4 grass *Andropogon virginicus* L. Each composite rhizosphere soil sample represented three root systems of the same species. Roots were gently dislodged from soil and neighboring roots and placed in a paper bag. After vigorous shaking, a subset of soil in the bag was processed for abiotic analysis (to represent rhizosphere soil environment) and another subset was stored at -80 °C until DNA extraction.

### *Soil chemical and physical characteristics*

Soils were processed for abiotic physical and chemical characterization in the same way as soils collected in 2015 and reported in Chapter 3. Briefly, these same methods are reiterated here. We measured gravimetric soil moisture by drying 20-30 g of field-moist soil at 105 °C for 24 hours. We calculated percent moisture as the difference in weight of moist and oven-dried soils divided by the oven-dried soil weight. Then, oven-dried samples were measured for pH by mixing a 1:1 (soil: water) solution. A subsample of oven-dried soil was ground and sieved using a 500 µm mesh and analyzed for total carbon and total nitrogen using an elemental analyzer (2400 CHNS Analyzer; Perkin Elmer; Waltham, Massachusetts, USA) at the Environmental and Agricultural Testing Service Laboratory (Department of Crop and Soil Sciences at North Carolina State University). To measure extractable inorganic N, approximately 5 g of field-moist soil was extracted with 45 ml of 2 M KCl and gravity filtered to collect extracts. Total phosphate ( $\text{PO}_4^{3-}$ ) was extracted by combining 0.1 g dried soil (ground and passed through a 500 µm sieve) with 0.5 ml of 50% w/v  $\text{Mg}(\text{NO}_3)$  and ashing for 2 hours at 550 °C. Samples were hydrated with 10 mL of 1 M HCl, shaken for 16 hours at 250 RPM, and the filtered (22 µm filter). Water extractable  $\text{PO}_4^{3-}$  was determined by combining 1 g dried soil (ground and passed through a 500 µm sieve) with deionized water, shaken for 1 hour, and filtered (22 µm filter). Ammonium ( $\text{NH}_4^+$ ), nitrate ( $\text{NO}_3^-$ ), and  $\text{PO}_4^{3-}$  ions in soil extracts were colorimetrically measured using a SmartChem 200 auto analyzer (Unity Scientific Milford, Massachusetts, USA) at the East Carolina University Environmental Research Laboratory.

### *Nucleic acid extraction from soil samples*

We extracted genomic DNA from soils using the Qiagen DNeasy PowerSoil Kit according to manufacturer's protocol. Genomic DNA extracts were diluted to 20 ng  $\mu\text{L}^{-1}$  prior to library preparation for ITS2 and 16S rRNA amplification and sequencing.

### *Fungal community analyses*

Soil DNA extractions were sent to GENEWIZ, Inc. (South Plainfield, NJ, US) for ITS2 amplification and sequencing. Briefly, the GENEWIZ, Inc. protocol is described here: 50-100 ng DNA were used to generate ITS2 amplicons using the forward primer  $F_{\text{ITS2}}$  sequence (5'-GTGAATCATCGARTC-3') and reverse primer  $R_{\text{ITS2}}$  (5'-TCCTCCGCTTATTGAT-3'). The primers were designed by GENEWIZ (South Plainfield, NJ, US). The barcoded PCR libraries were validated using an Agilent 2100 Bioanalyzer (Agilent Technologies, Palo Alto, CA, USA), and quantified by Qubit 2.0 fluorometry. Then, the libraries were multiplexed and sequenced on the Illumina MiSeq (Illumina, San Diego, CA, USA) platform using 2x250 paired-end reads (Illumina Reagent Kit v2, 500 reaction kit). Sequences were analyzed using the QIIME data analysis package for ITS rRNA. Contigs were assembled by joining paired-end reads and trimming barcode and primer sequences. Resulting contigs were quality filtered by removing sequences with length >200 bp length, ambiguous bases, and mean quality score of <20. The RDP Gold database and UCHIME algorithm were used to detect chimeric sequences. Sequences were grouped into operational taxonomic units (OTUs) at 97% sequence

similarity using the clustering program VSEARCH (1.9.6) with the UNITE ITS database (<https://unite.ut.ee/>). The Ribosomal Database Program (RDP) classifier was used to assign taxonomic category to all OTUs at confidence threshold of 0.8.

### *Bacterial community analyses*

These analyses were performed according to methods described in Chapter 3, but the methods are reiterated here. The same genomic DNA template used for fungal sequencing was also used as template in bacterial PCR reactions. Bacterial species were targeted using barcoded primers (515FB/806R) originally developed by the Earth Microbiome Project to target the V4 region of the bacterial 16S subunit of the ribosomal RNA gene (Caporaso et al., 2012). For each sample, three 50  $\mu\text{L}$  PCR libraries were prepared by combining 35.75  $\mu\text{L}$  molecular grade water, 5  $\mu\text{L}$  Amplitaq Gold 360 10x buffer, 5  $\mu\text{L}$   $\text{MgCl}_2$  (25 mM), 1  $\mu\text{L}$  dNTPs (40mM total, 10mM each), 0.25  $\mu\text{L}$  Amplitaq Gold polymerase, 1  $\mu\text{L}$  515 forward barcoded primer (10  $\mu\text{M}$ ), 1  $\mu\text{L}$  806 reverse primer (10  $\mu\text{M}$ ), and 1  $\mu\text{L}$  DNA template (10 ng  $\mu\text{L}^{-1}$ ). Thermocycler conditions for PCR reactions were as follows: initial denaturation (94  $^{\circ}\text{C}$ , 3 minutes); 30 cycles of 94  $^{\circ}\text{C}$  for 45 seconds, 50  $^{\circ}\text{C}$  for 30 seconds, 72  $^{\circ}\text{C}$  for 90 seconds; final elongation (72  $^{\circ}\text{C}$ , 10 minutes). Triplicate PCR reactions were combined and cleaned using the AMPure XP magnetic bead protocol (Axygen, Union City, California, USA). Cleaned PCR products were quantified using the QuantIT dsDNA BR assay (Thermo Scientific, Waltham, Massachusetts, USA) and diluted to a concentration of 10 ng  $\mu\text{L}^{-1}$  before pooling barcoded samples in equimolar concentration of 5 ng  $\mu\text{L}^{-1}$ . We sequenced the pooled

libraries using the Illumina MiSeq platform using paired end reads (Illumina Reagent Kit v2, 500 reaction kit) at the Indiana University Center for Genomics and Bioinformatics Sequencing Facility. Sequences were processed using the mothur (v1.40.1) (Schloss et al., 2009) MiSeq pipeline (Kozich et al., 2013). We assembled contigs from the paired-end reads, quality trimmed using a moving average quality score (minimum quality score 35), aligned sequences to the SILVA rRNA database (v128) (Quast et al., 2013), and removed chimeric sequences using the VSEARCH algorithm (Rognes et al., 2016). We created OTUs by first splitting sequences based on taxonomic class and then binning into OTUs based on 97% sequence similarity. The SILVA rRNA database (v128) (Quast et al., 2013) was then used to assign taxonomic designations to resulting OTUs.

### *Biolog phenotypic microarray assay and analyses*

Biolog Eco, Nitrogen (PM3B), and Phosphorus (PM4) phenotypic microarrays (Hayward, CA, USA) were used to measure microbial metabolic activity (i.e., substrate use rates and diversity). Each 96-well microarray plate contained multiple substrate sources: Eco plates contained one water control and 31 different C sources in triplicate, N plates contained one water control and 95 different N sources, P plates contained one water control and 59 different phosphate sources. In addition, P plates also contained one water control and 35 sulfur sources. However, sulfur data were omitted from further analyses due to positive results in water control. Each well contained tetrazolium dye which turns purple in the presence of NADH, which is a product of cellular respiration.

One Eco plate was inoculated for each composite soil sample (two soil cores, 12 cm depth, 3.1 cm diameter) representing different soil sources (i.e., bulk, forb rhizosphere, and grass rhizosphere) collected from the from the fertilization treatment plots (i.e., mowed/unfertilized and mowed/fertilized) within the four experimental blocks sampled (n=24). From each sample, a 0.5 g soil subsample was diluted with 2 mL of sterilized deionized water and combined with six sterilized 5 mm glass beads. Samples were gently shaken by hand, to limit damage to microbial cells, for 2 minutes and then centrifuged at 500 x g for 6 minutes at 4 °C to remove large soil particles and debris. Then, 600 µL of supernatant was combined with 14.4 mL of sterilized deionized water for a final dilution of 1:100. Each well was inoculated with 140 µL of the diluted soil solution and then incubated in the dark at room temperature (~20 °C).

In addition, N and P plates were inoculated in duplicate for each sample. For each soil sample, a 2 g subsample was diluted with 8 mL of sterilized deionized water and combined with 24-5 mm of sterilized glass beads. Samples were gently shaken by inverting samples by hand, to limit damage to microbial cells, for 2 minutes and then centrifuged at 500 x g for 6 minutes at 4 °C to remove large soil particles and debris. The final soil solution included 2.4 mL of supernatant combined with 500 µL of tetrazolium dye (100x), 4 mL of pyruvate (5 mM), and 53.1 mL of sterilized deionized water for a final dilution of 1:100. Unlike the Eco plate, N and P plates do not contain a C source or indicator dye and these components were added to the final soil solution. Each well was inoculated with 140 µL of soil solution and then incubated in the dark at room temperature (~20 °C).

To measure the color change of each microarray plate, we used a Biotek

Synergy spectrophotometer plate reader (BioTek Instruments, Inc., Winooski, VT, USA) at OD of 590 nm immediately after inoculation (T0), every 12 hours for the first 48 hours (T1-T3), and then every 24 hours (T4-T11) for a total duration of 12 days. Total substrate use for each microarray was determined as average well color development (AWCD). A caveat of using soil as starting material versus isolated cells is that the water control well will eventually display color development (i.e., positive result), due to small amounts of C substrates in the soil dilution. Therefore, well color development needs to be standardized to the water control well by subtracting the absorbance value of the water well from the substrate wells. Average well color development (AWCD) was calculated based on the following equation:  $AWCD = [\sum (C - R)] / n$ , where C represents the absorbance value of the control well, R is the mean absorbance of the response wells, and n is the number of substrates (31 for Eco plates, 95 for N plates, and 63 for P plates). The AWCD value is calculated for each time point. Substrate use diversity, which accounts for number of substrates and intensity of substrate use, was calculated as Shannon H' diversity using the *vegan::diversity* function (Oksanen, 2015). We determined the correlation of fungal community composition and bacterial community composition (based on Bray-Curtis dissimilarity matrices) with CNP substrate use profiles (based on Euclidean distance matrices for CNP profiles). We calculated the Mantel r statistic of each pair of matrix comparisons using the *vegan::mantel* function (Oksanen, 2015) with 999 permutations.

### *Statistical analyses*

All statistical analyses were performed in the R statistical environment (RStudio v1.1.383, Rv3.4.0) (R Core Team, 2019). Fungal and bacterial community sequences with low abundance OTUs represented less than 10 times (or  $\leq 0.004\%$  for fungal and  $\leq 0.0001\%$  for bacterial) in all samples were removed. Each group of samples (i.e., fungal or bacterial) was rarefied to the sample with the lowest total sequences within that group before performing further analyses. Fungal samples were rarefied to 9,284 OTUs and resampled, and bacterial samples were rarefied to 16,494 OTUs and resampled. We determined bacterial species diversity by calculating Shannon diversity index ( $H'$ ) because it accounts for species abundance and evenness, while also incorporating rare species (Kim et al., 2017; Shannon, 1948). We used the abundance-based Chao1 estimator to determine species richness because it is non-parametric and also considers rare species (Chao, 1984; Kim et al., 2017). Shannon diversity was calculated using the *vegan::diversity* function and Chao1 OTU richness using *vegan::estimate* (Oksanen, 2015).

To test for differences in fungal and bacterial OTU diversity and richness, and soil parameters (soil moisture, soil pH, total carbon, total nitrogen, KCl extractable ammonium and nitrate, HCl and water extractable phosphate, and percent organic matter), we used the two-way analysis of variance (ANOVA) to compare the main effects of soil source and fertilization treatment and the interaction. Significant interactions were compared with Tukey's HSD *post-hoc* analysis using the *agricolae::HSD.test* R function (de Mendiburu, 2019). In addition, we normalized sample-to-sample variation in sequence depth by taking the relative abundance of each OTU and dividing by the total number of OTUs for each soil community prior to

multivariate statistical analyses. We examined community diversity by visualizing fungal and bacterial community responses to nutrient additions and rhizosphere association using principal coordinates of analysis (PCoA) of fungal and bacterial community composition based on the Bray-Curtis dissimilarity matrix. We used permutational multivariate analysis of variance (PERMANOVA) to test for differences in community composition among treatments and within treatment using pairwise comparisons. Hypothesis testing using PERMANOVA was performed using the *vegan::adonis* function (Oksanen, 2015). Further, we examined the relationship between soil parameters and fungal and bacterial Bray-Curtis dissimilarity patterns using the *vegan::envfit* function (Oksanen, 2015). Soil parameters that were correlated to community patterns (significant at  $p < 0.05$ ) were represented on the PCoA plot as vectors scaled by the strength of their correlation. Fungal community composition (Bray-Curtis dissimilarity matrix), bacterial community composition (Bray-Curtis dissimilarity matrices), and soil property (Euclidean distance) matrix correlations were determined by calculating the Mantel  $r$  statistic based on Pearson correlations with 999 permutations using the *vegan::mantel* function (Oksanen, 2015). To identify specific community members that represented each soil source and fertilization treatment, we performed a Dufrene-Legendre indicator species analysis using the *labdsv::indval* function (Roberts, 2016). Indicator species analyses were conducted on each combination of fertilization and soil source groups.

## Results

### *Fertilization and plant effects on soil properties*

Only a subset of soil properties was distinct due to fertilization treatment and soil sources (Table 4.1, S4.1). Specifically, soil moisture was significantly higher in fertilized plots compared to unfertilized plots (36.6% vs. 34.4%,  $p=0.02$ ) (Table 4.1, S4.1). Also, HCl extractable  $\text{PO}_4^{3-}$  was significantly higher in fertilized ( $299.4 \pm 19.1$  to  $415.1 \pm 254.1$   $\mu\text{g PO}_4^{3-} \text{g}^{-1}$  soil) compared to unfertilized soils ( $123.9 \pm 11.9$  to  $301.7 \pm 126.4$   $\mu\text{g PO}_4^{3-} \text{g}^{-1}$  soil) (ANOVA,  $p=0.04$ , Tables 4.1 and S4.1). Soil organic matter concentrations were significantly higher in forb and grass rhizospheres ( $1.60 \pm 0.05$  to  $1.73 \pm 0.03$  %) compared to bulk soils ( $1.14 \pm 0.15$  to  $1.31 \pm 0.02$  %) (ANOVA,  $p=0.02$ , Tables 4.1 and S4.1). However, soil ammonium concentrations ( $0.15 \pm 0.02$  to  $0.30 \pm 0.08$   $\mu\text{g NH}_4^+\text{-N g}^{-1}$  dry soil) and total soil N concentrations ( $0.23 \pm 0.02$  to  $0.32 \pm 0.07$  %) were similar across soil sources and fertilization treatments, while nitrate concentrations were below detection limits.

### *Fungal and bacterial community diversity*

Fertilization most strongly influenced bacterial but not fungal diversity. Fungal Chao1 richness showed a slight decrease in fertilized plots, and Shannon H' diversity were similar between soil source and fertilization treatments (ANOVA, NS) (Fig. 4.1A, 4.1B). However, bacterial Chao1 richness and Shannon H' diversity were similar across soil sources but were significantly higher in fertilized compared to unfertilized treatments (source:  $p=0.03$ , treatment:  $p=0.01$ ) (Fig. 4.1C, 4.1D).

Fertilization but not soil source influenced fungal community composition.

Patterns in fungal community composition revealed that fertilization treatment explained 25.3% (PCoA axis 1) of the variation (Fig. 4.2). Further, fertilization (but not soil source) influenced fungal community structure (PERMANOVA,  $F=5.43$ ,  $R^2=0.19$ ,  $p=0.001$ ). The pattern in fungal community composition was associated with a subset set of soil properties. The following soil properties were correlated to fungal community patterns in fertilized plots:  $\text{NH}_4^+$  ( $r^2=0.33$ ,  $p=0.02$ ), HCl extractable  $\text{PO}_4^{3-}$  ( $r^2=0.42$ ,  $p=0.01$ ), total soil C ( $r^2=0.33$ ,  $p=0.02$ ), total soil N ( $r^2=0.41$ ,  $p=0.01$ ), and OM ( $r^2=0.32$ ,  $p=0.03$ ).

Both fertilization and soil source affected bacterial community composition. Fertilization treatment explained 29.6% (PCoA axis 1) and soil source explained 12.5% (PCoA axis 2) of the variation associated with bacterial communities. Hypothesis testing indicated that fertilization (PERMANOVA,  $F=3.69$ ,  $R^2=0.138$ ,  $p=0.003$ ) and soil source (PERMANOVA,  $F=1.77$ ,  $R^2=0.13$ ,  $p=0.03$ ) strongly influenced bacterial community composition. Further, results revealed that soil C:N ratio ( $r^2=0.58$ ,  $p=0.002$ ) was positively correlated to bacterial community composition in unfertilized bulk soils, while soil  $\text{NH}_4^+$  concentrations ( $r^2=0.38$ ,  $p=0.01$ ) were correlated with bacterial communities in fertilized bulk soils. In contrast, fertilized rhizosphere bacterial communities were positively correlated to total soil N ( $r^2=0.29$ ,  $p=0.04$ ), OM ( $r^2=0.48$ ,  $p=0.003$ ), and both HCl and water extractable  $\text{PO}_4^{3-}$  ( $r^2=0.77$ ,  $p=0.001$ ;  $r^2=0.47$ ,  $p=0.004$ , respectively).

### *Fungal and bacterial indicator species*

Different representative fungal taxa were associated with bulk soils and plant rhizosphere soils. The majority of fungal indicator species across all treatments were in

the phylum (i.e., number of significant indicator OTUs at  $p < 0.05$  that represent specific treatments) Ascomycota (23) with 4 representatives from Basidiomycota, 1 member from Mucoromycota, and 1 member from Chytridiomycota. Unfertilized bulk soils (16) had the greatest number of unique species, while fertilized bulk soils had the fewest fungal indicator species (1). This trend was opposite in plant rhizospheres, where unfertilized forb rhizospheres (4) had fewer unique taxa than fertilized forb rhizospheres (6). Further, the unfertilized grass rhizospheres (2) had fewer unique taxa than fertilized grass rhizospheres (4). Specific taxonomic designations for fungal indicator taxa are in supplemental Table S4.4.

In addition, distinct representative bacterial taxa were associated with bulk soils and plant rhizosphere soils. In bacterial communities, unfertilized (13) and fertilized (7) soils had the greatest number of unique bacterial indicator taxa. Unfertilized bulk soil had representatives from four different phyla (Acidobacteria (6), Planctomycetes (2), Proteobacteria (4), and Verrucomicrobia (1)). However, bulk soil indicator taxa represented the phylum Acidobacteria (6) with one OTU from Actinobacteria. Forb rhizospheres had the fewest unique taxa with the unfertilized treatment represented by a *Dyella* spp. and the fertilized treatment represented by a Planctomycetaceae OTU. Unfertilized grass rhizospheres were represented by three taxa from two phyla, Planctomycetes (1) and Proteobacteria (2), while fertilized grass rhizospheres did not contain any unique indicator OTUs based on our reporting criteria. Specific taxonomic designations for bacterial indicator taxa are included in supplemental Table S4.5.

## *Characterization of metabolic diversity using phenotypic microarray analysis*

### *Carbon (C)*

Fertilization treatment and soil source influenced C metabolic profiles. Specifically, C microarray AWCD (i.e., total substrate use rate) main effects of soil source (ANOVA,  $p < 0.001$ ), treatment (ANOVA,  $p < 0.001$ ), and the interaction (ANOVA,  $p = 0.008$ ) were significantly different with the highest AWCD values associated with fertilized forb and grass rhizosphere soils (Tukey  $p < 0.05$ ) (Fig. 4.4A, 4.4B; Tables S4.6A, S4.7A). When C microarray profiles were calculated as Shannon H' diversity indices, which accounts for the number of substrates used and intensity of substrate use, C metabolic diversity was significantly higher in forb and grass rhizospheres compared to bulk soils (Tukey HSD,  $p < 0.05$ ). Neither fungal taxonomic diversity ( $p = 0.78$ ) nor bacterial taxonomic diversity ( $p = 0.19$ ) had a linear relationship with C metabolic diversity.

### *Nitrogen (N)*

Fertilization treatment and soil source influenced N metabolic profiles. Specifically, N microarray AWCD main effects of soil source (ANOVA,  $p < 0.001$ ) and treatment (ANOVA,  $p < 0.001$ ), but not the interaction, were highest in fertilized soils and forb and grass rhizospheres compared to unfertilized soils (Tukey HSD,  $p < 0.05$ ) (Fig. 4.4C, 4.4D, Tables S4.6B, S4.7B). When N microarray profiles were calculated as Shannon H' diversity indices, N metabolic diversity was significantly higher in fertilized compared to unfertilized soils across all soil sources (ANOVA,  $p = 0.04$ ). In addition,

fungal taxonomic diversity ( $p=0.50$ ) was not linearly related to N metabolic diversity, but bacterial taxonomic diversity was linearly related to N metabolic diversity ( $R^2=0.14$ ,  $p=0.04$ ).

### *Phosphorus (P)*

Fertilization treatment and soil source influenced P metabolic profiles. Specifically, P microarray AWCD main effects of soil source (ANOVA,  $p<0.001$ ) and treatment (ANOVA,  $p<0.001$ ), but not the interaction, were highest in fertilized soils and forb and grass rhizospheres compared to unfertilized soils (Tukey HSD,  $p<0.05$ ) (Fig. 4.4E, 4.4F; Tables S4.6C, S4.7C). When P microarray profiles were calculated as Shannon H' diversity indices, P metabolic diversity had little variation across all samples but was significantly different by soil source (ANOVA,  $p=0.02$ ); with diversity highest in forb rhizospheres and lowest in bulk soils. Neither fungal taxonomic diversity (ANOVA,  $p=0.46$ ) nor bacterial taxonomic diversity (ANOVA,  $p=0.59$ ) had a linear relationship with P metabolic diversity.

### *Relationships among microbial communities, soil properties, and CNP metabolic profiles*

Patterns in bacterial community composition relate more strongly to patterns in soil characteristics and metabolic profiles than fungal community composition. Fungal and bacterial community patterns have a strong positive correlation (Mantel  $r=0.57$ ,  $p<0.001$ ) (Table 4.2). However, patterns in bacterial community composition had a

stronger relationship to patterns in CNP profiles and soil properties (Mantel  $r = 0.48$ ) and CNP substrate diversity (C: Mantel  $r = 0.36$ , N: Mantel  $r = 0.27$ , P: Mantel  $r = 0.25$ ) than fungal communities related to CNP profiles and soil properties (C: Mantel  $r = 0.19$ , N: Mantel  $r = 0.13$ , P: Mantel  $r = 0.12$ , soil: Mantel  $r = 0.19$ ) (Table 4.2). Further, C use profiles were correlated with soil properties (Mantel  $r = 0.28$ ) and N use profiles (Mantel  $r = 0.23$ ) but not P use profiles. Finally, the N use profiles were very strongly correlated with P use profiles (Mantel  $r = 0.86$ , Table 4.2).

## Discussion

In this study, fertilization increased species richness and diversity of bacterial communities but not fungal communities, possibly due to competition for N between fungi and plants. Despite relatively little difference in species richness and diversity in fungal communities, fertilization and plant-association affected both bacterial and fungal community composition. Due to the symbiotic relationship often observed in plant-fungal interactions, previous studies suggested that plant host has a greater impact on fungal communities than bacterial communities (Bergelson et al., 2019; Hannula et al., 2019). However, our results indicate that bacterial communities exhibit a stronger relationship with plant association in both fertilized and unfertilized plots; PCoA analysis of bacterial composition showed that rhizosphere communities were more similar to each other than to bulk soil communities within each fertilization treatment. In unfertilized plots grass and forb rhizospheres are more similar to each other than to bulk soils; but in fertilized plots bulk soils and grass rhizospheres are more similar to each other than forb

rhizospheres. In terms of plant benefits, N-fixing rhizobia bacteria, and to a lesser extent fungi, help supply plants with N while mycorrhizal fungi, and to a lesser bacteria, increase P supply to plants (Bulgarelli et al., 2013; Jach-Smith and Jackson, 2018; Van Der Heijden et al., 2016). This difference in plant-bacterial and plant-fungal relationships in our results may be because of N-limitation and P-availability within this wetland study system. That is, soil nitrate levels were below detection limits across all fertilization and soil sources while phosphate was detected in all soil samples. Another study found that in N-limited grassland ecosystems, N fertilization induces competition for N between plants and mycorrhizal fungi (Püschel et al., 2016).

In terms of metabolic potential of the total microbial community, our results suggest that both fertilization and plant-association increase C and N utilization and diversity and to a lesser degree P utilization and diversity. Plant rhizodeposition provides soil microorganisms with labile C substrates that promote decomposition of older soil organic matter (SOM) (Kuzyakov, 2010; Philippot et al., 2013). This cycling of SOM promotes N mining by microbes, thereby increasing plant available N. Some studies show that N fertilization decreases allocation of C in root exudates due to availability of N in soils (Kuzyakov et al., 2002; Phillips et al., 2009). However, within N-limited systems, fertilization tends to increase C and N cycling (Nowinski et al., 2008). Even with N fertilization, the supplied N may not be great enough to satisfy both plant and microbial demand. Therefore, in the presence of labile C from root exudates, N mining is still promoted. It is possible that N and P fertilization in naturally N-limited systems may exacerbate N limitation due to the unlimited availability of P in soils in the present study. Similarly, in a past experiment conducted in P-limited tropical soils, N

fertilization and litter additions stimulated microbial activity which was likely a result of labile C from plants inducing P-mining (Soong et al., 2018).

Bacterial communities are likely more active than fungal communities within this low-nutrient wetland due competition between plants and fungal communities for limited N resources (Püschel et al., 2016). In this study, CNP metabolic profiles more strongly correlated to soil bacterial than to fungal community composition. Also, bacterial diversity and microbial metabolic potential were highest in fertilized rhizospheres. Although phenotypic microarrays represent a fraction of the total soil microbial community (bacteria and fungi) that can grow under laboratory conditions, together, these results suggest that soil bacterial communities more than fungal communities have a greater impact on soil nutrient cycling in bulk and rhizosphere soils within this wetland. In a study by Van Der Heijden et al., 2016, when N and P is limited, fungal and bacterial taxa complement each other in providing N and P to grassland plants. However, even with fertilization, our wetland system has low availability of N but high availability of P possibly resulting in plant-fungal competition for the limited N resource.

Overall, the present study highlights that rhizosphere communities are particularly sensitive to nutrient enrichments, especially in soils that are chronically N-limited. While wetlands are more often considered C sinks, this study and others support that nutrient additions have the potential to promote C and N cycling and increase SOM decomposition in oligotrophic wetlands (Bodker et al., 2015; Morris and Bradley, 1999; Nowinski et al., 2008). Therefore, long-term fertilization has the potential to increase C cycling, especially within plant rhizospheres, leading to decreased wetland C storage potential.

## Figures and Tables

**Table 4.1.** (A) Soil physiochemical properties after 15 years of fertilization and mowing disturbance. Average (mean  $\pm$  SD) soil properties (temperature, gravimetric moisture, pH, extractable nitrate and ammonium concentrations, total C% and N%, and C:N ratio) across unfertilized and fertilized plots and among soil sources (bulk, forb rhizosphere, and grass rhizosphere). Main effects that are significantly differently (ANOVA  $p < 0.05$ ) are bolded. Letters represent significant differences between soil sources (Tukey's HSD  $p < 0.05$ ). ANOVA summary Table S4.1.

	Unfertilized			Fertilized		
	Bulk	Forb	Grass	Bulk	Forb	Grass
Temperature °C	13.5 ± 1.3	-	-	13.5 ± 1.0	-	-
<b>Moisture (%)</b>	34.4 ± 0.8 <b>a</b>	-	-	36.6 ± 1.1 <b>b</b>	-	-
pH	3.89 ± 0.24	-	-	4.06 ± 0.22	-	-
NO <sub>3</sub> <sup>-</sup> -N (ug/g dry soil)	MDL	MDL	MDL	MDL	MDL	MDL
NH <sub>4</sub> <sup>+</sup> -N (µg/g dry soil)	0.26 ± 0.26	0.24 ± 0.13	0.19 ± 0.08	0.30 ± 0.18	0.17 ± 0.03	0.15 ± 0.02
<b>PO<sub>4</sub><sup>3-</sup> HCl (µg/g dry soil)</b>	123.9 ± 11.9 <b>a</b>	301.7 ± 126.4 <b>a</b>	237.4 ± 186.5 <b>a</b>	299.4 ± 19.1 <b>b</b>	353.4 ± 128.0 <b>b</b>	415.1 ± 254.1 <b>b</b>
PO <sub>4</sub> <sup>3-</sup> water (µg/g dry soil)	0.19 ± 0.16	11.5 ± 21.5	11.8 ± 22.1	2.9 ± 1.7	14.0 ± 11.5	14.5 ± 18.4
Total C (%)	4.44 ± 0.51	5.32 ± 0.72	5.90 ± 1.70	5.11 ± 0.89	5.60 ± 1.08	5.47 ± 2.01
Total N (%)	0.23 ± 0.02	0.29 ± 0.04	0.30 ± 0.09	0.27 ± 0.04	0.32 ± 0.07	0.30 ± 0.12
Soil C:N (wt:wt)	19.70 ± 1.30	18.49 ± 0.74	19.55 ± 0.32	19.09 ± 1.08	17.85 ± 1.35	18.53 ± 1.14
<b>Organic Matter %</b>	1.14 ± 0.15 <b>a</b>	1.71 ± 2.61e-6 <b>b</b>	1.73 ± 0.03 <b>b</b>	1.31 ± 0.02 <b>a</b>	1.70 ± 0.06 <b>b</b>	1.60 ± 0.05 <b>b</b>

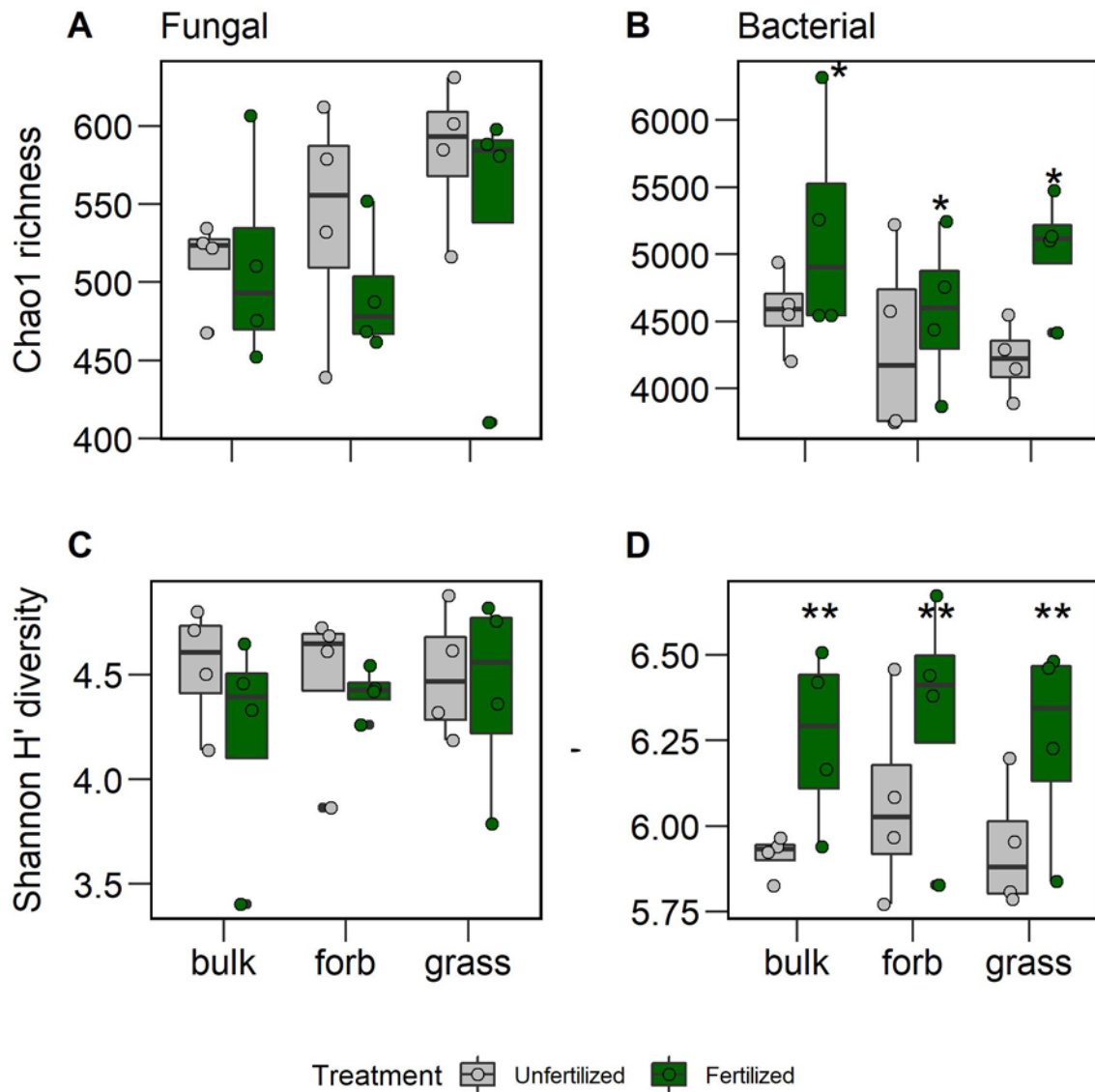


**Figure 4.1.** Boxplots of fungal and bacterial diversity based on mean (A) Chao1 richness and (B) Shannon H' Diversity Index associated with soil source (bulk, grass rhizosphere, forb rhizosphere). Colors indicate fertilization treatment (gray = unfertilized, green = fertilized) at mowed plots. Asterisks (\*) indicate significant differences between fertilization treatments: \*  $p=0.02$ , \*\*  $p=0.01$ .

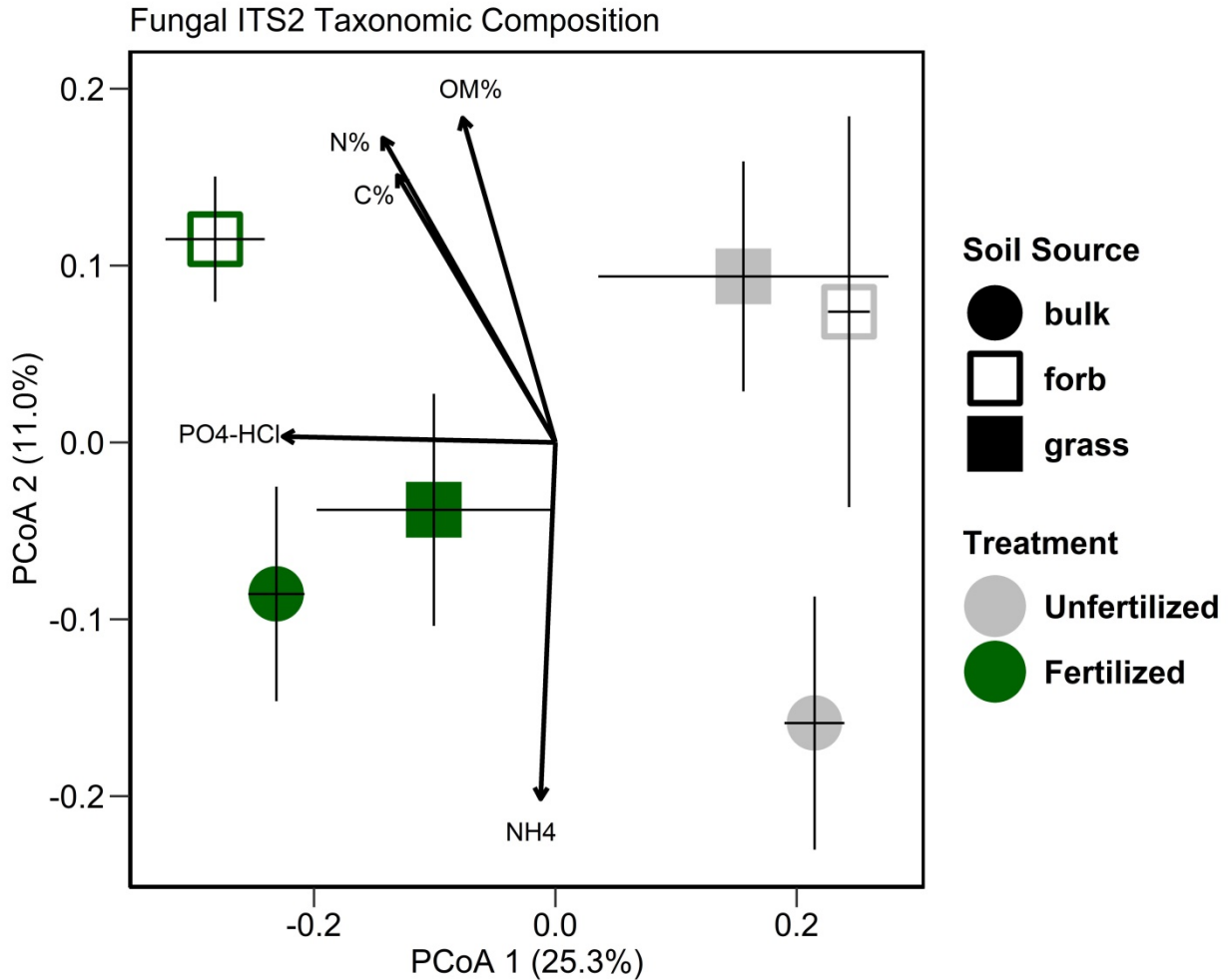


**Figure 4.2.** Ordination based on PCoA of Bray-Curtis dissimilarity matrix illustrating fungal ITS2 community composition. Colors represent fertilization treatment (gray = unfertilized, green = fertilized) and symbols represent soil source (bulk soil = circle, grass rhizosphere = open square, forb rhizosphere = filled square). Vectors represent soil factors that are correlated ( $p < 0.05$ ) to patterns in bacterial community composition (C%= percent soil carbon, N%= percent soil nitrogen, OM%= percent organic matter, NH<sub>4</sub>= ammonium mg g<sup>-1</sup> soil, PO<sub>4</sub>-HCl= phosphate mg g<sup>-1</sup> soil).

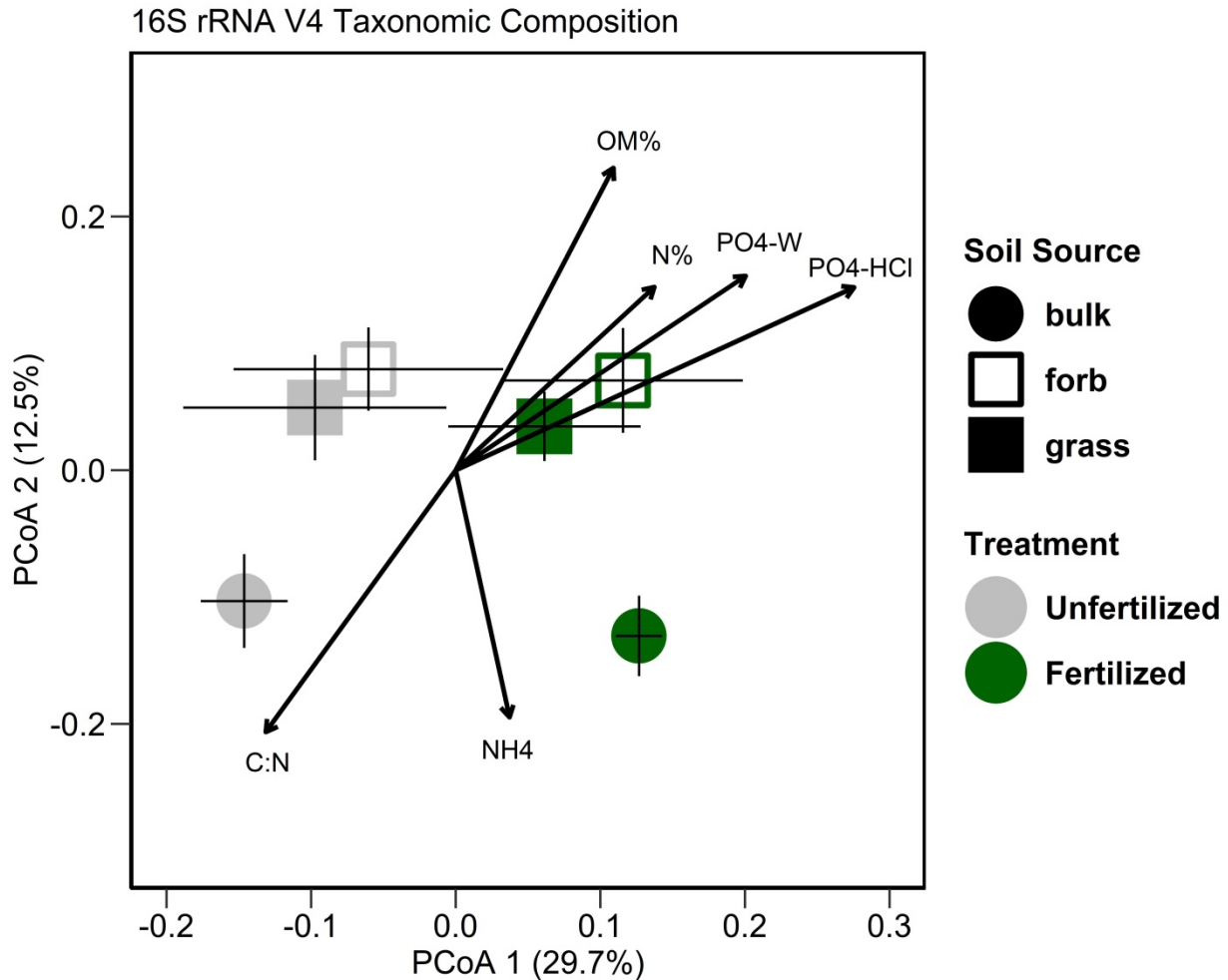


**Figure 4.3.** Ordination based on PCoA of Bray-Curtis dissimilarity matrix illustrating bacterial 16S rRNA community composition. Colors represent fertilization treatment (gray = unfertilized, green = fertilized) and symbols represent soil source (bulk soil = circle, grass rhizosphere = open square, forb rhizosphere = filled square). Vectors represent soil factors that are correlated ( $p < 0.05$ ) to patterns in bacterial community composition (C:N= percent soil C to percent N ratio, N%= percent soil N, OM%= percent organic matter, NH<sub>4</sub>= ammonium mg g<sup>-1</sup> soil, PO<sub>4</sub>-HCl= phosphate mg g<sup>-1</sup> soil from HCl extraction, PO<sub>4</sub>-W= phosphate mg g<sup>-1</sup> soil from water extraction).

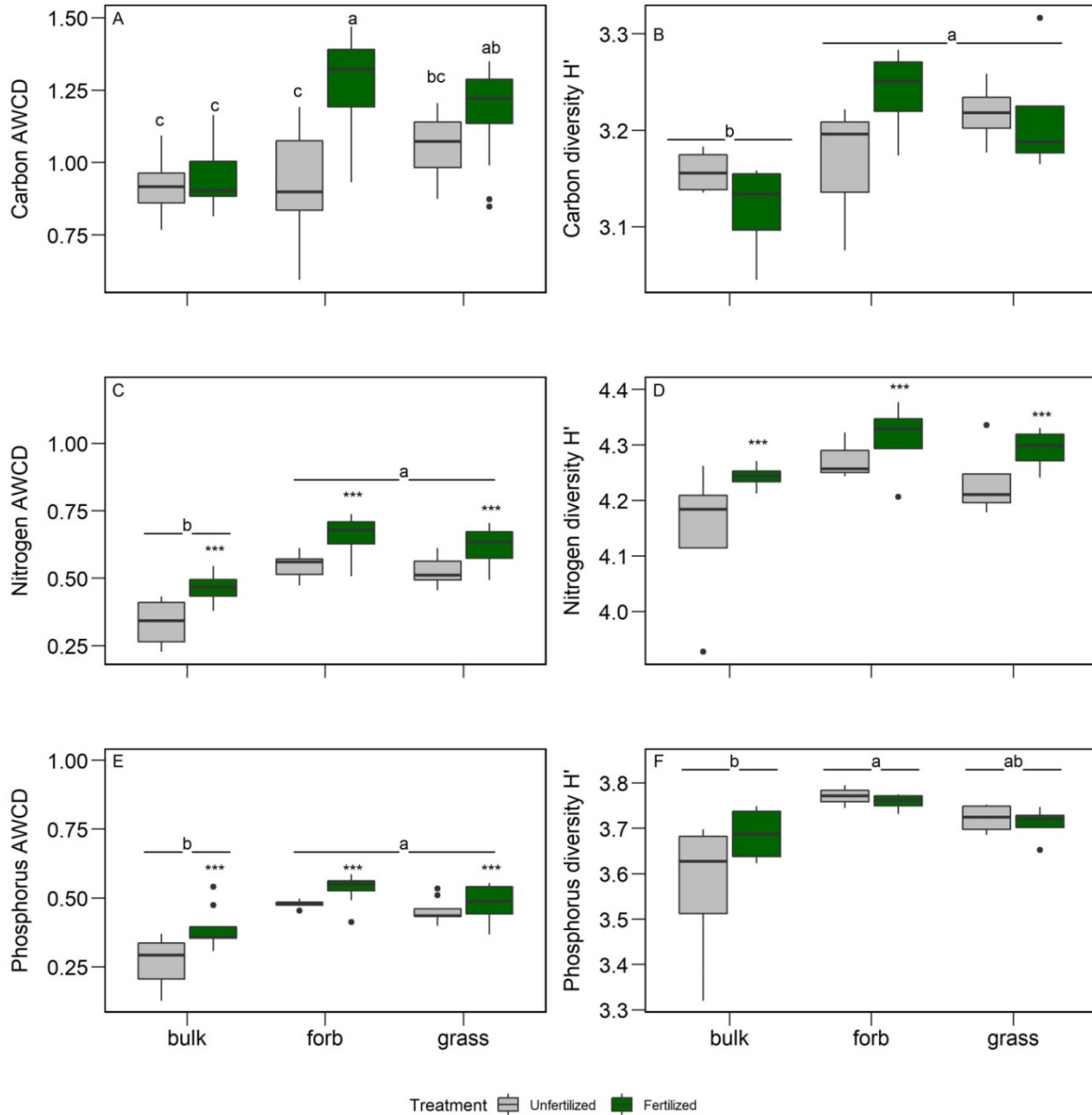


**Figure 4.4.** Boxplots of phenotypic microarray average well color development (AWCD) and Shannon H' diversity grouped by fertilization treatment and soil source for (A, B) carbon, (C, D) nitrogen, (E, F) phosphorus microarrays. Soil sources are bulk, forb rhizospheres, and grass rhizospheres. Colors represent fertilization treatment (gray = unfertilized, green = fertilized). Asterisks (\*\*\*) indicate significant differences in fertilization treatments ( $p < 0.05$ ). Letters indicate significant differences in soil source or interaction groups (Tukey  $p \leq 0.05$ ).

## Supplemental Figures and Tables

**Table S4.1.** Summary of two-way ANOVA comparing soil properties among soil source (bulk, grass rhizosphere, and forb rhizosphere), fertilization treatments and the interaction in mowed plots. Treatment effects that were significantly different ( $p < 0.05$ ) are bolded.

	Treatment		Source		Treatment × Source	
	F-value	P-value	F-value	P-value	F-value	P-value
<b>Moisture (%)</b>	<b>10.67</b>	<b>0.017</b>	-	-	-	-
pH	1.17	0.32	-	-	-	-
NH <sub>4</sub> <sup>+</sup> -N (µg/g dry soil)	0.18	0.68	1.22	0.32	0.31	0.74
Total C (%)	0.11	0.74	1.08	0.36	0.53	0.60
Total N (%)	0.60	0.45	1.76	0.20	0.40	0.67
Soil C:N (wt:wt)	3.32	0.09	2.99	0.08	0.10	0.90
<b>PO<sub>4</sub><sup>3+</sup> (µg/g dry soil) HCl extraction</b>	<b>4.96</b>	<b>0.04</b>	1.61	0.28	0.47	0.63
PO <sub>4</sub> <sup>3+</sup> (µg/g dry soil) water extraction	0.18	0.68	1.44	0.26	0.0002	1.00
<b>OM (%)</b>	0.04	0.84	<b>5.61</b>	<b>0.02</b>	0.75	0.49

**Table S4.2.** Summary of two-way ANOVA comparing fungal Chao1 richness (A), fungal Shannon H' diversity (B), bacterial Chao 1 richness (C), and bacterial Shannon H' diversity (D), metrics among soil source and fertilization treatments. Source represents bulk, grass rhizosphere, and forb rhizosphere and treatment represents fertilized and unfertilized mowed treatments. Treatment effects that were significantly different ( $p < 0.05$ ) are bolded.

(A) Fungal Chao1 richness

Main Effect	SumSq	MeanSq	NumDF	F-value	Pr(>F)
Source	13284	6641.9	2	1.712	0.209
Fertilization	5216	5216.3	1	1.344	0.261
Source x Treatment	2512	1256.1	2	0.324	0.728

(B) Fungal Shannon diversity

Main Effect	SumSq	MeanSq	NumDF	F-value	Pr(>F)
Source	0.036	0.018	2	0.122	0.886
Treatment	0.136	0.136	1	0.914	0.352
Source x Treatment	0.095	0.047	2	0.319	0.731

(C) Bacterial Chao1 richness

Main Effect	SumSq	MeanSq	NumDF	F-value	Pr(>F)
Source	717970	358985	2	1.130	0.345
<b>Treatment</b>	1805724	1805724	1	5.684	<b>0.028</b>
Source x Treatment	317561	158780	2	0.500	0.615

(D) Bacterial Shannon diversity

Main Effect	SumSq	MeanSq	NumDF	F-value	Pr(>F)
Source	0.068	0.034	2	0.511	0.608
<b>Treatment</b>	0.567	0.567	1	8.504	<b>0.010</b>
Source x Treatment	0.006	0.003	2	0.412	0.960

**Table S4.3.** Summary of (A) fungal community PERMANOVA main effects soil source (bulk, grass rhizosphere, and forb rhizosphere), fertilization treatment, and interaction of mowed plots, (B) bacterial community PERMANOVA, and (C) soil properties PERMANOVA. Treatment effects that were significantly different ( $p < 0.05$ ) are bolded.

(A) Fungal community main effects

Main Effect	SumSq	F-value	R <sup>2</sup>	P-value
Source	0.567	1.463	0.102	0.077
<b>Treatment</b>	1.072	5.533	0.192	<b>0.001</b>
Source × Treatment	0.454	1.171	0.081	0.251

(B) Bacterial community main effects

Main Effect	SumSq	F-value	R <sup>2</sup>	P-value
<b>Source</b>	0.281	1.788	0.133	<b>0.030</b>
<b>Treatment</b>	0.293	3.741	0.140	<b>0.001</b>
Source × Treatment	0.120	0.762	0.057	0.759

(C) Soil properties main effects

Main Effect	SumSq	F-value	R <sup>2</sup>	P-value
Source	71592	1.601	0.119	0.218
<b>Treatment</b>	109310	4.907	0.181	<b>0.052</b>
Source × Treatment	20817	0.467	0.035	0.652

**Table S4.4:** Summary of fungal taxa (OTUs) characteristic to each soil source (bulk, grass rhizosphere, and forb rhizosphere) and fertilization treatment based on indicator species analysis. These are the top OTUs (>1% relative abundance) that are significantly ( $p < 0.02$ ) associated with each soil source and treatment group.

OTU_ID	Cluster	IndVal	Prob	Classification Domain; Phylum; Class; Order; Family; Genus
OTU3	bulk unfertilized	0.302	0.003	Fungi; Ascomycota; Eurotiomycetes; Eurotiales; Aspergillaceae; Penicillium
OTU23	bulk unfertilized	0.942	0.004	Fungi
OTU109	bulk unfertilized	0.9	0.002	Fungi; Ascomycota
OTU354	bulk unfertilized	0.628	0.001	Fungi; Ascomycota

OTU178	bulk unfertilized	0.656	0.003	Fungi; Ascomycota
OTU153	bulk unfertilized	0.867	0.004	Fungi; Ascomycota
OTU177	bulk unfertilized	0.772	0.009	Fungi; Ascomycota; Orbiliomycetes; Orbiliales
OTU182	bulk unfertilized	0.407	0.013	Fungi; Mucoromycota; Umbelopsidomycetes; Umbelopsidales; Umbelopsidaceae; Umbelopsis; Umbelopsis dimorpha
OTU159	bulk unfertilized	0.884	0.001	Fungi; Ascomycota
OTU1181	bulk unfertilized	0.5	0.003	Fungi
OTU2133	bulk unfertilized	0.657	0.013	Fungi; Ascomycota; Leotiomyces; Leotiomyces ord Incertae sedis; Pseudeurotiaceae; Pseudeurotium; Pseudeurotium hygrophilum
OTU2120	bulk unfertilized	0.455	0.003	Fungi
OTU424	bulk unfertilized	0.855	0.001	Fungi; Ascomycota
OTU2447	bulk unfertilized	0.695	0.014	Fungi
OTU370	bulk unfertilized	0.638	0.016	Fungi; Ascomycota
OTU1206	bulk unfertilized	0.474	0.017	Fungi
OTU69	bulk fertilized	0.721	0.013	Fungi; Ascomycota
OTU111	bulk fertilized	0.563	0.013	Fungi; Ascomycota
OTU473	bulk fertilized	0.693	0.019	Fungi; Ascomycota; Sordariomycetes; Sordariales; Lasiosphaeriaceae; Echria
OTU25	forb unfertilized	0.453	0.009	Fungi; Ascomycota
OTU46	forb unfertilized	0.481	0.006	Fungi; Ascomycota; Sordariomycetes; Hypocreales; Ophiocordycipitaceae; Tolypocladium
OTU127	forb unfertilized	0.508	0.015	Fungi
OTU327	forb unfertilized	0.583	0.001	Fungi; Ascomycota; Leotiomyces; Helotiales
OTU62	forb fertilized	0.485	0.004	Fungi; Basidiomycota; Tremellomycetes; Filobasidiales; Piskurozymaceae; Solicoccozyma; Solicoccozyma terricola
OTU148	forb fertilized	0.430	0.006	Fungi; Ascomycota
OTU191	forb fertilized	0.660	0.002	Fungi; Ascomycota; Sordariomycetes; Hypocreales; Hypocreales fam Incertae sedis; Myxocephala; Myxocephala albida
OTU200	forb fertilized	0.552	0.002	Fungi; Chytridiomycota; Rhizophydiomycetes; Rhizophydiales; Terramycetaceae

OTU170	forb fertilized	0.666	0.019	Fungi; Ascomycota; Sordariomycetes; Sordariales; Chaetomiaceae; Chaetomium; Chaetomium homopilatum
OTU353	forb fertilized	0.629	0.008	Fungi; Basidiomycota; Agaricomycetes; Auriculariales
OTU213	grass unfertilized	0.537	0.004	Fungi; Ascomycota; Dothideomycetes; Pleosporales
OTU314	grass unfertilized	0.712	0.007	Fungi; Basidiomycota; Agaricomycetes; Trechisporales; Hydnodontaceae; Trechispora
OTU77	grass fertilized	0.735	0.01	Fungi; Basidiomycota; Agaricomycetes; Agaricales
OTU42	grass fertilized	0.963	0.007	Fungi; Ascomycota; Sordariomycetes; Hypocreales; Nectriaceae
OTU240	grass fertilized	0.576	0.019	Fungi; Ascomycota; Sordariomycetes; Chaetosphaeriales; Chaetosphaeriaceae; Chaetosphaeria; Chaetosphaeria fusiformis
OTU492	grass fertilized	0.716	0.004	Fungi; Ascomycota; Dothideomycetes; Pleosporales

**Table S4.5:** Summary of bacterial taxa (OTUs) characteristic to each soil source (bulk, grass rhizosphere, and forb rhizosphere) and fertilization treatment based on indicator species analysis. These are the top OTUs (>1% relative abundance) that are significantly ( $p < 0.02$ ) associated with each soil source and treatment group.

OTU	Cluster	IndVal	Prob	Classification Domain; Phylum; Class; Order; Family; Genus
Otu00030	bulk unfertilized	0.340	0.003	Bacteria; Acidobacteria; Acidobacteria Gp2; Gp2; Gp2; Gp2
Otu00043	bulk unfertilized	0.344	0.012	Bacteria; Proteobacteria; Alphaproteobacteria; Rhodospirillales; Rhodospirillales ; Rhodospirillales
Otu00057	bulk unfertilized	0.390	0.004	Bacteria; Proteobacteria; Proteobacteria ; Proteobacteria ; Proteobacteria ; Proteobacteria
Otu00058	bulk unfertilized	0.292	0.012	Bacteria; Proteobacteria; Alphaproteobacteria; Rhizobiales; Rhizobiales ; Rhizobiales
Otu00081	bulk unfertilized	0.326	0.01	Bacteria; Verrucomicrobia; Spartobacteria; Spartobacteria; Spartobacteria

Otu00119	bulk unfertilized	0.309	0.004	Bacteria; Acidobacteria; Acidobacteria Gp2; Gp2; Gp2; Gp2
Otu00123	bulk unfertilized	0.432	0.001	Bacteria; Acidobacteria; Acidobacteria Gp1; Gp1; Gp1; Gp1
Otu00139	bulk unfertilized	0.294	0.018	Bacteria; Acidobacteria; Acidobacteria Gp3; Gp3; Gp3; Gp3
Otu00159	bulk unfertilized	0.365	0.012	Bacteria; Proteobacteria; Betaproteobacteria; Betaproteobacteria; Betaproteobacteria; Betaproteobacteria
Otu00160	bulk unfertilized	0.413	0.01	Bacteria; Planctomycetes; Planctomycetia; Planctomycetales; Planctomycetaceae; Planctomycetaceae
Otu00209	bulk unfertilized	0.413	0.019	Bacteria; Acidobacteria; Acidobacteria Gp1; Gp1; Gp1; Gp1
Otu00265	bulk unfertilized	0.6	0.002	Bacteria; Acidobacteria; Acidobacteria Gp1; Gp1; Gp1; Gp1
Otu00366	bulk unfertilized	0.421	0.009	Bacteria; Planctomycetes; Planctomycetia; Planctomycetales; Planctomycetaceae; Planctomycetaceae
Otu00021	bulk fertilized	0.290	0.006	Bacteria; Actinobacteria; Actinobacteria; Solirubrobacterales; Solirubrobacterales; Solirubrobacterales
Otu00036	bulk fertilized	0.348	0.002	Bacteria; Acidobacteria; Acidobacteria Gp1; Gp1; Gp1; Gp1
Otu00073	bulk fertilized	0.437	0.001	Bacteria; Acidobacteria; Acidobacteria Gp2; Gp2; Gp2; Gp2
Otu00101	bulk fertilized	0.319	0.011	Bacteria; Acidobacteria; Acidobacteria Gp2; Gp2; Gp2; Gp2
Otu00212	bulk fertilized	0.352	0.008	Bacteria; Acidobacteria; Acidobacteria Gp1; Gp1; Gp1; Gp1
Otu00243	bulk fertilized	0.324	0.005	Bacteria; Acidobacteria; Acidobacteria Gp2; Gp2; Gp2; Gp2
Otu00253	bulk fertilized	0.419	0.005	Bacteria; Acidobacteria; Acidobacteria Gp2; Gp2; Gp2; Gp2
Otu00142	forb unfertilized	0.384	0.007	Bacteria; Proteobacteria; Gammaproteobacteria; Xanthomonadales; Xanthomonadaceae; Dyella
Otu00235	forb	0.253	0.008	Bacteria; Planctomycetes; Planctomycetia;

	fertilized			Planctomycetales; Planctomycetaceae; Planctomycetaceae
Otu00061	grass unfertilized	0.241	0.02	Bacteria; Proteobacteria; Alphaproteobacteria; Alphaproteobacteria incertae sedis; Rhizomicrobium; Rhizomicrobium
Otu00117	grass unfertilized	0.385	0.007	Bacteria; Planctomycetes; Planctomycetia; Planctomycetales; Planctomycetaceae; Planctomycetaceae
Otu00470	grass unfertilized	0.308	0.011	Bacteria; Proteobacteria; Gammaproteobacteria; Gammaproteobacteria; Gammaproteobacteria; Gammaproteobacteria

**Table S4.6.** Analysis of variance summary of main effects for AWCD of (A) carbon microarray, (B) nitrogen microarray, and (C) phosphorus microarray among soil source and fertilization treatments. Source represents bulk, grass rhizosphere, and forb rhizosphere and treatment represents fertilized and unfertilized mowed treatments. Treatment effects that were significantly different ( $p < 0.05$ ) are bolded.

(A) Carbon microarray AWCD ANOVA Summary

Main Effect	SumSq	MeanSq	NumDF	F-value	Pr(>F)
<b>Source</b>	0.492	0.246	2	10.993	<b>&lt;0.001</b>
<b>Treatment</b>	0.402	0.402	1	17.967	<b>&lt;0.001</b>
<b>Source × Treatment</b>	0.232	0.116	2	5.185	<b>0.008</b>

(B) Nitrogen microarray AWCD ANOVA Summary

Main Effect	SumSq	MeanSq	NumDF	F-value	Pr(>F)
<b>Source</b>	0.363	0.181	2	39.035	<b>&lt;0.001</b>
<b>Treatment</b>	0.159	0.159	1	34.136	<b>&lt;0.001</b>
Source × Treatment	0.003	0.002	2	0.320	0.728

(C) P microarray AWCD ANOVA Summary

Main Effect	SumSq	MeanSq	NumDF	F-value	Pr(>F)
<b>Source</b>	0.267	0.133	2	30.953	<b>&lt;0.001</b>
<b>Treatment</b>	0.066	0.066	1	15.334	<b>0.0003</b>
Source × Treatment	0.0183	0.009	2	2.121	0.133

**Table S4.7.** Analysis of variance summary of main effects for Shannon H' diversity of carbon microarray (A), nitrogen microarray (B), and phosphorus microarray (C) among soil source and fertilization treatments. Source represents bulk, grass rhizosphere, and forb rhizosphere and treatment represents fertilized and unfertilized mowed treatments. Treatment effects that were significantly different ( $p < 0.05$ ) are bolded.

(A) Carbon microarray Shannon H' diversity

Main Effect	SumSq	MeanSq	NumDF	F-value	Pr(>F)
<b>Source</b>	0.029	0.015	2	5.255	<b>0.02</b>
Treatment	0.0005	0.0005	1	0.176	0.681
Source × Treatment	0.013	0.006	2	2.286	0.132

(B) Nitrogen microarray Shannon H' diversity

Main Effect	SumSq	MeanSq	NumDF	F-value	Pr(>F)
Source	0.040	0.020	2	3.250	0.064
<b>Treatment</b>	0.029	0.029	1	4.710	<b>0.044</b>
Source × Treatment	0.004	0.002	2	0.355	0.706

(C) Phosphorus microarray Shannon H' diversity

Main Effect	SumSq	MeanSq	NumDF	F-value	Pr(>F)
<b>Source</b>	0.070	0.035	2	5.274	<b>0.017</b>
Treatment	0.009	0.009	1	1.336	0.264
Source × Treatment	0.022	0.111	2	1.686	0.215

## References

- Bengtson, P., Barker, J., Grayston, S.J., 2012. Evidence of a strong coupling between root exudation, C and N availability, and stimulated SOM decomposition caused by rhizosphere priming effects. *Ecol. Evol.* 2, 1843–1852. <https://doi.org/10.1002/ece3.311>
- Bergelson, J., Mittelstrass, J., Horton, M.W., 2019. Characterizing both bacteria and fungi improves understanding of the Arabidopsis root microbiome. *Sci. Rep.* 9, 1–11. <https://doi.org/10.1038/s41598-018-37208-z>
- Bertin, C., Yang, X., Weston, L.A., 2003. The role of root exudates and allelochemicals in the rhizosphere. *Plant Soil* 256, 67–83. <https://doi.org/10.1023/A:1026290508166>
- Bodker, J.E., Turner, R.E., Tweel, A., Schulz, C., Swarzenski, C., 2015. Nutrient-enhanced decomposition of plant biomass in a freshwater wetland. *Aquat. Bot.* 127, 44–52. <https://doi.org/10.1016/j.aquabot.2015.08.001>
- Bulgarelli, D., Schlaeppi, K., Spaepen, S., Ver Loren van Themaat, E., Schulze-Lefert, P., 2013. Structure and functions of the bacterial microbiota of plants. *Annu. Rev. Plant Biol.* 64, 807–38. <https://doi.org/10.1146/annurev-arplant-050312-120106>
- Campbell, B.J., Polson, S.W., Hanson, T.E., Mack, M.C., Schuur, E.A.G., 2010. The effect of nutrient deposition on bacterial communities in Arctic tundra soil. *Environ. Microbiol.* 12, 1842–1854. <https://doi.org/10.1111/j.1462-2920.2010.02189.x>
- Caporaso, J.G., Lauber, C.L., Walters, W. a, Berg-Lyons, D., Huntley, J., Fierer, N., Owens, S.M., Betley, J., Fraser, L., Bauer, M., Gormley, N., Gilbert, J. a, Smith, G., Knight, R., 2012. Ultra-high-throughput microbial community analysis on the Illumina HiSeq and MiSeq platforms. *ISME J.* 6, 1621–1624. <https://doi.org/10.1038/ismej.2012.8>
- Carvalhais, L.C., Dennis, P.G., Fedoseyenko, D., Hajirezaei, M.R., Borriss, R., Von Wirén, N., 2011. Root exudation of sugars, amino acids, and organic acids by maize as affected by nitrogen, phosphorus, potassium, and iron deficiency. *J. Plant Nutr. Soil Sci.* 174, 3–11. <https://doi.org/10.1002/jpln.201000085>
- Chao, A., 1984. Board of the Foundation of the Scandinavian Journal of Statistics Nonparametric Estimation of the Number of Classes in a Population Author ( s ): Anne Chao Source : Scandinavian Journal of Statistics , Vol . 11 , No . 4 ( 1984 ), pp . 265-270 Published by. *Scand. J. Stat.* 11, 265–270.
- Dakora, F.D., Phillips, D.A., 2002. Root exudates as mediators of mineral acquisition in low-nutrient environments. *Plant Soil* 245, 35–47. <https://doi.org/10.1023/A:1020809400075>
- de Mendiburu, F., 2019. R Package ‘ agricolae . ’
- Deng, J., Gu, Y., Zhang, J., Xue, K., Qin, Y., Yuan, M., Yin, H., He, Z., Wu, L., Schuur, E.A.G., Tiedje, J.M., Zhou, J., 2015. Shifts of tundra bacterial and archaeal

- communities along a permafrost thaw gradient in Alaska. *Mol. Ecol.* 24, 222–234. <https://doi.org/10.1111/mec.13015>
- Goodwillie, C., Franch, W.R., 2006. An experimental study of the effects of nutrient addition and mowing on a ditched wetland plant community: Results of the first year. *J. North Carolina Acad. Sci.* 122, 106–117.
- Goodwillie, C., McCoy, M.W., Peralta, A.L., n.d. Long-term fertilization, mowing, and ditch drainage interact in the dynamics of a wetland plant community. *Ecosphere*.
- Gorka, S., Dietrich, M., Mayerhofer, W., Gabriel, R., Wiesenbauer, J., Martin, V., Zheng, Q., Imai, B., Prommer, J., Weidinger, M., Schweiger, P., Eichorst, S.A., Wagner, M., Richter, A., Schintlmeister, A., Woebken, D., Kaiser, C., 2019. Rapid transfer of plant photosynthates to soil bacteria via ectomycorrhizal hyphae and its interaction with nitrogen availability. *Front. Microbiol.* 10, 1–20. <https://doi.org/10.3389/fmicb.2019.00168>
- Haichar, F. el Z., Santaella, C., Heulin, T., Achouak, W., 2014. Root exudates mediated interactions belowground. *Soil Biol. Biochem.* 77, 69–80. <https://doi.org/10.1016/j.soilbio.2014.06.017>
- Hannula, S.E., Kielak, A.M., Steinauer, K., Huberty, M., Jongen, R., De Long, J.R., Heinen, R., Bezemer, T.M., 2019. Time after time: Temporal variation in the effects of grass and forb species on soil bacterial and fungal communities. *MBio* 10, 1–16. <https://doi.org/10.1128/mBio.02635-19>
- Hill, B.H., Elonen, C.M., Herlihy, A.T., Jicha, T.M., Serenbetz, G., 2017. Microbial ecoenzyme stoichiometry, nutrient limitation, and organic matter decomposition in wetlands of the conterminous United States. *Wetl. Ecol. Manag.* 1–15. <https://doi.org/10.1007/s11273-017-9584-5>
- Huo, C., Luo, Y., Cheng, W., 2017. Rhizosphere priming effect: A meta-analysis. *Soil Biol. Biochem.* 111, 78–84. <https://doi.org/10.1016/j.soilbio.2017.04.003>
- Jach-Smith, L.C., Jackson, R.D., 2018. N addition undermines N supplied by arbuscular mycorrhizal fungi to native perennial grasses. *Soil Biol. Biochem.* 116, 148–157. <https://doi.org/10.1016/j.soilbio.2017.10.009>
- Jones, D.L., Nguyen, C., Finlay, R.D., 2009. Carbon flow in the rhizosphere: Carbon trading at the soil-root interface. *Plant Soil* 321, 5–33. <https://doi.org/10.1007/s11104-009-9925-0>
- Kim, B.R., Shin, J., Guevarra, R.B., Lee, Jun Hyung, Kim, D.W., Seol, K.H., Lee, Ju Hoon, Kim, H.B., Isaacson, R.E., 2017. Deciphering diversity indices for a better understanding of microbial communities. *J. Microbiol. Biotechnol.* 27, 2089–2093. <https://doi.org/10.4014/jmb.1709.09027>
- Kozich, J.J., Westcott, S.L., Baxter, N.T., Highlander, S.K., Schloss, P.D., 2013. Development of a dual-index sequencing strategy and curation pipeline for analyzing

- amplicon sequence data on the miseq illumina sequencing platform. *Appl. Environ. Microbiol.* 79, 5112–5120. <https://doi.org/10.1128/AEM.01043-13>
- Kuzyakov, Y., 2010. Soil Biology & Biochemistry Priming effects : Interactions between living and dead organic matter. *Soil Biol. Biochem.* 42, 1363–1371. <https://doi.org/10.1016/j.soilbio.2010.04.003>
- Kuzyakov, Y., Blagodatskaya, E., 2015. Microbial hotspots and hot moments in soil: Concept & review. *Soil Biol. Biochem.* 83, 184–199. <https://doi.org/10.1016/j.soilbio.2015.01.025>
- Kuzyakov, Y., Domanski, G., 2000. Carbon input by plants into the soil. Review. *J. Plant Nutr. Soil Sci.* 421–431.
- Kuzyakov, Y., Siniakina, S. V., Ruehlmann, J., Domanski, G., Stahr, K., 2002. Effect of nitrogen fertilisation on below-ground carbon allocation in lettuce. *J. Sci. Food Agric.* 82, 1432–1441. <https://doi.org/10.1002/jsfa.1202>
- Lal, R., 2008. Carbon sequestration. *Philos. Trans. R. Soc. B Biol. Sci.* <https://doi.org/10.1098/rstb.2007.2185>
- Leff, J.W., Jones, S.E., Prober, S.M., Barberán, A., Borer, E.T., Firn, J.L., Harpole, W.S., Hobbie, S.E., Hofmockel, K.S., Knops, J.M.H., McCulley, R.L., La Pierre, K., Risch, A.C., Seabloom, E.W., Schütz, M., Steenbock, C., Stevens, C.J., Fierer, N., 2015. Consistent responses of soil microbial communities to elevated nutrient inputs in grasslands across the globe. *Proc. Natl. Acad. Sci.* 112, 10967–10972. <https://doi.org/10.1073/pnas.1508382112>
- Lundberg, D.S., Lebeis, S.L., Paredes, S.H., Yourstone, S., Gehring, J., Malfatti, S., Tremblay, J., Engelbrektson, A., Kunin, V., del Rio, T.G., Edgar, R.C., Eickhorst, T., Ley, R.E., Hugenholtz, P., Tringe, S.G., Dangl, J.L., 2012. Defining the core *Arabidopsis thaliana* root microbiome. *Nature* 488, 86–90. <https://doi.org/10.1038/nature11237>
- Matthews, A., Pierce, S., Hipperson, H., Raymond, B., 2019. Rhizobacterial Community Assembly Patterns Vary Between Crop Species. *Front. Microbiol.* 10, 1–13. <https://doi.org/10.3389/fmicb.2019.00581>
- Meier, I.C., Finzi, A.C., Phillips, R.P., 2017. Root exudates increase N availability by stimulating microbial turnover of fast-cycling N pools. *Soil Biol. Biochem.* 106, 119–128. <https://doi.org/10.1016/j.soilbio.2016.12.004>
- Mitsch, W.J., Bernal, B., Nahlik, A.M., Mander, Ü., Zhang, L., Anderson, C.J., Jørgensen, S.E., Brix, H., 2013. Wetlands, carbon, and climate change. *Landsc. Ecol.* 28, 583–597. <https://doi.org/10.1007/s10980-012-9758-8>
- Morris, J.T., Bradley, P.M., 1999. Effects of nutrient loading on the carbon balance of coastal wetland sediments. *Limnol. Oceanogr.* 44, 699–702. <https://doi.org/10.4319/lo.1999.44.3.0699>

- Nguyen, L.T.T., Osanai, Y., Lai, K., Anderson, I.C., Bange, M.P., Tissue, D.T., Singh, B.K., 2018. Responses of the soil microbial community to nitrogen fertilizer regimes and historical exposure to extreme weather events: Flooding or prolonged-drought. *Soil Biol. Biochem.* 118, 227–236. <https://doi.org/10.1016/j.soilbio.2017.12.016>
- Nowinski, N.S., Trumbore, S.E., Schuur, E.A.G., MacK, M.C., Shaver, G.R., 2008. Nutrient addition prompts rapid destabilization of organic matter in an arctic tundra ecosystem. *Ecosystems* 11, 16–25. <https://doi.org/10.1007/s10021-007-9104-1>
- Oksanen, J., 2015. *Vegan : ecological diversity* 1, 1–12. <https://doi.org/10.1029/2006JF000545>
- Peñuelas, J., Sardans, J., Rivas-ubach, A., Janssens, I.A., 2012. The human-induced imbalance between C, N and P in Earth's life system. *Glob. Chang. Biol.* 18, 3–6. <https://doi.org/10.1111/j.1365-2486.2011.02568.x>
- Philippot, L., Raaijmakers, J.M., Lemanceau, P., Van Der Putten, W.H., 2013. Going back to the roots: The microbial ecology of the rhizosphere. *Nat. Rev. Microbiol.* 11, 789–799. <https://doi.org/10.1038/nrmicro3109>
- Phillips, R.P., Bernhardt, E.S., Schlesinger, W.H., 2009. Elevated CO<sub>2</sub> increases root exudation from loblolly pine (*Pinus taeda*) seedlings as an N-mediated response. *Tree Physiol.* 29, 1513–1523. <https://doi.org/10.1093/treephys/tpp083>
- Püschel, D., Janoušková, M., Hujslová, M., Slavíková, R., Gryndlerová, H., Jansa, J., 2016. Plant–fungus competition for nitrogen erases mycorrhizal growth benefits of *Andropogon gerardii* under limited nitrogen supply. *Ecol. Evol.* 6, 4332–4346. <https://doi.org/10.1002/ece3.2207>
- Quast, C., Pruesse, E., Yilmaz, P., Gerken, J., Schweer, T., Yarza, P., Peplies, J., Glöckner, F.O., 2013. The SILVA ribosomal RNA gene database project: Improved data processing and web-based tools. *Nucleic Acids Res.* 41, 590–596. <https://doi.org/10.1093/nar/gks1219>
- R Core Team, 2019. *R: A language and environment for statistical computing*. R Found. Stat. Comput. Vienna, Austria.
- Riggs, C.E., Hobbie, S.E., Bach, E.M., Hofmockel, K.S., Kazanski, C.E., 2015. Nitrogen addition changes grassland soil organic matter decomposition. *Biogeochemistry* 125, 203–219. <https://doi.org/10.1007/s10533-015-0123-2>
- Roberts, D., 2016. Package ‘labdsv.’
- Rognes, T., Flouri, T., Nichols, B., Quince, C., Mahé, F., 2016. VSEARCH: a versatile open source tool for metagenomics. *PeerJ* 4, e2584. <https://doi.org/10.7717/peerj.2584>
- Schloss, P.D., Westcott, S.L., Ryabin, T., Hall, J.R., Hartmann, M., Hollister, E.B., Lesniewski, R. a., Oakley, B.B., Parks, D.H., Robinson, C.J., Sahl, J.W., Stres, B., Thallinger, G.G., Van Horn, D.J., Weber, C.F., 2009. Introducing mothur: Open-

source, platform-independent, community-supported software for describing and comparing microbial communities. *Appl. Environ. Microbiol.* 75, 7537–7541. <https://doi.org/10.1128/AEM.01541-09>

Shannon, C.E., 1948. A Mathematical Theory of Communication. *Bell Syst. Tech. J.* 27, 379–423. <https://doi.org/10.1002/j.1538-7305.1948.tb01338.x>

Soong, Jennifer L., Marañon-Jimenez, S., Cotrufo, M.F., Boeckx, P., Bodé, S., Guenet, B., Peñuelas, J., Richter, A., Stahl, C., Verbruggen, E., Janssens, I.A., 2018. Soil microbial CNP and respiration responses to organic matter and nutrient additions: Evidence from a tropical soil incubation. *Soil Biol. Biochem.* 122, 141–149. <https://doi.org/10.1016/j.soilbio.2018.04.011>

Soong, Jennifer L., Marañon-Jimenez, S., Cotrufo, M.F., Boeckx, P., Bodé, S., Guenet, B., Peñuelas, J., Richter, A., Stahl, C., Verbruggen, E., Janssens, I.A., Boeckx, P., Peñuelas, J., Stahl, C., Richter, A., Soong, J.L., Janssens, I.A., Bodé, S., Verbruggen, E., Marañon-Jimenez, S., Cotrufo, M.F., 2018. Soil microbial CNP and respiration responses to organic matter and nutrient additions: Evidence from a tropical soil incubation. *Soil Biol. Biochem.* 122, 141–149. <https://doi.org/10.1016/j.soilbio.2018.04.011>

Treseder, K.K., 2008. Nitrogen additions and microbial biomass: a meta-analysis of ecosystem studies. *Ecol. Lett.* 1111–1120. <https://doi.org/10.1111/j.1461-0248.2008.01230.x>

Uroz, S., Buée, M., Murat, C., Frey-Klett, P., Martin, F., 2010. Pyrosequencing reveals a contrasted bacterial diversity between oak rhizosphere and surrounding soil. *Environ. Microbiol. Rep.* 2, 281–288. <https://doi.org/10.1111/j.1758-2229.2009.00117.x>

Van Der Heijden, M.G.A., Bardgett, R.D., Van Straalen, N.M., 2008. The unseen majority: Soil microbes as drivers of plant diversity and productivity in terrestrial ecosystems. *Ecol. Lett.* <https://doi.org/10.1111/j.1461-0248.2007.01139.x>

Van Der Heijden, M.G.A., Bruin, S. De, Luckerhoff, L., Van Logtestijn, R.S.P., Schlaeppi, K., 2016. A widespread plant-fungal-bacterial symbiosis promotes plant biodiversity, plant nutrition and seedling recruitment. *ISME J.* 10, 389–399. <https://doi.org/10.1038/ismej.2015.120>

Vranova, V., Rejsek, K., Skene, K.R., Janous, D., Formanek, P., 2013. Methods of collection of plant root exudates in relation to plant metabolism and purpose: A review. *J. Plant Nutr. Soil Sci.* 176, 175–199. <https://doi.org/10.1002/jpln.201000360>

Wallander, H., Nilsson, L.O., Hagerberg, D., Rosengren, U., 2003. Direct estimates of C:N ratios of ectomycorrhizal mycelia collected from Norway spruce forest soils. *Soil Biol. Biochem.* 35, 997–999. [https://doi.org/10.1016/S0038-0717\(03\)00121-4](https://doi.org/10.1016/S0038-0717(03)00121-4)

Wang, R., Balkanski, Y., Boucher, O., Ciais, P., Peñuelas, J., Tao, S., 2015. Significant contribution of combustion-related emissions to the atmospheric phosphorus budget. *Nat. Geosci.* 8, 48–54. <https://doi.org/10.1038/ngeo2324>

- Worrich, A., Stryhanyuk, H., Musat, N., König, S., Banitz, T., Centler, F., Frank, K., Thullner, M., Harms, H., Richnow, H.H., Miltner, A., Kästner, M., Wick, L.Y., 2017. Mycelium-mediated transfer of water and nutrients stimulates bacterial activity in dry and oligotrophic environments. *Nat. Commun.* 8. <https://doi.org/10.1038/ncomms15472>
- Wu, F.Y., Chung, A.K.C., Tam, N.F.Y., Wong, M.H., 2012. Root exudates of wetland plants influenced by nutrient status and types of plant cultivation. *Int. J. Phytoremediation* 14, 543–553. <https://doi.org/10.1080/15226514.2011.604691>
- Zarraonaindia, I., Owens, S., Weisenhorn, P., West, K., Hampton-Marcell, J., Lax, S., Bokulich, N., Mills, D., Martin, G., Taghavi, S., Lelie, van der, D., Gilbert, J., 2015. The Soil Microbiome Influences Grapevine-Associated Microbiota. *MBio*. <https://doi.org/10.1128/mBio.02527-14.Editor>
- Zhang, C., Niu, D., Hall, S.J., Wen, H., Li, X., Fu, H., Wan, C., Elser, J.J., 2014. Effects of simulated nitrogen deposition on soil respiration components and their temperature sensitivities in a semiarid grassland. *Soil Biol. Biochem.* 75, 113–123. <https://doi.org/10.1016/j.soilbio.2014.04.013>
- Zhu, B., Gutknecht, J.L.M., Herman, D.J., Keck, D.C., Firestone, M.K., Cheng, W., 2014. Rhizosphere priming effects on soil carbon and nitrogen mineralization. *Soil Biol. Biochem.* 76, 183–192. <https://doi.org/10.1016/j.soilbio.2014.04.033>

## CONCLUSION

We should not underestimate the global implications of the world's tiniest engineers. Soil microorganisms are one of the most important groups of organisms on Earth, and it is expected that soil bacteria and fungi have the ability to mitigate and worsen climate change (Cavicchioli et al., 2019; Jansson and Hofmockel, 2019). Microorganisms are responsible for regulating ecosystem processes such as biogeochemical cycles, plant production, and greenhouse gas emissions (Bardgett and Van Der Putten, 2014; Bodelier, 2011; Delgado-Baquerizo et al., 2018; Philippot et al., 2013). During the Anthropocene, industrial processes and land use change have produced vast amounts of greenhouse gases (GHGs) and increased nutrient (e.g., nitrogen (N) and phosphorus (P)) deposition onto Earth's ecosystems (Guignard et al., 2017). These human induced changes can directly influence microbial activity (Leff et al., 2015). As a result, global nutrient cycles are altered, which further increase GHG emissions that can worsen climate change (Jansson and Hofmockel, 2019).

Over the last three decades, there has been an explosion in research focused on how microbial diversity relates to ecosystem functions (Bardgett and Van Der Putten, 2014; Tiedje et al., 1999). Despite ongoing research efforts, much of the microbial world and associated activities remain uncharacterized (Bardgett and Van Der Putten, 2014; Tiedje et al., 1999). This is because multiple abiotic and biotic environmental factors, such as soil moisture, nutrient concentrations, and plant carbon inputs, directly and indirectly affect microbially driven ecosystem functions (Jansson and Hofmockel, 2019). Further, interacting abiotic and biotic processes make microbial patterns and activities challenging to predict. This dissertation addresses how specific abiotic and biotic

processes affect microbial community structure and nutrient cycling functions. Specifically, this dissertation explored how soil moisture, soil nutrient concentrations, and plant presence impact microbial community structure and carbon (C) and N cycling functions in wetland soils.

Wetlands are areas of conservation and restoration because they provide many ecosystem benefits such as processing pollutants and storing C (Mitsch et al., 2013). Microbial activity in soils and sediments contribute to wetland ecosystem benefits (Bodelier and Dedysh, 2013). Wetlands naturally accumulate C due to anoxic soil conditions inhibiting aerobic microbial soil organic matter (SOM) decomposition, which slows down C losses to the atmosphere (Jansson and Hofmockel, 2019). However, saturated soils with low N availability can promote anaerobic microbial decomposition of SOM resulting in production of the potent GHG methane (CH<sub>4</sub>) (Demuzere et al., 2014). When N is available for microbially activity, these anoxic conditions can also support microbial N removal processes which can improve water quality (Reisinger et al., 2016). Further, the presence of plants can significantly enhance microbial activity by providing C sources to fuel microbial processes (Kuzyakov and Blagodatskaya, 2015; Philippot et al., 2013) and by facilitating gas exchange between plant aboveground and belowground components (Chanton, 2005; Hu et al., 2015). Taken together, microbial interactions with plants, nutrients, and water can affect microbially driven ecosystem functions in different ways.

This dissertation suggests that soil hydrology can have a long lasting effect on microbial community composition, and that the interaction of current soil moisture conditions along with the presence of plants can significantly decrease GHG production

(Chapters 1 and 2). In terms of new wetland construction and design (Chapter 1), saturated but not permanently flooded land areas have the greatest potential for N removal by denitrification and decreased GHG emissions. Specifically, when saturated zones are flooded, denitrification rates are similar to rates measured in permanently flooded soils. This result warrants deeper temporal investigations to elucidate when N removal processes decline and when CH<sub>4</sub> production increases after flood waters saturate soils. Understanding how the movement and duration of flood waters influence transitions between microbial processes can inform wetland management. For example, the management of water retention can provide the maximum pollutant removal benefits while inhibiting CH<sub>4</sub> production as precipitation patterns change. Further, plants should always be included in wetland construction due to their ability to mediate GHG production. Even though our restored wetland study (Chapter 2) showed that plants can reduce GHG production, other studies have demonstrated that plants can increase GHG production by transporting CH<sub>4</sub> from belowground (Carmichael et al., 2014; Hu et al., 2015). Therefore, future studies should evaluate the efficacy of different plant species (monoculture and mixed species communities), that are commonly used in wetland construction and restoration, to control GHG production. To that end, a meta-analysis of studies estimating GHGs with and without plants would be valuable to broadly understanding the actual C storage potential of wetlands.

Nutrient availability for plant and microbial communities are important C cycling control points (Kuzyakov and Blagodatskaya, 2015). Increased nutrient availability in soils can increase C cycling rates especially in naturally low-nutrient ecosystems (Bengtson et al., 2012; Nowinski et al., 2008). Through human activities such as burning

of fuels and biomass and mining of phosphorus (P), N and P can become airborne (Guignard et al., 2017). These nutrients get transported and deposited onto ecosystems that are spatially disconnected from the nutrient sources (Ireland et al., 2014). While wetlands are typically considered C sinks (i.e., net C fixed and stored is more than C lost), indirect nutrient additions may be increasing C cycling and reducing C stocks especially in low-nutrient wetlands (Bengtson et al., 2012; Nowinski et al., 2008). In this dissertation, the focal coastal plain wetland represents a low-nutrient ecosystem receiving experimental nutrient additions. Chapters 3 and 4 revealed a positive feedback in that nutrient addition increased soil bacterial diversity which stimulated an increase in C, N, and P cycling, especially in plant rhizospheres. This is in contrast to grassland or agricultural ecosystems, where nutrient enrichment decreases microbial respiration and these negative feedbacks dominate (Leff et al., 2015; Nguyen et al., 2018). These studies warrant further investigation into SOM decomposition in oligotrophic, low-nutrient wetlands to better understand when positive versus negative plant-microbe feedbacks occur. Additionally, comparing microbial community C cycling responses to nutrient additions in oligotrophic wetlands to more intensive agricultural systems could provide insights into mechanisms driving positive and negative plant-microbe interactions.

In conclusion, the microbial process of SOM decomposition results in the production of carbon dioxide in oxic soils and CH<sub>4</sub> in anoxic soils. This process represents a control point where microbial activity can speed up (i.e., produce GHG emissions) or slow down (i.e., reduce GHG emissions) climate change effects. Further, nutrient enrichment of soils can have contrasting effects on microbial SOM

decomposition such that historically low-nutrient ecosystems respond with increases in C cycling while high-nutrient ecosystems respond with decreases in C cycling. Continuing to research how microbial diversity and environmental factors interact to affect soil C storage can inform better management of microbial engineers to mitigate the effects of climate change.

## References

- Bardgett, R.D., Van Der Putten, W.H., 2014. Belowground biodiversity and ecosystem functioning. *Nature* 515, 505–511. <https://doi.org/10.1038/nature13855>
- Bengtson, P., Barker, J., Grayston, S.J., 2012. Evidence of a strong coupling between root exudation, C and N availability, and stimulated SOM decomposition caused by rhizosphere priming effects. *Ecol. Evol.* 2, 1843–1852. <https://doi.org/10.1002/ece3.311>
- Bodelier, P.L.E., 2011. Toward understanding, managing, and protecting microbial ecosystems. *Front. Microbiol.* 2, 1–8. <https://doi.org/10.3389/fmicb.2011.00080>
- Bodelier, P.L.E., Dedysh, S.N., 2013. Microbiology of wetlands. *Front. Microbiol.* 4, 2–5. <https://doi.org/10.3389/fmicb.2013.00079>
- Carmichael, M.J., Bernhardt, E.S., Bräuer, S.L., Smith, W.K., 2014. The role of vegetation in methane flux to the atmosphere: should vegetation be included as a distinct category in the global methane budget? *Biogeochemistry* 119, 1–24. <https://doi.org/10.1007/s10533-014-9974-1>
- Cavicchioli, R., Ripple, W.J., Timmis, K.N., Azam, F., Bakken, L.R., Baylis, M., Behrenfeld, M.J., Boetius, A., Boyd, P.W., Classen, A.T., Crowther, T.W., Danovaro, R., Foreman, C.M., Huisman, J., Hutchins, D.A., Jansson, J.K., Karl, D.M., Koskella, B., Mark Welch, D.B., Martiny, J.B.H., Moran, M.A., Orphan, V.J., Reay, D.S., Remais, J. V., Rich, V.I., Singh, B.K., Stein, L.Y., Stewart, F.J., Sullivan, M.B., van Oppen, M.J.H., Weaver, S.C., Webb, E.A., Webster, N.S., 2019. Scientists' warning to humanity: microorganisms and climate change. *Nat. Rev. Microbiol.* 17, 569–586. <https://doi.org/10.1038/s41579-019-0222-5>
- Chanton, J.P., 2005. The effect of gas transport on the isotope signature of methane in wetlands. *Org. Geochem.* 36, 753–768. <https://doi.org/10.1016/j.orggeochem.2004.10.007>
- Delgado-Baquerizo, M., Oliverio, A.M., Brewer, T.E., Benavent-gonzález, A., Eldridge, D.J., Bardgett, R.D., Maestre, F.T., Singh, B.K., Fierer, N., 2018. A Global Atlas of the Dominant Bacteria Found in Soil. *Science* (80-. ). 325, 320–325. <https://doi.org/10.1126/science.aap9516>
- Demuzere, M., Orru, K., Heidrich, O., Olazabal, E., Geneletti, D., Orru, H., Bhave, A.G., Mittal, N., Feliu, E., Faehnle, M., 2014. Mitigating and adapting to climate change: Multi-functional and multi-scale assessment of green urban infrastructure. *J. Environ. Manage.* 146, 107–115. <https://doi.org/10.1016/j.jenvman.2014.07.025>
- Guignard, M.S., Leitch, A.R., Acquisti, C., Eizaguirre, C., Elser, J.J., Hessen, D.O., Jeyasingh, P.D., Neiman, M., Richardson, A.E., Soltis, P.S., Soltis, D.E., Stevens, C.J., Trimmer, M., Weider, L.J., Woodward, G., Leitch, I.J., 2017. Impacts of Nitrogen and Phosphorus: From Genomes to Natural Ecosystems and Agriculture. *Front. Ecol. Evol.* 5. <https://doi.org/10.3389/fevo.2017.00070>

- Hu, Q., Cai, J., Yao, B., Wu, Q., Wang, Y., Xu, X., 2015. Plant-mediated methane and nitrous oxide fluxes from a carex meadow in Poyang Lake during drawdown periods. *Plant Soil*. <https://doi.org/10.1007/s11104-015-2733-9>
- Ireland, A.W., Clifford, M.J., Booth, R.K., 2014. Widespread dust deposition on North American peatlands coincident with European land-clearance. *Veg. Hist. Archaeobot.* 23, 693–700. <https://doi.org/10.1007/s00334-014-0466-y>
- Jansson, J.K., Hofmockel, K.S., 2019. Soil microbiomes and climate change. *Nat. Rev. Microbiol.* <https://doi.org/10.1038/s41579-019-0265-7>
- Kuzyakov, Y., Blagodatskaya, E., 2015. Microbial hotspots and hot moments in soil: Concept & review. *Soil Biol. Biochem.* 83, 184–199. <https://doi.org/10.1016/j.soilbio.2015.01.025>
- Leff, J.W., Jones, S.E., Prober, S.M., Barberán, A., Borer, E.T., Firn, J.L., Harpole, W.S., Hobbie, S.E., Hofmockel, K.S., Knops, J.M.H., McCulley, R.L., La Pierre, K., Risch, A.C., Seabloom, E.W., Schütz, M., Steenbock, C., Stevens, C.J., Fierer, N., 2015. Consistent responses of soil microbial communities to elevated nutrient inputs in grasslands across the globe. *Proc. Natl. Acad. Sci.* 112, 10967–10972. <https://doi.org/10.1073/pnas.1508382112>
- Mitsch, W.J., Bernal, B., Nahlik, A.M., Mander, Ü., Zhang, L., Anderson, C.J., Jørgensen, S.E., Brix, H., 2013. Wetlands, carbon, and climate change. *Landsc. Ecol.* 28, 583–597. <https://doi.org/10.1007/s10980-012-9758-8>
- Nguyen, L.T.T., Osanai, Y., Lai, K., Anderson, I.C., Bange, M.P., Tissue, D.T., Singh, B.K., 2018. Responses of the soil microbial community to nitrogen fertilizer regimes and historical exposure to extreme weather events: Flooding or prolonged-drought. *Soil Biol. Biochem.* 118, 227–236. <https://doi.org/10.1016/j.soilbio.2017.12.016>
- Nowinski, N.S., Trumbore, S.E., Schuur, E.A.G., MacK, M.C., Shaver, G.R., 2008. Nutrient addition prompts rapid destabilization of organic matter in an arctic tundra ecosystem. *Ecosystems* 11, 16–25. <https://doi.org/10.1007/s10021-007-9104-1>
- Philippot, L., Raaijmakers, J.M., Lemanceau, P., Van Der Putten, W.H., 2013. Going back to the roots: The microbial ecology of the rhizosphere. *Nat. Rev. Microbiol.* 11, 789–799. <https://doi.org/10.1038/nrmicro3109>
- Reisinger, A.J., Groffman, P.M., Rosi-Marshall, E.J., 2016. Nitrogen-cycling process rates across urban ecosystems. *FEMS Microbiol. Ecol.* 92, fiw198. <https://doi.org/10.1093/femsec/fiw198>
- Tiedje, J.M., Asuming-Brempong, S., Nüsslein, K., Marsh, T.L., Flynn, S.J., 1999. Opening the black box of soil microbial diversity. *Appl. Soil Ecol.* 13, 109–122. [https://doi.org/10.1016/S0929-1393\(99\)00026-8](https://doi.org/10.1016/S0929-1393(99)00026-8)

